PREPARATION AND CHARACTERIZATION OF POLYMER COMPOSITES CONTAINING BORON COMPOUNDS

A THESIS SUBMITTED TO
THE GRADUATE SCHOOL OF NATURAL AND APPLIED SCIENCES
OF
MIDDLE EAST TECHNICAL UNIVERSITY

BY

ELİF TOPÇUOĞLU

IN PARTIAL FULFILLMENT OF THE REQUIREMENTS
FOR
THE DEGREE OF MASTER OF SCIENCE
IN
CHEMICAL ENGINEERING

AUGUST 2016

Approval of thesis:

PREPARATION AND CHARACTERIZATION OF POLYMER COMPOSITES CONTAINING BORON COMPOUNDS

submitted by **ELİF TOPÇUOĞLU** in partial fulfillment of the requirements for the degree of **Master of Science in Chemical Engineering Department, Middle East Technical University** by,

Prof. Dr. Gülbin Dural Ünver _____
Dean, Graduate School of **Natural and Applied Sciences**

Prof. Dr. Halil Kalıpçılar _____
Head of Department, **Chemical Engineering**

Prof. Dr. Göknur Bayram _____
Supervisor, **Chemical Engineering Dept., METU**

Prof. Dr. Naime Aslı Sezgi _____
Co-Supervisor, **Chemical Engineering Dept., METU**

Examining Committee Members:

Assoc. Prof. Dr. Özcan Köysüren _____
Energy and Materials Eng. Dept., Ankara University

Prof. Dr. Göknur Bayram _____
Chemical Engineering Dept., METU

Prof. Dr. Naime Aslı Sezgi _____
Chemical Engineering Dept., METU

Assoc. Prof. Dr. Çerağ Dilek Hacıhabiboğlu _____
Chemical Engineering Dept., METU

Asst. Prof. Dr. Erhan Bat _____
Chemical Engineering Dept., METU

Date: 09.08.2016

I hereby declare that all information in this document has been obtained and presented in accordance with academic rules and ethical conduct. I also declare that, as required by these rules and conduct, I have fully cited and referenced all material and results that are not original to this work.

Name, Last name: Elif TOPÇUOĞLU

Signature:

ABSTRACT

PREPARATION AND CHARACTERIZATION OF POLYMER COMPOSITES CONTAINING BORON COMPOUNDS

Topçuoğlu, Elif

M.S., Department of Chemical Engineering
Supervisor: Prof. Dr. Göknur Bayram
Co-Supervisor: Prof. Dr. Naime Aslı Sezgi

August 2016, 155 pages

Epoxy (EP) is a thermosetting polymer which has high dimensional stability. However, the brittleness, low resistance to impact failure and flammability are some limitations of the epoxy polymer. These properties limit the usage of epoxy in the applications where high mechanical strength and flame retardancy properties are needed.

The purposes of this study are to improve both mechanical and flame retardancy properties of epoxy by the addition of boron containing compounds (BCC) mainly boron carbide (B_4C), and to characterize the prepared composites in terms of their mechanical, flame retardancy, thermal, electrical properties and morphologies.

In this study, as-received boron carbide particles were first characterized in terms of their structural, thermal, electrical properties and morphologies. X-Ray Diffraction (XRD) analysis revealed the presence of B_4C. Scanning Electron Microscopy (SEM) showed that the particles are irregular in shape and with the size of 3-8 microns.

Epoxy composites containing 0.5, 1, 3, 5 and 8% boron carbide were characterized using Fourier Transform Infrared Spectroscopy (FTIR), tensile and impact tests, Limiting Oxygen Index (LOI), and UL-94 tests, Differential Scanning Calorimetry (DSC) analysis, Thermal Gravimetric Analysis (TGA) and two point probe electrical resistivity measurements. It was determined that epoxy-based composites containing 3% B_4C had 44 MPa tensile strength, 13.4 kJ/m^2 impact strength and LOI value of 23%.

The properties of the epoxy-based composites containing BCC such as zinc borate (ZnB), boric acid (BA), calcium borate (CaB) and melamine phosphate (MP) were investigated using the same characterization techniques.

Among all the composites of the study, EP/10MP/3B_4C composite exhibited the highest flame retardancy property with a LOI value of 27.5% and V-0 rating in UL-94 test.

Impact strength of EP/3B_4C composite (13.4 kJ/m^2) was found to be higher than that of the neat epoxy (11.1 kJ/m^2) and EP/10MP/3B_4C composite (6.4 kJ/m^2).

Keywords: Epoxy, boron carbide, composite, mechanical characterization, flame retardancy

ÖZ

BOR BİLEŞİKLERİ İÇEREN POLİMER KOMPOZİTLERİNİN HAZIRLANMASI VE KARAKTERİZASYONU

Topçuoğlu, Elif

Yüksek Lisans, Kimya Mühendisliği
Tez Yöneticisi: Prof. Dr. Göknur Bayram
Ortak Tez Yöneticisi: Prof. Dr. Naime Aslı Sezgi

Ağustos 2016, 155 sayfa

Epoksi (EP), yüksek boyutsal kararlılığa sahip bir termoset polimerdir. Ancak, kırılganlık, çarpma dayanımının düşük olması ve yanıcı olması epoksi polimerlerinin bazı dezavantajlarıdır. Bu özellikler, epoksinin yüksek mekanik mukavemet ve alev geciktirici özellikler gerektiren uygulamalarda kullanılmasını sınırlandırmaktadır.

Bu çalışmanın amaçları, epoksiye başlıca bor karbür (B_4C) olmak üzere bor içeren bileşikler (BCC) ekleyerek epoksinin mekanik ve alev geciktirici özelliklerini iyileştirmek ve hazırlanan kompozit malzemelerin mekanik, alev geciktirici, termal, elektriksel özelliklerini ve morfolojilerini karakterize etmektir.

Bu çalışmada alınan bor karbür partikülleri öncelikle, yapısal, termal, elektriksel ve yüzey özellikleri açısından karakterize edilmiştir. X-ışını kırınımı (XRD) analizi,

B_4C varlığını açığa çıkarmıştır. Taramalı elektron mikroskobu (SEM) analizi, partiküllerin şekil olarak düzensiz ve 3-8 mikron boyutlarında olduğunu göstermiştir.

%0.5, 1, 3, 5 ve 8 miktarlarında bor karbür içeren epoksi kompozitler, fourier dönüşümlü kızılötesi spektroskopisi (FTIR), çekme ve darbe testleri, sınırlayıcı oksijen indeksi (LOI), ve dikey yanma testleri (UL-94), diferansiyel taramalı kalorimetre (DSC) analizi, termogravimetrik analiz (TGA), ve iki nokta temaslı özdirenç ölçümü ile karakterize edilmiştir. %3 B_4C içeren epoksi-bazlı kompozitin 44 MPa çekme dayanımı, 13.4 kJ/m^2 darbe dayanımı ve %23 LOI değerine sahip olduğu belirlenmiştir.

Çinko borat (ZnB), borik asit (BA) ve kalsiyum borat (CaB) içeren BCC, ve melamin fosfat (MP) yanmayı geciktiricilerini içeren epoksi-bazlı kompozitlerin özellikleri aynı karakterizasyon teknikleri kullanılarak araştırılmıştır.

Çalışmanın bütün kompozitleri arasında, EP/10MP/3B_4C kompoziti %27.5 LOI değeri ve UL-94 testindeki V-0 değeri ile en yüksek yanmayı geciktirici özelliği ortaya koymuştur.

EP/3B_4C kompozitinin darbe dayanımı (13.4 kJ/m^2), saf epoksininkinden (11.1 kJ/m^2) ve EP/10MP/3B_4C kompozitinden (6.4 kJ/m^2) daha fazla olarak bulunmuştur.

Anahtar kelimeler: Epoksi, bor karbür, kompozit, mekanik karakterizasyon, alev geciktirici

To my lovely family,

ACKNOWLEDGEMENTS

I wish to express my deepest gratitude to my supervisor, Prof. Dr. Göknur Bayram, for her continuous support, encouragement, and guidance at all levels of my study. I also present my sincere gratitude to my co-supervisor Prof. Dr. Naime Aslı Sezgi for her valuable advices, encouragement and guidance throughout this study. I acquired valuable experience during my study under their supervision that will help me through my future career.

I would like to thank the financial support from Middle East Technical University Scientific Research Fund (BAP) through the grant number BAP-07-02-2014-007-451. I also want to thank METU Central Laboratory and all the technicians of Chemical Engineering Department of Middle East Technical University. I would like to thank Mihrican Açıkgöz from Department of Chemical Engineering for DSC and TGA analysis, for teaching me how to use the instruments and giving me the opportunity to use them. I want to thank Yavuz Güngör from Department of Chemical Engineering for his technical helps and advices for the mechanical tests.

I also thank Merve Özkutlu and Berrak Erkmen for their helps throughout my thesis not only as lab mates but also as dearest enjoyable friends. We solved the problems that we have faced in the laboratory during our studies but we shared and laughed more. Therefore I appreciate their kind friendship and all the good times that we had.

I would like to thank my dear colleagues Elif İrem Şenyurt, Fatma Şahin Çakanyıldırım, Özge Çimen, Dilara Gülçin Çağlayan, Merve Sarıyer, Özge Batır, Özge Şen and all the C-block residents. I feel very lucky that I had the chance to work with them. I want to thank Arzu Aslan for her valuable support.

My dearest friend Sezin Güner, without your support and valuable friendship not the studies but the life would be much harder. I am thankful that I have another sister like

you. Also, I am thanking to my lovely friends Hande Akar and Sadık Tunçay for their endless support at any time in my life.

Foremost I am grateful to the life from the deepest of my heart that it introduced me the man that I loved. I am very thankful to my fiance Özgen Buğdaycı for his love, courage, patience, knowledge and everything both in my thesis and our whole life.

Not last but least, my awesome family, İsmail Saraloğlu, Süheyla Saraloğlu and my devoted mom Zerrin Saraloğlu without your endless support and love, my success wouldn't have been possible. My special thanks go to my beloved little sister Eda Topçuoğlu Özdeniz who I love the most. I appreciate her love, endless moral support, care and everything. Also I am thankful to Selçuk Özdeniz and little Özdeniz for giving me the moral that I needed in the very stressful times of writing thesis.

TABLE OF CONTENTS

ABSTRACT v

ÖZ vii

ACKNOWLEDGEMENTS x

TABLE OF CONTENTS xii

LIST OF TABLES xvii

LIST OF FIGURES xix

NOMENCLATURE xxiv

1. INTRODUCTION 1

2. BACKGROUND 5

2.1 Boron 5

2.1.1 Boron in the World 6

2.1.2 Boron in Turkey 6

2.1.3 Boron Carbide (B_4C) 7

2.1.3.1 Structure of boron carbide 8

2.1.3.2 Production of boron carbide 9

2.1.3.2.1 Carbothermal synthesis of boron carbide 10

2.2 Epoxy 10

2.3 Epoxy Composites 13

2.4 Flammability and Thermal Decomposition of Epoxy 14

2.5 Polymer Combustion 15

2.6 Flame Retardancy 16

2.6.1 Flame Retardant Mechanism 18

2.6.1.1 Physical Action 18

2.6.1.2 Chemical Action 18
2.6.2 Flame Retardants 19
2.6.2.1 Boron Containing Flame Retardants 20
2.6.2.1.1 Zinc Borate 20
2.6.2.1.2 Boric Acid 21
2.6.2.1.3 Calcium Borate 22
2.6.2.1.4 Boron Carbide 22
2.6.2.2 Nitrogen-Based Flame Retardants 22
2.6.2.3 Melamine-based Flame Retardants 23
2.6.2.3.1 Melamine Phosphate 23
2.6.2.4 Phosphorus-Based Flame Retardants 24
2.7 Improvement of Mechanical Properties 25
2.8 Characterization Techniques 26
2.8.1 Mechanical Characterization 26
2.8.1.1 Tensile Test 26
2.8.1.2 Impact Test 29
2.8.1.3 Shore Hardness Test 29
2.8.2 Flame Retardancy Characterization 30
2.8.2.1 Limiting Oxygen Index (LOI) Test 30
2.8.2.2 UL-94 Vertical Burning Test 31
2.8.3 Morphological Analysis 33
2.8.3.1 Scanning Electron Microscopy (SEM) 33
2.8.4 X-Ray Spectroscopy (XPS) 33
2.8.5 Fourier Transform Infrared (FTIR) Spectroscopy 34
2.8.6 X-ray Diffraction (XRD) Analysis 35
2.8.7 Thermal Characterization 35
2.8.7.1 Differential Scanning Calorimetry (DSC) 35

2.8.7.2 Thermal Gravimetric Analysis (TGA) 36
2.8.8 Electrical Characterization 37
2.8.8.1 Electrical Resistivity Measurement 37
2.9 Previous Studies 38
2.9.1 Flame Retardancy of Epoxy 38
2.9.2 Mechanical Properties of Epoxy 40
2.10 Motivation of the Study 41
3. EXPERIMENTAL 43
3.1 Materials 43
3.1.1 Epoxy Resin 43
3.1.2 Curing Agent 44
3.1.3 Boron Carbide 44
3.1.4 Zinc Borate (ZnB) 45
3.1.5 Boric Acid (BA) 45
3.1.6 Calcium Borate (CaB) 46
3.1.7 Melamine Phosphate (MP) 46
3.1.8 Solvent (Acetone) 46
3.2 Preparation of Epoxy Polymer and Epoxy-based Composites 47
3.2.1 Preparation of Neat Epoxy 47
3.2.2 Preparation of Epoxy-based Composites 49
3.3 Characterization Methods 52
3.3.1 X-Ray Diffraction (XRD) 52
3.3.2 Scanning Electron Microscopy (SEM) 52
3.3.3 X-Ray Photoelectron Spectroscopy (XPS) 52
3.3.4 Thermal Gravimetric Analysis (TGA) 52
3.3.5 Fourier Transformed Infrared (FTIR) Spectroscopy 52
3.3.6 Mechanical Characterization of EP-based Composites 53

3.3.6.1 Tensile Test 53
3.3.6.2 Impact Test 54
3.3.6.3 Shore D Hardness Test 55
3.3.7 Flame Retardancy Characterization of EP-based Composites 55
3.3.7.1 Limiting Oxygen Index Test (LOI) 55
3.3.7.2 UL-94 Vertical Burning Test 56
3.3.8 Differential Scanning Calorimetry (DSC) 56
3.3.9 Electrical Characterization of EP/B_4C Composites 56
4. RESULTS AND DISCUSSION 59
4.1 FTIR Results of Epoxy/Boron Carbide Composites 70
4.2 XRD Analysis of Epoxy/Boron Carbide Composites 71
4.3 Scanning Electron Microscopy (SEM) Analysis 72
4.3.1 SEM Analysis of EP/B_4C Composites 72
4.3.2. SEM Analysis of Epoxy/Boron Containing Compound Composites and Epoxy/Melamine Phosphate Composites 81
4.4 Mechanical Analysis of Epoxy-Based Composites 87
4.4.1 Mechanical Properties of Epoxy/Boron Carbide Composites 87
4.4.2 Mechanical Properties of Epoxy/Boron Containing Compound Composites and Epoxy/Melamine Phosphate Composites 93
4.5 Flammability Analysis of Epoxy-Based Composites 97
4.5.1 Flammability Properties of Epoxy/Boron Carbide Composites 97
4.5.2 Flammability Properties of Epoxy/Boron Containing Compound Composites and Epoxy/Melamine Phosphate Composites 100
4.6 Thermal Analyses of Epoxy-Based Composites 104
4.6.1 Thermal Properties of Epoxy/Boron Carbide Composites 104
4.6.2 Thermal Properties of Epoxy/Boron Containing Compound Composites and Epoxy/Melamine Phosphate Composites 107
4.7 Electrical Resistivities of Epoxy/Boron Carbide Composites 109

5. CONCLUSIONS 113

REFERENCES 115

A. X-RAY DIFFRACTION DATA 125

B. RESULTS OF DSC ANALYSIS 135

C. RESULTS OF MECHANICAL ANALYSIS 137

D. RESULTS OF DSC AND TGA ANALYSES OF EPOXY-BASED COMPOSITES 139

E. SINTERING OF BORON CARBIDE 155

LIST OF TABLES

TABLES

Table 2.1 The properties of boron 5
Table 2.2 The properties of stoichiometric B_4C 7
Table 2.3 The criteria for classification of samples for UL-94 test 33
Table 3.1 The properties of Polires 188 ……43
Table 3.2 The properties of Cetepox 1393 H. 44
Table 3.3 The properties of B_4C 44
Table 3.4 Chemical analysis data of B_4C 45
Table 3.5 The properties of ZnB 45
Table 3.6 The properties of BA. 45
Table 3.7 The properties of CaB. 46
Table 3.8 The properties of MP 46
Table 3.9 The properties of acetone 47
Table 3.10 The compositions of epoxy/boron carbide composites. 51
Table 3.11 The compositions of epoxy/boron containing compounds composites. 51
Table 3.12 Dimensions of the dog bone shape sample. 54
Table 3.13 Dimensions of the impact test sample. 55
Table 4.1 Atomic amount of boron and carbon in the as-received boron carbide. .. 64
Table 4.2 Shore D hardness values of neat epoxy and EP/B_4C composites. 92
Table 4.3 Shore D hardness values of epoxy-boron containing compound composites and epoxy/melamine phosphate composites. 93
Table 4.4 The flammability test results of neat epoxy and epoxy/boron carbide composites. 98
Table 4.5 The flammability test results of epoxy/boron containing compound composites and epoxy/melamine phosphate composites. 100
Table 4.6 Thermal degradation temperatures and char yields of neat epoxy and epoxy/boron carbide composites. 106
Table 4.7 Thermal degradation temperatures and char yields of epoxy/boron containing compound composites and epoxy/melamine phosphate composites….109

Table A.1 XRD data of trigonal boron. 125
Table A.2 XRD data of rhombohedral boron carbide. 127
Table A.3 XRD data of B_2O_3. 128
Table A.4 XRD data of Fe_3O_4. 128
Table A.5 XRD data of Fe_2O_3. 129
Table A.6 XRD data of graphite. 131
Table A.7 XRD data of as-received B_4C. 132
Table A.8 XRD data of B_4C heated in air atmosphere. 133
Table A.9 XRD data of B_4C heated in argon atmosphere. 134
Table C.1 Tensile test data of neat epoxy and EP/B_4C composites. 137
Table C.2 Impact test data of neat epoxy and EP/B_4C composites. 137
Table C.3 Tensile test data of epoxy/boron containing compound composites and epoxy/melamine phosphate composites. 138
Table C.4 Impact test data of epoxy/boron containing compound composites and epoxy/melamine phosphate composites. 138

LIST OF FIGURES

FIGURES

Figure 2.1 The rhombohedral structure of boron carbide 8
Figure 2.2 B-C Phase Diagram 9
Figure 2.3 Epoxide group 10
Figure 2.4 Photos of epoxy polymers used in (a) paints and coatings, (b) adhesives, (c) electronic materials and (d) airplanes 11
Figure 2.5 The structure of DGEBA 11
Figure 2.6 Reactions in the production of DGEBA 12
Figure 2.7 Curing reaction of DGEBA and cycloaliphatic diamine 13
Figure 2.8 Thermal degradation of epoxy cured with amines 15
Figure 2.9 Polymer combustion process 16
Figure 2.10 Stages of a fire. 17
Figure 2.11 Boric acid and boroxine network 21
Figure 2.12 Chemical structure of melamine 23
Figure 2.13 Toughening of polymer with rigid filler 26
Figure 2.14 Tensile testing machine and test specimen 27
Figure 2.15 Stress-strain curve 28
Figure 2.16 Schematic of Charpy impact test apparatus 29
Figure 2.17 Shore hardness scale 30
Figure 2.18 Shore durometer apparatus 30
Figure 2.19 Limiting oxygen index test apparatus 31
Figure 2.20 UL-94 vertical burning test apparatus 32
Figure 2.21 Photoemission process 34
Figure 2.22 Typical DSC curve of a thermoset polymer 36
Figure 2.23 TGA plot 37
Figure 2.24 Schematic of electrical resistivity measurement 38
Figure 3.1 Block diagram for the neat epoxy preparation. 48
Figure 3.2 Block diagram for the preparation of epoxy composites containing flame retardant additive. 50

Figure 3.3 Shimadzu Autograph AG-100 KNIS MS universal tensile testing instrument. 53
Figure 3.4 Ceast Resil Impactor 6967 instrument. 54
Figure 3.5 Dynisco Polymer LOI test instrument. 56
Figure 3.6 Two Probe measurement device, Keithley 2400 SourceMeter. 57
Figure 4.1 XRD pattern of as-received boron carbide 60
Figure 4.2 XRD pattern of boron carbide after heat treatment under different atmospheres: Air, Ar. 62
Figure 4.3 SEM Micrographs of boron carbide particles (a) 10,000x magnification, (b) 20,000x magnification. 63
Figure 4.4 XPS spectrum of boron carbide. 64
Figure 4.5 TGA plots of boron carbide under different atmospheres. 65
Figure 4.6 Time-dependent weight gain of boron carbide under nitrogen atmosphere. 66
Figure 4.7 FTIR spectrum of boron carbide. 67
Figure 4.8 Curing mechanism of epoxy [68]. 68
Figure 4.9 FTIR spectra of epoxy resin, curing agent and cured epoxy sample. 69
Figure 4.10 FTIR spectra of neat epoxy and epoxy/boron carbide composites. 70
Figure 4.11 XRD patterns of EP/B_4C composites. 71
Figure 4.12 SEM images of Neat EP (a) 1,000x magnification, (b) 5,000x magnification, (c) 10,000x magnification, and (d) 20,000x magnification. 72
Figure 4.13 SEM images of EP/0.5B_4C composites (a) 1,000x magnification, (b) 5,000x magnification, (c) 10,000x magnification, and (d) 20,000x magnification. 73
Figure 4.14 SEM images of tensile samples of EP/0.5B_4C composites (a) 1,000x magnification, (b) 5,000x magnification, (c) 10,000x magnification, and (d) 20,0000x magnification. 74
Figure 4.15 SEM images of EP/1B_4C composites (a) 1,000x magnification, (b) 5,000x magnification, (c) 10,000x magnification, and (d) 20,000x magnification. 75
Figure 4.16 SEM images of EP/3B_4C composites (a) 1,000x magnification, (b) 5,000x magnification, (c) 10,000x magnification, and (d) 20,000x magnification. 76
Figure 4.17 SEM images of tensile samples of EP/3B_4C composites (a) 1,000x magnification, (b) 5,000x magnification, (c) 10,000x magnification, and (d) 20,000x magnification. 77

Figure 4.18 SEM images of EP/5B_4C composites (a) 1,000x magnification, (b) 5,000x magnification, (c) 10,000x magnification, and (d) 20,000x magnification. 78
Figure 4.19 SEM images of EP/8B_4C composites (a) 1,000x magnification, (b) 5,000x magnification, (c) 10,000x magnification, and (d) 20,000x magnification. 79
Figure 4.20 SEM images of tensile samples of EP/8B_4C composites (a) 1,000x magnification, (b) 5,000x magnification, (c) 10,000x magnification, and (d) 20,000x magnification..... 80
Figure 4.21 SEM images of samples of (a) EP/1ZnB at 1,000x magnification, (b) EP/1ZnB at 5,000x magnification, (c) EP/1BA at 1,000x magnification, (d) EP/1BA at 5,000x magnification, (e) EP/1CaB at 1,000x magnification, and (f) EP/1CaB at 5,000x magnification..... 82
Figure 4.22 SEM images of samples of (a) EP/3B_4C/1ZnB at 1,000x magnification, (b) EP/3B_4C/1ZnB at 5,000x magnification, (c) EP/3B_4C/1BA at 1,000x magnification, (d) EP/3B_4C/1BA at 5,000x magnification, (e) EP/3B_4C/1CaB at 1,000x magnification, and (f) EP/3B_4C/1CaB at 5,000x magnification. 84
Figure 4.23 EDX spectra of (a) EP/1CaB, (b)EP/3B_4C/1ZnB, and (c) EP/3B_4C/1CaB composites. 85
Figure 4.24 SEM images of samples of (a) EP/10MP at 1,000x magnification, (b) EP/10MP at 5,000x magnification, (c) EP/10MP/3B_4C at 1,000x magnification, (d) EP/10MP/3B_4C at 5,000x magnification, (e) EP/10MP/3B_4C/1ZnB at 1,000x magnification, and (f) EP/10MP/3B_4C/1ZnB at 5,000x magnification. 86
Figure 4.25 Tensile strengths of neat epoxy and epoxy/boron carbide composites. 88
Figure 4.26 Elastic moduli of neat epoxy and epoxy/boron carbide composites..... 89
Figure 4.27 Elongation at break of neat epoxy and epoxy/boron carbide composites. 90
Figure 4.28 Impact strengths of neat epoxy and epoxy/boron carbide composites. 91
Figure 4.29 Tensile strengths of epoxy/boron containing compound composites and epoxy/melamine phosphate composites. 94
Figure 4.30 Elastic moduli of epoxy/boron containing compound composites and epoxy/melamine phosphate composites. 95
Figure 4.31 Elongation at break of epoxy/boron containing compound composites and epoxy/melamine phosphate composites. 96

Figure 4.32 Impact strengths of epoxy/boron containing compound composites and epoxy/melamine phosphate composites. 97
Figure 4.33 Photographs of the burned samples after LOI test a) Neat EP, ... 99
Figure 4.34 Photographs of the burned samples after LOI test a) Neat Epoxy,..... 101
Figure 4.35 Photographs of the burned samples after LOI test a) Neat Epoxy..... 102
Figure 4.36 Photographs of the burned samples after LOI test a) Neat Epoxy..... 104
Figure 4.37 Change of T_g with respect to boron carbide addition. 105
Figure 4.38 TGA plots of neat epoxy and epoxy/boron carbide composites under nitrogen atmosphere. 105
Figure 4.39 T_g values of epoxy-boron containing compound composites and epoxy/melamine phosphate composites. 107
Figure 4.40 TGA plots of epoxy/boron containing compound composites and epoxy/melamine phosphate composites under nitrogen atmosphere. 108
Figure 4.41 log(resistivity) values for neat epoxy, EP/B_4C composites and B_4C.. 110
Figure 4.42 log(resistivity) values for epoxy/boron containing compound composites and epoxy/melamine phosphate composites. 111
Figure B.1 DSC curve of cured and uncured epoxy sample. 135
Figure D.1 DSC Thermogram of Neat EP. 139
Figure D.2 DSC Thermogram of EP/0.5B_4C. 140
Figure D.3 DSC Thermogram of EP/1B_4C. 140
Figure D.4 DSC Thermogram of EP/3B_4C. 141
Figure D.5 DSC Thermogram of EP/5B_4C. 141
Figure D.6 DSC Thermogram of EP/8B_4C. 142
Figure D.7 DSC Thermogram of EP/1ZnB. 142
Figure D.8 DSC Thermogram of EP/1BA. 143
Figure D.9 DSC Thermogram of EP/1CaB. 143
Figure D.10 DSC Thermogram of EP/3B_4C/1ZnB. 144
Figure D.11 DSC Thermogram of EP/3B_4C/1BA. 144
Figure D.12 DSC Thermogram of EP/3B_4C/1CaB. 145
Figure D.13 DSC Thermogram of EP/10MP. 145
Figure D.14 DSC Thermogram of EP/10MP/3B_4C. 146
Figure D.15 DSC Thermogram of EP/10MP/3B_4C/1ZnB. 146
Figure D.16 Dr-TGA Thermogram of Neat EP. 147

Figure D.17 Dr-TGA Thermogram of EP/0.5B_4C. 147
Figure D.18 Dr-TGA Thermogram of EP/1B_4C. 148
Figure D.19 Dr-TGA Thermogram of EP/3B_4C. 148
Figure D.20 Dr-TGA Thermogram of EP/5B_4C. 149
Figure D.21 Dr-TGA Thermogram of EP/8B_4C. 149
Figure D.22 Dr-TGA Thermogram of EP/1ZnB..... 150
Figure D.23 Dr-TGA Thermogram of EP/1BA. 150
Figure D.24 Dr-TGA Thermogram of EP/1CaB..... 151
Figure D.25 Dr-TGA Thermogram of EP/3B_4C/1ZnB. 151
Figure D.26 Dr-TGA Thermogram of EP/3B_4C/1BA. 152
Figure D.27 Dr-TGA Thermogram of EP/3B_4C/1CaB. 152
Figure D.28 Dr-TGA Thermogram of EP/10MP. 153
Figure D.29 Dr-TGA Thermogram of EP/10MP/3B_4C. 153
Figure D.30 Dr-TGA Thermogram of EP/10MP/3B_4C/1ZnB. 154
Figure E.1 Pressed boron carbide……155

NOMENCLATURE

E	Elastic Modulus, MPa
F	Maximum Force, N
L_o	Initial Length, mm
L_f	Final Length, mm
S	Cross Sectional Area, mm^2
S_o	Initial Cross Sectional Area, mm^2

Greek Letters

σ	Tensile Strength, MPa
ε	Strain

Abbreviations

B_4C	Boron Carbide
BA	Boric Acid
BCC	Boron Containing Compounds
CaB	Calcium Borate
DGEBA	Diglycidyl Ether of Bisphenol A
DSC	Differential Scanning Calorimetry
EP	Epoxy

FTIR	Fourier Transform Infrared Spectroscopy
LOI	Limiting Oxygen Index, %
MP	Melamine Phosphate
SEM	Scanning Electron Microscopy
TGA	Thermal Gravimetric Analysis
XPS	X-Ray Photoelectron Spectroscopy
XRD	X-Ray Diffraction Spectroscopy
ZnB	Zinc Borate

CHAPTER 1

INTRODUCTION

Polymer materials are widely used in a wide range of applications in our daily lives due to their fundamental properties such as ductility and low weight. It is also easy to produce polymers. Despite their advantages, they also have some disadvantages which limit their usage areas. Generally polymers have lower mechanical properties when compared with metals and ceramics. However, the addition of organic or inorganic fillers can improve their mechanical properties [1]. Another disadvantage of polymers is their flammability. Also, combustion of the polymers results in the production of the toxic gases and smoke. The fire retardancy properties of polymers can be improved with addition of fillers which are called fire retardants [2].

Epoxy polymers are widely used as thermosetting polymers with their exceptional mechanical properties, thermal stability, resistance to solvents, chemical and moisture resistance, excellent adherence properties [3]. Therefore, they are used as coatings, adhesives, insulating materials, laminates in mainly aerospace, electronics and transportation industries [4]. However, high flammability, brittleness and low toughness are the main drawbacks of epoxy polymer [5].

Flame retardancy is an important phenomenon. Fire affects the buildings, and goods so there are huge economic and social consequences of fire. In a fire, deaths are caused mostly not by the flame but the inhalation of smoke and toxic gases, which are evolved from polymer combustion [6].

Flame retardancy has physical and chemical mechanisms. In a physical approach, it can work by reducing ignition or if the ignition has already started, burning of the material occurs with a lower efficiency. The flame retardant additive can improve the flame retardancy properties of a polymer in several ways. It can act as a barrier between polymer and the fire by generating inert gases. This barrier isolates the surface from oxygen. It also dilutes fuel while inhibiting the formation of combustible gases. On the other hand, flame retardant additive decreases the heat evolved [6, 7]. In a chemical approach, the flame retardant can join the chains of the polymers thus the flame retardancy properties can be enhanced [8].

Two or more flame retardants can be used together to improve the flame retardancy properties of a polymer. If there is a combined effect of these flame retardants which is more effective than that of the single usage of a flame retardant, then it can be said that there is a synergism between those flame retardant additives. These co-additives are usually named as synergists [6].

Among a lot of different kinds, halogen-containing flame retardants with antimony oxide are the mostly used ones in especially epoxy matrices. However, the usage of halogenated flame retardants causes corrosive products and toxic gases while the combustion occurs. For this reason, new studies are being developed using different fire retardants containing boron, phosphorus, sulfur, nitrogen, and silicon which are named as halogen-free flame retardants [5].

Mechanical properties are significant for epoxy composites. Their fracture behaviour and brittleness values are lower than that of the metals. Therefore development of mechanical properties by addition of fillers are in great interest. The effects of the fillers on the mechanical properties of the composite depend upon type, shape, and size of the fillers and interfacial bonding [9]. Tensile strength is related with the load transfer from the matrix to the filler. For this reason, the bonding between the filler and the matrix should be strong enough to improve the tensile strength of the epoxy composites. If there are debonding and voids between the filler and the matrix, tensile strength decreases. On the other hand, addition of inorganic fillers should increase the fracture toughness of the epoxy composites [10].

Toughness, which can be determined by the impact test, is the capability of material to absorb energy until the fracture of the sample. It is inversely proportional to brittleness [11]. There have been studies in the literature which are related to increasing the fracture toughness of epoxy with different methods. One of the methods for toughening is the addition of a hard filler, and it leads to matrix-filler debonding which results as voids in the epoxy matrix [12].

Boron carbide (B_4C) is a ceramic material which is the third hardest material next to diamond and cubic boron nitride [13]. It is extremely hard and has thermal stability, high melting point, high capacity of neutron absorption and abrasion resistance. It is also a semiconductor. Boron carbide is used as a filler in polymeric matrices, abrasive coatings, refractory applications, electronic and nuclear applications [14].

Composites are described as materials combining two or more constituents. They have better desired properties than the properties that constituents have alone. In a composite, the constituents are separate phases and can be dispersed randomly or in an oriented way. The continuous phase is known as the matrix of the composite and the dispersed phase is named as reinforcement or filler. The matrix, fillers and the interaction between these phases are important parameters in determining the properties of the composites [15].

In this thesis; the main objective is to improve the flame retardancy and mechanical properties of epoxy polymer with the addition of boron carbide and other boron containing compounds (BCC). Since boron carbide is a hard and tough material, it is expected from boron carbide to improve mechanical properties of the epoxy composites. Hence, it is intended to extend the use of boron carbide as an additive in epoxy systems and to specifically analyze its effects in the presence or absence of other additives on fire retardant, mechanical properties, electrical, thermal properties and morphologies of the epoxy composites.

This thesis is comprised of three main parts. The first part of the study includes the characterization of as-received boron carbide particles. These as-received particles were analyzed first in terms of their surface, thermal properties and morphologies to have sufficient information about their properties which have not been given by the manufacturers. Boron carbide particles were sintered in appropriate conditions and

then the produced sintered boron carbide was used to characterize boron carbide electrically.

In the second part of the study, neat epoxy samples were produced from bisphenol A co-epichlorohydrin based epoxy resin and cycloaliphatic polyamine based hardener with a ratio of 100:54. Boron carbide content was varied as 0.5, 1, 3, 5 and 8 wt.% in the epoxy resin and the epoxy/B_4C composites were produced with the same procedure used in neat epoxy preparation. The fire retardancy properties of the neat epoxy samples and the composites were studied. The produced neat epoxy samples and the composites were characterized in terms of flame retardation, mechanical, thermal, morphological and electrical tests.

In the third part, the epoxy composites were prepared with the addition of different boron containing compounds such as calcium borate, zinc borate and boric acid separately, and each of them was combined with the selected composition of boron carbide in epoxy matrix. It is aimed to see if there is a synergistic effect between boron carbide and these boron containing compounds. Also the composites were analyzed in terms of their flame retardation, mechanical, thermal properties and morphologies.

To our knowledge, the literature does not have much studies about the preparation and characterization of epoxy and boron carbide composites. Moreover, there is not any comprehensive study which includes mechanical, thermal, electrical, flame retardation properties and morphologies of epoxy/B_4C composites. Also the addition of boron carbide together with other boron containing compounds to epoxy polymer have not been studied in the literature in terms of their flame retardancy characterization.

CHAPTER 2

BACKGROUND

2.1 Boron

The pure elemental boron was first discovered in 1808 by English chemist H. Davy and French chemists Baron L.J. Thenard and J.L. Gay-Lussac.

Boron is an element which is represented with B in the periodic table. It is a semiconductor material. The physical properties of elemental boron are given in Table 2.1.

Table 2.1 The properties of boron [16].

Property	**Value**
Molecular formula	B
Density, g/cm^3 at 300 K	2.34
Melting point, K	2573
Boiling point, K	4275
Molar volume, cm^3/mole	4.68

In boron containing compounds, boron acts as a nonmetal compound. On the other hand boron is an electrical conductor like carbon. Crystallized boron has optical and morphological characteristics of diamond. In addition the rigidity of the crystallized boron is similar to that of diamond.

In nature, boron can be observed in different allotropic forms. One of them is amorphous and the other types are crystalline polymorphic forms. Alpha and beta rhombohedral forms of boron are the most commonly studied crystalline polymorphic forms. The alpha type may decompose at 1200 °C and form the beta types at 1500 °C. In addition to this, above their melting points, all types of pure boron can undergo a transformation to become beta rhombohedral [16].

2.1.1 Boron in the World

Thousand years ago Tibet used boron salts for the first time. After this, Babylonians melt artefacts with boron salts. Then, boron salts have been used by Egyptians for mummifying and by Ancient Greeks and Romans for cleaning. Boron salts were produced as drug by Arabs.

After Marco Polo brought boron to Europe in 13th century, boric acid was produced in Italy in 1830. In 1852, industrial borax mining began in Chile. After the boron reserves were found and processed in USA, the country has become the biggest boron supplier in the world [17].

2.1.2 Boron in Turkey

In nature, boron cannot be found in elemental form. Borax is naturally present as a mineral. The boron containing minerals are based on boron oxide, sodium and calcium. The most common natural boron minerals are tincal ($Na_2B_4O_7.10H_2O$), ulexite ($NaCaB_5O_9.8H_2O$), colemanite ($Ca_2B_6O_{11}.5H_2O$), and kernite ($Na_2B_4O_7.4H_2O$) among the 230 different types.

Turkey has an important geological formation and high potential of different types of minerals. The most important and commercially available boron minerals are tincal, ulexite and colemanite. Turkey takes the first place among all the countries with the 72.5% of boron reserves of the world.

The boron containing compounds can be produced by refining boron containing minerals. The most preferred boron containing compounds are boric acid (H_3BO_3), boron oxide (B_2O_3), sodium perborate ($Na_2B_4O_7.5H_2O$), borax pentahydrate

($Na_2B_4O_7.10H_2O$), borax decahydrate ($Na_2B_4O_7.5H_2O$), and anhydrous borax ($Na_2B_4O_7$).

Turkey is the largest producer and trader of boron with a share of 47.2% followed by USA with a share of 27.6%.

Boron containing compounds have been used in a large variety of application areas such as detergents, nuclear applications, electronics, fuels, nanotechnology, vehicles, polymeric composites, energy, automotive sector. But the real demand for boron containing compounds is in the area of agriculture, flame retardants, glass, insulation materials and detergents [16, 18].

2.1.3 Boron Carbide (B_4C)

Boron carbide is a boron containing compound which was first discovered in 1858. In 1894, B_6C was prepared by H. Moissan. The stoichiometric ratio of B_4C was first provided in 1934 [19].

Nowadays boron carbide can be produced in a homogeneity range from $B_{4.3}C$ to $B_{10.4}C$ [20]. The properties of boron carbide are given in Table 2.2.

Table 2.2 The properties of stoichiometric B_4C [19].

Property	**Value**
Molecular formula	B_4C
Density, g/cm^3	2.52
Melting point, °C	2490
Knoop hardness, kg/mm^2	3770±80

Boron carbide is one of the important materials of the nonmetallic material group with superior properties. After diamond and cubic boron nitride it is the hardest material. Boron carbide is used in a wide variety of applications such as abrasives, coatings, nuclear and military applications due to its physical and chemical properties. These properties include high hardness, high modulus, high melting point and low density. It is resistant to abrasion. Boron carbide is chemically inert. It is thermally stable and it can be used as high temperature semiconductor material in

microelectronic industries. Also having neutron capture ability makes boron carbide an appropriate material to be used in nuclear applications. Considering all the features that boron carbide have, it can be used for applications requiring high technologies [14, 21].

2.1.3.1 Structure of boron carbide

The structure of boron carbide has been obtained for quite a while. Boron carbide has a rhombohedral unit cell which has 12-atom icosahedral units located at eight corners of the structure [19]. The structure of boron carbide is shown in Figure 2.1.

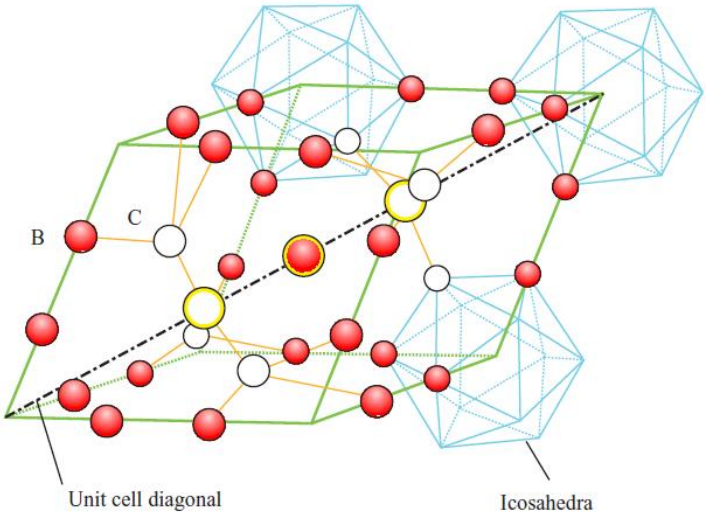

Figure 2.1 The rhombohedral structure of boron carbide [20].

For the B_4C stoichiometry, icosahedra corresponds to $B_{11}C$ and it has C-B-C bonds. If the boron content increases in the compound, then the boron atoms are kept in icosahedra while carbon atoms switch with boron atoms. Then the $B_{11}C$ icosahedra is replaced with B_{12} icosahedra and C-B-B bonds are formed [22]. While the density of the unit cell increases, the volume of the unit cell decreases linearly with an increase in the carbon content. Figure 2.2 shows the B-C diagram.

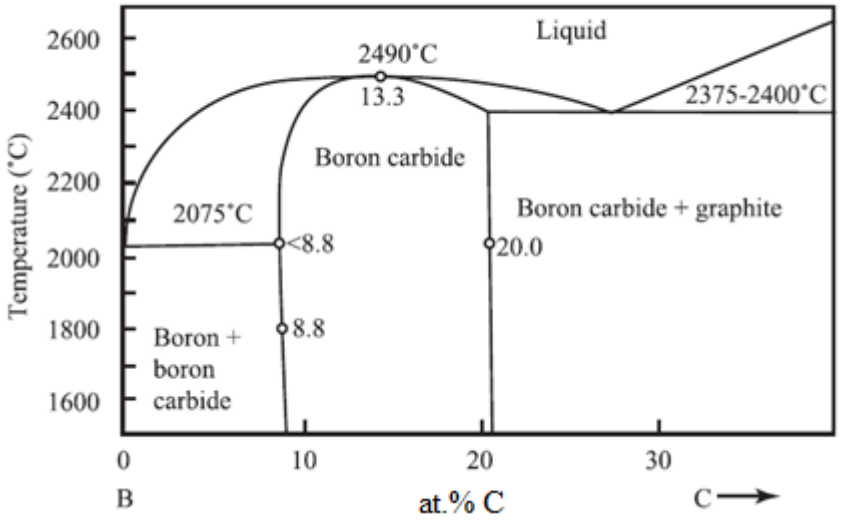

Figure 2.2 B-C Phase Diagram [20].

The rigid cage structure which comes from the close bonding of atoms in rhombohedral unit cell gives boron carbide the hardness and refractory properties. Because of this closeness of the bonds, its melting point is above 2300°C. The melting point of boron carbide depends on the content of the boron carbide but for the stoichiometric ratio of B_4C it is known as 2490 °C.

The variations of boron carbide stoichiometry come from the varying boron and carbon contents. It is accepted that there is a wide range of carbon solubility from 8 to 20 at. %. In this range of carbon content there is a stable phase of boron carbide and boron. Above 20 at.% of carbon content, there exist a stable phase of boron carbide and graphite. It has relatively lower melting point and it is followed by a eutectic point of 30 at.% carbon content [14].

2.1.3.2 Production of boron carbide

There have been a plenty of research to produce boron carbide powder with different processing techniques: hot pressing, pressureless sintering, chemical vapor deposition and carbothermic reduction of boron oxide (B_2O_3) or boric acid (H_3BO_3). Among the various production methods, boron carbide which was used in this study was produced by the supplier through the reduction of boric acid with carbon.

2.1.3.2.1 Carbothermal synthesis of boron carbide

Elemental boron and carbon can be used for the direct production of boron carbide. In the case of synthesis of boron carbide from boron and carbon, the process becomes expensive. By considering the cost of the process, carbothermic synthesis of boron carbide from B_2O_3 or H_3BO_3 is used frequently in industry. These boron containing compounds can be reduced with a carbon source which is usually coke in an electric heating furnace at temperatures higher than 2000°C. A grinding process is applied to boron carbide which is produced [23, 24].

The following reaction (Equation 2.1) shows the carbothermic reduction of boric acid:

$$4H_3BO_3 + 7C \longrightarrow B_4C + 6CO + 6H_2O \qquad (2.1)$$

2.2 Epoxy

Epoxy resin is known as the low molecular weight polymer which consists of epoxide groups as shown in Figure 2.3. It was first discovered in 1909 by D. Prileschajew [25].

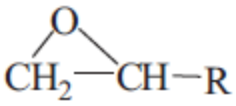

Figure 2.3 Epoxide group [25].

Epoxy resins can be cured with a various types of curing agents such as amine, alkali and catalytic curing agents and anhydrides. The properties of epoxy change with type of both the epoxy resin and curing agent. Since they have many advantages such as superior mechanical properties, chemical and heat resistance, outstanding adhesion to different surfaces they can be used in a wide range of engineering applications such as industrial tooling, aerospace industry, biomedical systems, high performance adhesives, fiber-reinforced composites, encapsulating technology, paints and coatings. Figure 2.4 shows the application areas of epoxy resins [26].

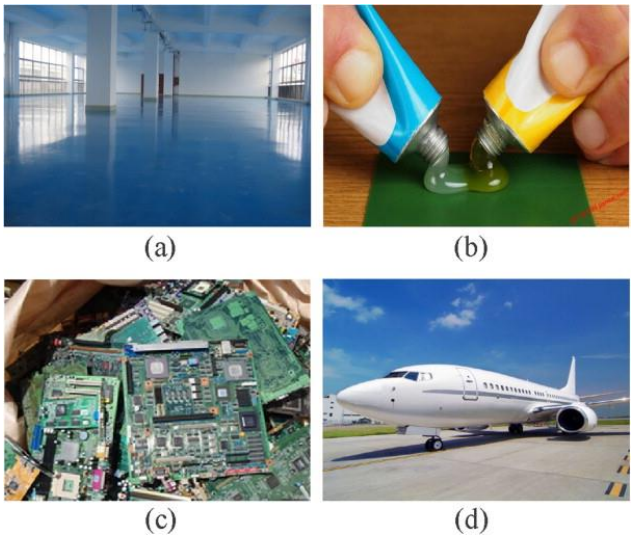

Figure 2.4 Photos of epoxy polymers used in (a) paints and coatings, (b) adhesives, (c) electronic materials and (d) airplanes [26].

The lack of fire retardation which is the main disadvantage of epoxy resin limits the usage areas of epoxy especially in the application areas where the flame retardancy property is important such as electronics, coatings, etc. Another drawback of epoxy is its brittleness. Therefore, improving the impact resistance of epoxy is an important issue hence the epoxy composites can be used in high performance application areas [27].

The types of epoxy resins can be considered in the order of importance as glycidylation of bisphenol A, bisphenol F, phenol novolacs, diaminodiphenyl methane, p-aminophenol, aliphatic diols, aliphatic and cycloaliphatic carboxylic acids. Among them the most commonly used epoxy resin is diglycidyl ether of bisphenol A (DGEBA) which is produced from the reaction of bisphenol A (BPA) and epichlorohydrin in the presence of sodium hydroxide. The structure of DGEBA is shown in Figure 2.5.

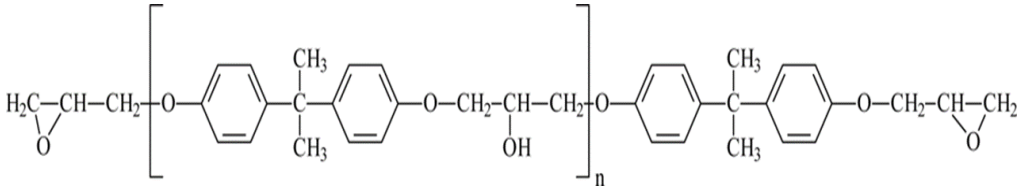

Figure 2.5 The structure of DGEBA [26].

Bisphenol A is a colorless solid which is produced from the reaction of phenol and acetone in the presence of acid. Epichlorohydrin is a liquid which does not have color. It has an odor of chlorinated hydrocarbon solvents. Epichlorohydrin is produced by chlorination of propylene. The product of chlorination reaction is reacted with hypochlorous acid. By the stripping reaction, epichlorohydrin can be obtained in the presence of caustic soda at high temperature [28]. Figure 2.6 shows the reaction of bisphenol A and epichlorohydrin to yield DGEBA.

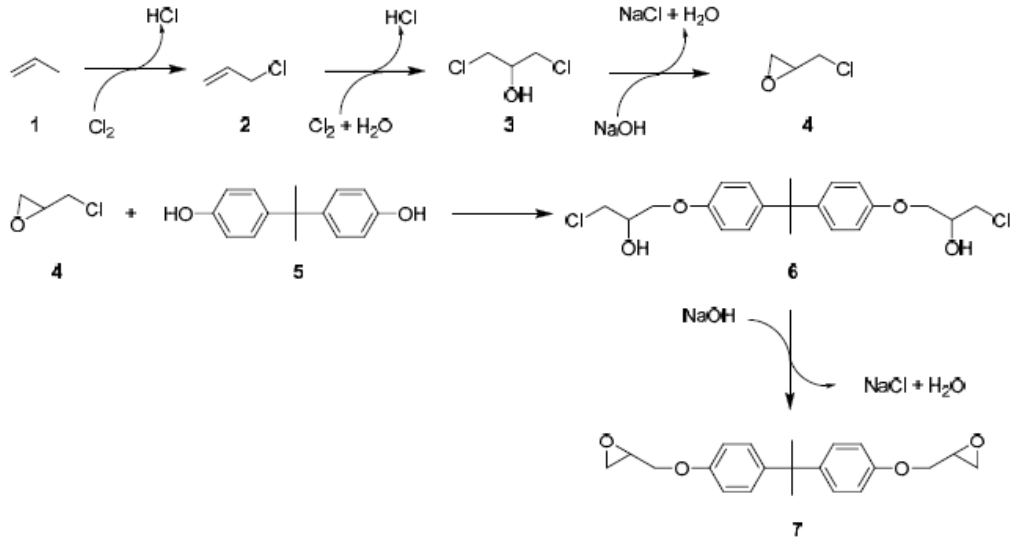

Figure 2.6 Reactions in the production of DGEBA [29].

In general epoxy resins can be cured at room temperature but in order to improve and promote the curing, heat can be applied.

Epoxide groups in thermoset polymers create a reactive site for crosslinking in the reaction with the curing agent. The curing agents generally have reactive hydrogen which belong to nitrogen, sulfur or oxygen [29].

Curing agents can be classified by their chemical compositions as amine, alkali and catalytic curing agents and anhydrides. The most preferred ones are the amine curing agents. They create three dimensional network with epoxy resins. Figure 2.7 shows the crosslinking reaction between DGEBA and cycloaliphatic diamine based curing agent [26].

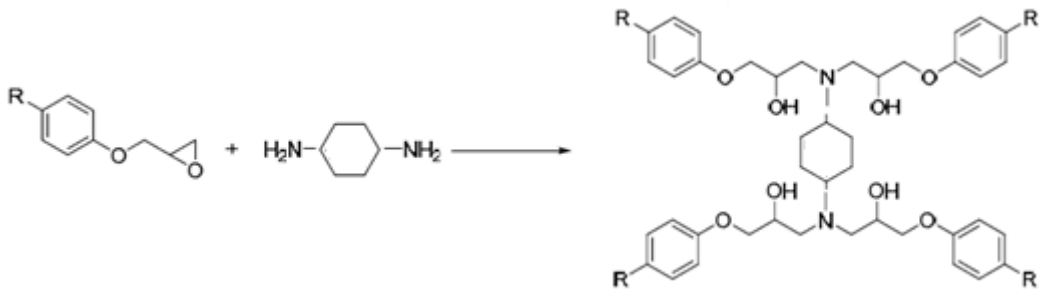

Figure 2.7 Curing reaction of DGEBA and cycloaliphatic diamine [29].

2.3 Epoxy Composites

Composites are the materials which are made with the combination of two or more constituents to have better physical or chemical properties than the individual constituents. They can naturally occur or they can be produced intentionally. In the finished structure, the constituents remain distinct and separate.

Composites have basic components called as matrix and reinforcement. Reinforcement materials are significant because they can enhance the selected property or properties of a matrix material.

Epoxy resin can be used as matrix in polymer composites which are benefited in a wide range of different engineering applications such as adhesives, coatings, etc. Epoxy composites can be classified as fiber reinforced composites, particulate reinforced composites and nanocomposites [27].

Epoxy-based composites have fabulous properties such as high performance to cost ratio and easy processing in many applications. Glass transition temperature, crosslinking density, toughness and dimensional stability are the parameters which are related to each other and provide epoxy to be used in aforementioned applications.

When the glass transition temperature decreases, the crosslinking density which stiffen the molecular network of epoxy composites decreases and consequently toughness increases [30]. Dimensional stability also decreases with a decrease in glass transition temperature. These requirements should be considered while preparing the epoxy composites. The important part is to enhance these properties

while preserving the other properties which the material has already have [31]. For example increasing the fire retardancy of epoxy composites with addition of a reinforcement can cause a decrease in mechanical or thermal properties. There has to be an optimization between the properties of epoxy composites. Another example is the addition of reinforcement which plays a role as toughener can decrease the glass transition temperature therefore decrease the crosslinking density while increasing the fracture toughness and impact strength in some cases [32].

2.4 Flammability and Thermal Decomposition of Epoxy

Epoxy has many advantageous properties thus it is utilized in different application areas. However, the flammability is the main disadvantage of epoxies like the other polymers. Especially in the application areas where the high flame retardancy is needed, the flammability of epoxy restricts its usage. Therefore, many studies have been focused on improving the fire retardancy properties of epoxy [5, 33].

The thermal properties of epoxy polymer depend on the structure of the epoxy, type and amount of the curing agent and crosslinking density [34].

Cured epoxy decomposes and releases toxic gases, heat, soot and smoke into the atmosphere when it is introduced with high temperatures like 300-400°C. During the thermal decomposition of the polymer, three reactions occur in the condensed phase of the flame. The generation of radical species is the main reaction caused by the end-chain or random-chain scissions. At the same time, another reaction which is called as chain stripping occurs with the rejection of different kinds of atoms and functional groups which do not belong to the polymer backbone. Finally, crosslinking reactions occur between different radicals which are produced with chain scission to form a thermally stable char on the surface of the composite [35].

While the epoxy is being burned, the secondary alcohol in the epoxy structure dehydrates and forms vinylene ethers. Chain scission takes place in allylic position since the formed allylic ether C-O bond is less stable than original C-O. Also secondary amine group goes into chain scission. Amines generally evaporate or remain in the residue and experience to become char. While the thermal decomposition goes further, ends of the aliphatic chains create flammable volatiles

such as acetone, alcohol and some kinds of hydrocarbons or contribute charring [34]. The thermal degradation reactions of epoxy which is cured by amine curing agent is shown in Figure 2.8.

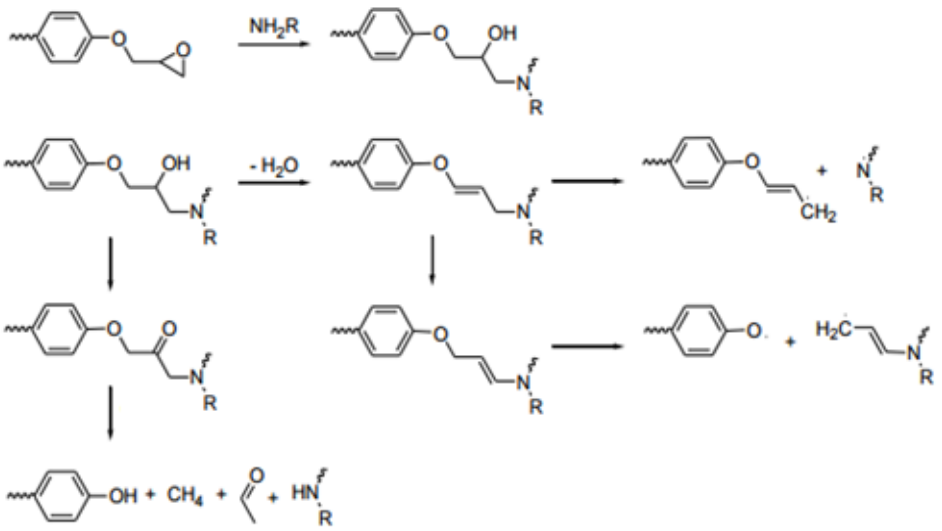

Figure 2.8 Thermal degradation of epoxy cured with amines [35].

2.5 Polymer Combustion

Polymers are combustible materials since they contain high amount of carbon and hydrogen. For a combustion process there needs to be a combustible and a combustive material with a source of heat. In an increase of the ambient temperature acts the bonds in the polymeric material and they start to mobilize [2].

Physical and chemical changes occur during application of heat to the polymer material. If the heat is high enough to ignite the mixture of oxygen in the air, solid polymer surface starts to burn. In further steps of fire, with the effect of temperature of the flames, flammable volatiles arise from the polymer due to the decomposition of the polymer. Also these flammable volatiles burn on the polymer surface and fire continues with the generation of the combustion products [6, 36]. Figure 2.9 shows a simple combustion process of a polymer.

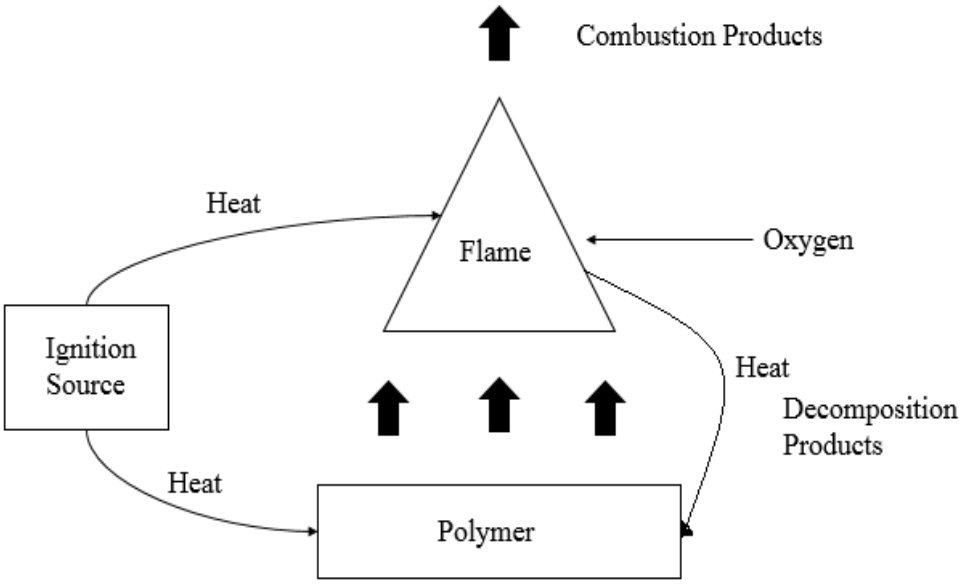

Figure 2.9 Polymer combustion process [6].

The gasification of polymers is a complicated process. The solid polymer disassembles to its small parts which are totally different chemical compounds. So every chemical compound has its own equilibrium vapor pressure. While the small parts that have higher vapor pressure vaporizes the heavy parts stay in the condensed phase. Also in the condensed phase, these heavier parts decompose and create lighter compounds that vaporize. The residue can be carbonaceous char, inorganic residue or a mixture of both of them. If the residue is carbonaceous char then it can act as barrier between the flame and the polymer so prevents the further decomposition of polymer. If the residue is an inorganic compound, then it may form a glassy layer on the surface of the polymer and protect the polymer from penetration of the flammable volatiles [36].

2.6 Flame Retardancy

Flame is a gas phase combustion process which can be classified in two categories. One of them is a premixed flame which is a combination of flammable volatiles and oxygen. The flame in the Bunsen burner can be given as an example to this category. The second one is the diffusion flame. The oxygen that is needed for the combustion diffuses from the environment. The best example for this flame is the one from a candle. In a burning process of a candle, wax is melted by the heat and the fuel

molecules in the wax are vaporized. They decompose at temperatures of 600 and 800 °C. The vaporized products react with oxygen in the air and sustain a consistent flame [6].

The process of a fire can be classified into three stages. The first stage of a fire is the initiating stage which includes the incipient and growth of the fire. Then fully developed fire stage begins and it is followed by decay stage. The plot given in Figure 2.10 shows the stages in a burning process. Polymers always burn at fully developed stage. So the precautions for the fire retardancy have to be taken before the fire starts [37].

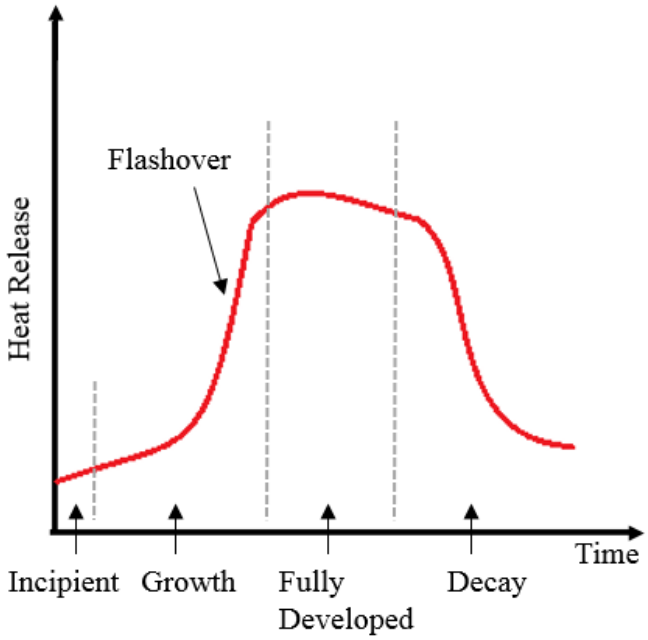

Figure 2.10 Stages of a fire**.**

Flame retardancy is to make a material less likely to ignite or if it is ignited then to make it burn less efficiently. Retarding a flame can be achieved with several possible ways. These are: decreasing the necessary heat, the amount of flammable volatiles, the oxygen concentration in the environment of the material being burned and the ignition temperature of the material. The manipulated decomposition processes and formation of char yield, which is a barrier between the polymer surface and the flame, are also the possible ways of retarding fire [2, 6, 37].

2.6.1 Flame Retardant Mechanism

Flame retardant additives restrain burning of a material. They can serve their duty of fire retardancy with chemical or physical processes which depend on the type of the flame retardant additive, in gas, liquid or solid state. They interrupt a specific process of burning such as heating, decomposition, etc.

2.6.1.1 Physical Action

Flame retardancy of a polymer can be provided with a variant physical actions. One of them is cooling the surface. Flame retardant additives decompose with high temperature and in addition to exothermic reactions, some endothermic reactions take place. These endothermic reactions use the heat therefore the environment cools down eventually and the heat that is required for the continuous burning process is also decreased. For example, aluminum hydroxide is a cooling type flame retardant.

Another physical action of flame retardant additives is formation of a protective layer on the surface of the polymer. While the burning continues, the flame retardant additives can form a layer which can be a solid, liquid or a gaseous phase, on the surface of the polymer. This layer formation leads to cooling of the condensed phase and followed by the reduction of pyrolysis gases. The polymer is also isolated from the oxygen which is required for combustion. Boron containing compounds and phosphorus can be given as examples for the flame retardant additives which forms protective layer on the polymers to be protected.

Besides these actions, dilution of the combustible gases is another physical action of flame retardants. Flame retardants dilute the fuel in both gaseous and solid phases by releasing inert gases and decrease the ignition limit by forming a less combustible gas mixture. For example, aluminum hydroxide is used for its dilution effect [2, 38].

2.6.1.2 Chemical Action

The important chemical reactions to prevent further combustion and retard fire take place in the solid and gas phases.

When the reactions in the gas phase have been taken into consideration, the free radical mechanism of the combustion process is deactivated with association of flame retardant additives. The halogenated flame retardants release free radicals such as Br•

and Cl• to the gas phase to react with highly reactive radicals like H• and OH• to yield less reactive or even inert molecules. In this way of chemical modifications, the combustion processes are inhibited, the burning environment becomes cooler and the amount of combustible volatiles are decreased.

In the solid phase, the fire retardancy is handled by formation of a protective carbon or glassy layer on the polymer surface by the degradation of polymer chains. This layer interfere between gas phase and solid phase. Flame retardants accelerate the rupture of the polymer chains. Thus polymer bonds change location and get further away from the fire. Phosphorus compounds are the examples of fire retardants act chemically to form protective layer on the surface of the materials into which they are added [2, 37].

2.6.2 Flame Retardants

A flame retardant material can be an additive, reactive or combination of both when they are incorporated into the polymer system.

Reactive flame retardants are the materials which can react chemically with the polymer in the existence of a starting material. The reaction between the polymer and the flame retardant makes them perfectly combined, and this increases the fire retardancy. They are generally used in thermoset polymers.

Additive type flame retardants are added to the polymer system before, during or after polymerization. In this type of flame retardants there are no reactions between the polymer and the additive. They are generally used in thermoplastics but also they have a usage area in thermoset polymers.

Combination of additive and reactive flame retardants can be synergistic or antagonistic with each other. They can have positive or negative effect of being together rather than used alone [37].

Types of flame retardants which are commonly used in researches, industry and also in this thesis study will be explained in detail.

2.6.2.1 Boron Containing Flame Retardants

Boron containing compounds are used as flame retardants, afterglow suppressants, smoke suppressants and anti-cracking agent in halogen free and halogen based polymer systems. In latest studies, borates such as zinc borate, melamine borate, boron phosphate and borosiloxane have been started to be used as flame retardants in addition to commonly used boron containing flame retardants such as boric acid and sodium borate [37, 38].

Flame retardant mechanism of boron-based flame retardants occurs in the condensed phase and gas phase of the polymer. They supply crosslinking between OH• groups and the crosslinking leads to char formation. On the other hand, they form a glassy layer when they are exposed to high temperatures. That glassy layer stabilizes the char, which is the residue of burning, also prevents the further decomposition of material. In addition, glassy layer prevents dripping of the burning material and it also acts as a barrier between the surface and flame so that it protects the surface, isolates the oxygen that sustains the burning process. Some borates also release water while burning and cool the burning zone [39].

Boron-based flame retardants can be said as environmentally friendly, cheaper and less toxic alternatives to traditional flame retardant additives. Also they can be added in epoxy systems as flame retardant additive alone or with some other commercial flame retardants because of their synergistic effects [40, 41].

In the following sections commercially used boron containing flame retardants, especially the ones that were used in this thesis are described.

2.6.2.1.1 Zinc Borate

Zinc borate is the most used boron based flame retardant with the molecular formula of $2ZnO \cdot 3B_2O_3 \cdot 3.5H_2O$. Frequent use of zinc borate as a flame retardant in polymers comes from its ability to keep its hydration water up to 290°C. After its endothermic decomposition reaction in the temperature range of 290-450°C, it releases its dehydration water and forms boron oxide and boric acid on the surface. At temperatures above 500 °C the boron oxide layer flows and creates a glassy layer. On

the other hand boric acid dehydrates and forms char layer which isolates the oxygen inlet [2, 42].

In addition, the combustion of zinc borate does not release toxic gases into the environment.

Zinc borate is usually used as halogen free flame retardant additive in polymer systems. Zinc borate serves as smoke and afterglow suppressants in a matter of fire. Also it is used as char promoter, corrosion inhibitor, wear resistance agent and lubricant in the polymers. It can be used with other flame retardants since it is a synergistic flame retardant [42].

2.6.2.1.2 Boric Acid

Boric acid is a flame retardant additive which is commonly used in many different flame retardancy applications. Not only boric acid but also the boroxine network, which is formed during heating process in a possible fire, leads to formation of protective char layer and inhibits the fuel to be carried for further burning [35]. This boroxine network is shown in Figure 2.11.

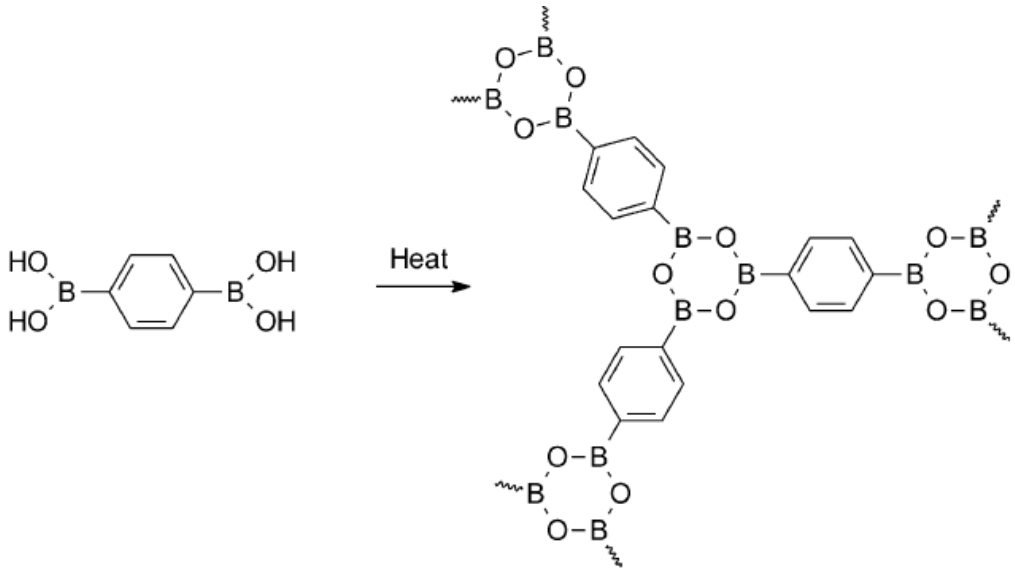

Figure 2.11 Boric acid and boroxine network [35].

The mechanism of flame retardancy of boric acid can be explained in three stages. The first stage is the endothermic decomposition of boric acid. The second step is the release of its crystal water in two stages and dilution in the gas phase. Final step is the formation of a high density char structure in the condensed phase [35].

After releasing its crystal water in two stages, the residue is the mainly boron oxide. Boron oxide softens at 350°C and flows at 500°C [2]. Boric acid decreases the thermal stability of epoxy since it has low dehydration temperature. Also it increases the time to ignition value in case of subjecting to flame [41].

2.6.2.1.3 Calcium Borate

Different types of calcium borates are produced by the reaction of boric acid and calcium hydroxide. Among all kinds of calcium borates, colemanite with the formula of $2CaO{\cdot}3B_2O_3{\cdot}5H_2O$ has the most usage areas as flame retardant in polymer systems than the other types of calcium borates [39]. The flame retardancy mechanism of calcium borate in epoxy resin can be explained as follows: calcium oxide, that calcium borate has already have, promotes the crosslinking of epoxy by absorbing water from phenols in the curing agent. In addition to this, calcium oxide and water form calcium hydroxide which takes part in improving the flame retardancy of polymer due to releasing of water from its structure [41].

2.6.2.1.4 Boron Carbide

Boron carbide is a carbon containing borate which can be used as a flame retardant additive. The addition of boron carbide into a polymer system results in a formation of a hard layer on the surface, developing mechanical strengths such as compression and peel strength throughout the fire. In this way, it inhibits the expansion which is a result of high temperatures, and postpones the weight loss of the formed layer at very high temperatures like 1000°C [39].

2.6.2.2 Nitrogen-Based Flame Retardants

Nitrogen-based flame retardants have a wide range of application areas. They are generally used with phosphorus containing compounds since they have synergistic effects together. However, nitrogen-based flame retardants are still effective alone as the flame retardants.

Thermal decomposition of a large portion of nitrogen-based flame retardants is endothermic and affects as a heat sink. The decomposition products are generally large amounts of inert gases such as ammonia and nitrogen to dilute the fuel of the fire and prevent the spread of flames by moving the heat away and intumescent. Nitrogen-based flame retardants are usually utilized with phosphorus compounds to create phosphoric acid followed by propagating the char formation. Ammonia, melamine, urea and guadine can be given as examples of nitrogen-based flame retardants [39].

2.6.2.3 Melamine-based Flame Retardants

Melamine, its salts and its product of condensation are mostly utilized as the flame retardant material.

It is a crystalline material having a melting temperature of 354°C. It dilutes the oxygen and the flammable volatiles since it sublimates at approximately 200 °C. Moreover melamine decomposes endothermically so it works as a heat sink when exposed to fire. As a result of decomposition, it also releases non-flammable gases such as CO_2, ammonia and water. It is soluble in hot water. Figure 2.12 shows the chemical structure of melamine [39].

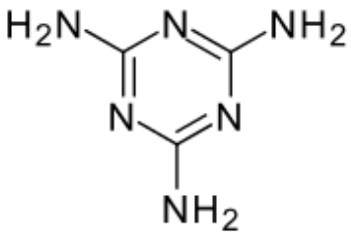

Figure 2.12 Chemical structure of melamine [43].

Melamine is mostly used with phosphorus compounds since they have synergism.

2.6.2.3.1 Melamine Phosphate

Melamine phosphate is a broadly utilized flame retardant additive which is also used as intumescent flame retardant additive. It is produced by the reaction of phosphoric acid and melamine [44].

Melamine phosphate is thermally decompose to melamine polyphosphate with discharging of phosphoric acid and melamine. The discharged phosphoric acid shows flame retardant effect just like the phosphorus-based flame retardants [2].

Melamine polyphosphate, which comes from the thermal decomposition of melamine phosphate, is generally utilized with other flame retardant additives like phosphates, metal hydroxides and metal phosphinates. Melamine polyphosphate has a small effect on glass transition temperature and has a good thermal stability. Thermal decompositions of melamine compounds are endothermic and as a result of decomposition, inert gases such as ammonia etc. are released to the environment. These inert gases dilute the fuel, and cause flame to be retarded. Also phosphoric acid is formed as a decomposition product and it boosts the char formation on the surface of the polymer [35].

2.6.2.4 Phosphorus-Based Flame Retardants

Phosphorus-based flame retardants are known as halogen-free flame retardants and used for different kinds of polymeric materials and various applications. Unlike some other additives they are effective both in condensed and gas phases. They are successful as a flame retardant additive especially in materials with high oxygen contents.

The flame retardancy mechanism of these additives can be explained as follows: phosphorus enhances the char formation by thermal decomposition of phosphorus into phosphoric acid in the condensed phase together with formation of a glassy layer and an intumescent. In the gas phase, the reactions of the chains and oxidation of hydrocarbons decelerate the flame and this is called as inhibition of flame [45]. The release of phosphorus-containing volatiles from the oxidation reactions dilute the fuel. Nevertheless, the oxygen concentration of phosphorus additive is important to contribute to reduction of the flame. On the other hand, another dilution process comes from the release of inert gases [35].

The efficiency of flame retardancy changes with both the chemical structure of phosphorus-based flame retardant and the interaction of this phosphorus-based flame retardant with its environment during the pyrolysis. In addition, the efficiency of flame retardancy mechanism depends on the type of the polymer. So different

phosphorus-based flame retardant additives can be used with each other to see their synergistic effect in different types of polymeric materials [45]. These phosphorus-based flame retardant additives can also be added to the polymer system during polymerization or after polymerization as an additive [40].

2.7 Improvement of Mechanical Properties

It is mentioned that there are lots of advantages of epoxies. However, there are also some disadvantages of epoxies such as brittleness and low toughness which are related to their mechanical properties.

Toughness is described as the amount of energy that a material can absorb until the fracture. Therefore it is a magnitude of sample's resistance to fracture. It is directly proportional to impact strength. Toughness of epoxy resins can be improved with different types of processes. The most frequently used method for improving toughness is the addition of toughener to the epoxy matrix. This toughener can be rubber, rigid and hard fillers, and thermoplastics [46].

Toughening mechanism of addition of inorganic fillers can be explained as debonding between the filler and the matrix, formation of shear bands and formation of stress concentration locations in the composite [47].

In the literature, the most common proposition is that the debonding begins before yielding. The debonding between the matrix and the filler creates stress softening points which comes from the formation of shear bands. Stress softening causes a decrease in stiffness of the composite, and shows a reduction in the slope of stress versus strain curve [47].

Figure 2.13 shows the toughening of polymer with an addition of rigid filler. As it is seen, the interfaces of the matrix and the filler expand as a result of stress application. The polymer chains yield this expansion. Therefore the absorbing energy capacity increases with the formation of shear bands. That means an increase in toughness [47].

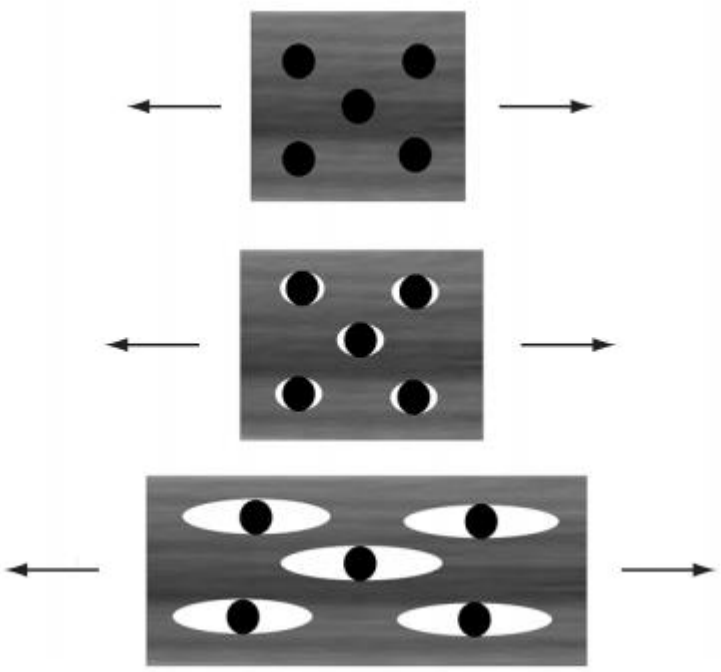

Figure 2.13 Toughening of polymer with rigid filler [47].

Boron carbide is a rigid material. Hence the addition of boron carbide is expected to increase the toughness of the polymer composite.

2.8 Characterization Techniques

A variety of techniques are used to characterize the desired properties of a polymer, composite or the filler. The characterization techniques which are used in this study are expressed in the following subsections.

2.8.1 Mechanical Characterization

If the material is produced for a special use which needs to withstand to a certain load or requires some rigidity then the information have to be obtained by the mechanical tests. For these purposes there are many mechanical testing methods to characterize the material. Tensile, impact and hardness tests are some of the mechanical characterization methods that are used in this study [48].

2.8.1.1 Tensile Test

The most widely recognized kind of test to determine the mechanical properties of a material is the tensile test also called as tension test. Using the tensile test, the

fundamental data such as tensile strength, elastic modulus and elongation at break can be obtained.

Dog bone shaped specimens are prepared and fixed into clamps on machine which applies load and pulls the material at a constant speed as shown in Figure 2.14.

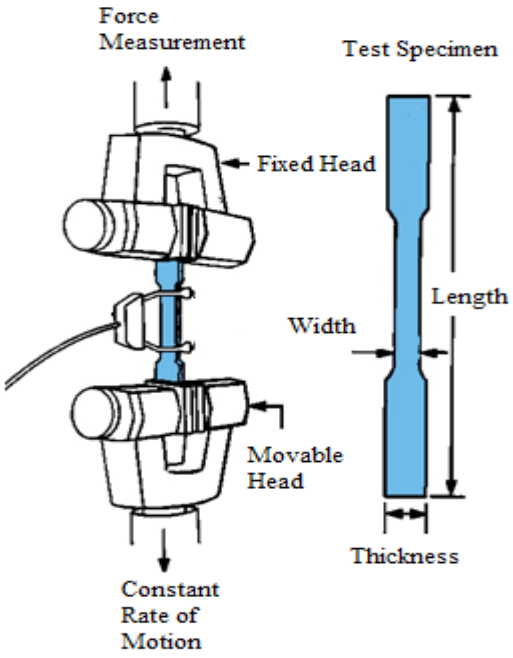

Figure 2.14 Tensile testing machine and test specimen [49].

Test proceeds until a breakage appears. Throughout the test, the applied force and change in gauge length are recorded and strain-stress curve which is shown in Figure 2.15 can be drawn with this data. After that, the mechanical properties can be calculated using this curve [48].

As can be seen from Figure 2.15, ultimate stress corresponds to the stress where the fracture occurs. Yield stress can be defined as the maximum stress that a material can withstand before plastic deformation.

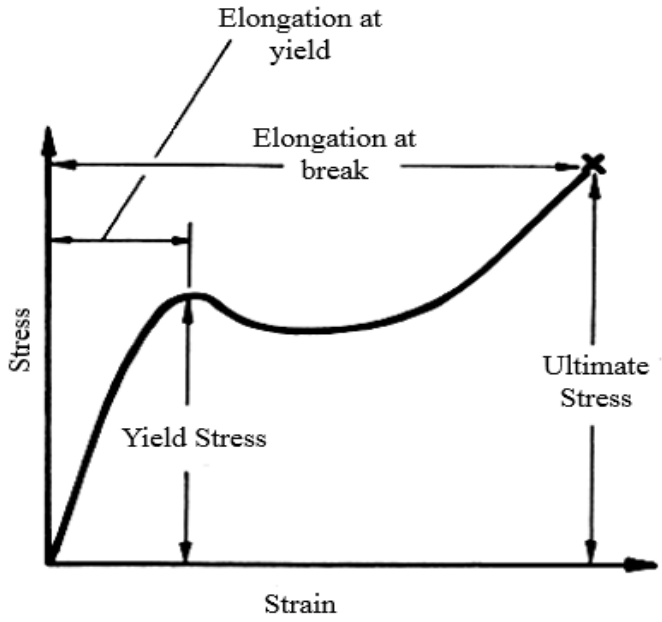

Figure 2.15 Stress-strain curve [50].

The tensile strength (σ) is the maximum stress that a material can withstand. It can be calculated using Equation (2.2), where σ is tensile strength, F is maximum applied force and S_0 is the initial cross section area of the specimen.

$$\sigma = \frac{F}{S_0} \tag{2.2}$$

Ductility of the materials can be explained as the percent elongation in area or length. The strain (ε) is the value of plastic strain at fracture and can be calculated by Equation (2.3) where L_f is the final length and L_0 is the initial length of the specimen.

$$\varepsilon = \frac{L_f - L_0}{L_0} \tag{2.3}$$

In elastic region strain and stress are directly proportional to each other. So elastic modulus (E) is the slope of this linear portion of stress-strain curve and can be calculated by Equation (2.4) where ε is strain and σ is tensile strength [48].

$$E = \frac{\sigma}{\varepsilon} \tag{2.4}$$

2.8.1.2 Impact Test

Impact test is a mechanical characterization method to measure the materials' ability to resist impact load [51]. The apparatus of impact test is shown in Figure 2.16. Charpy and Izod types of the specimens are commonly used in impact testing.

In the test, pendulum hits the specimen from its center and the specimen breaks by absorbing an energy which is the potential energy difference of the pendulum before and after the impact. The energy is recorded and divided by the area of the test specimen to obtain the impact strength [15].

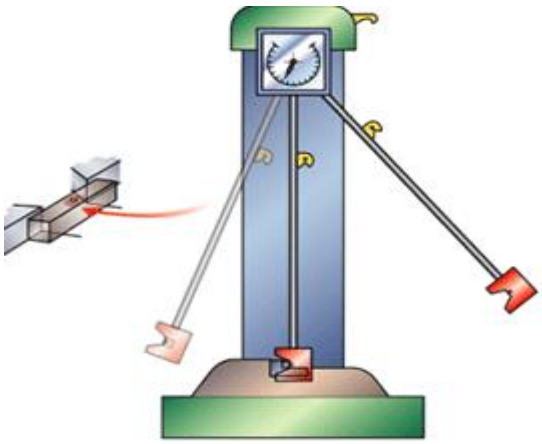

Figure 2.16 Schematic of Charpy impact test apparatus [52].

2.8.1.3 Shore Hardness Test

The hardness of polymers is usually measured using Shore and Rockwell hardness tests. Shore Hardness test measures the resistance of material to indentation. There are different scales of Shore hardness depending on the hardness of the specimen which is tested. Shore A scale is used for softer materials and Shore D scale is used for relatively harder materials. The scale is shown in Figure 2.17. There are also some other kinds of Shore scales such as Shore 0 and Shore H but uncommonly used in polymer sector [53].

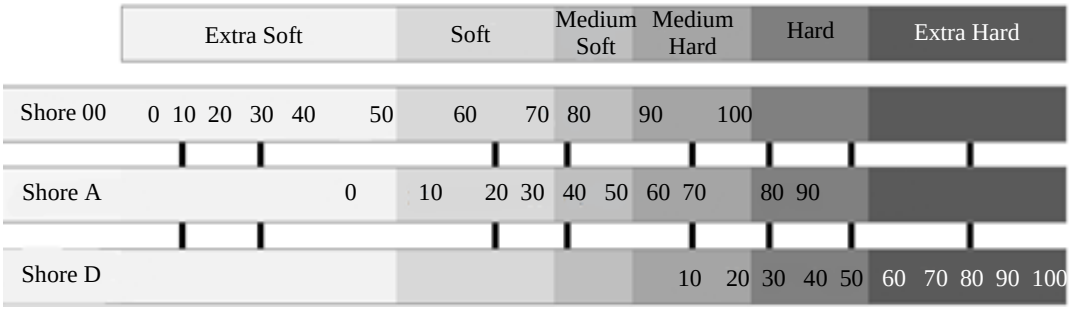

Figure 2.17 Shore hardness scale [54].

Durometer is the apparatus of the Shore hardness measurement and it is shown in Figure 2.18. The hardness value is identified by the drilling of the indenter into the specimen and can be read from the dial gauge of the apparatus. This test is generally used to have relative hardness value and also get information about the flexibility of the specimen [53].

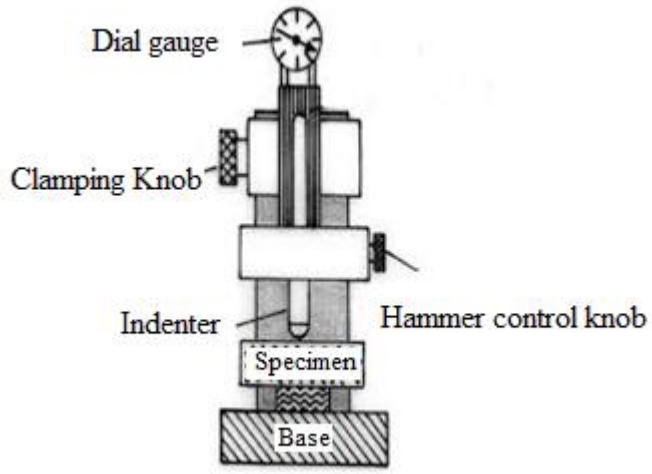

Figure 2.18 Shore durometer apparatus [55].

2.8.2 Flame Retardancy Characterization

2.8.2.1 Limiting Oxygen Index (LOI) Test

Limiting oxygen index test shows the flammability of substances. It evaluates the minimum oxygen concentration in a mixture of O_2 and N_2 to start the ignition and sustain the flame on the material for 3 minutes or a length of 5 cm [56]. The LOI

value can be calculated from Equation (2.5) where $[O_2]$ and $[N_2]$ are the concentrations of oxygen and nitrogen, respectively.

$$\text{LOI } (O_2\,\%) = \frac{[O_2]}{[O_2]+[N_2]} \times 100 \tag{2.5}$$

The corresponding experimental apparatus of LOI is shown in Figure 2.19.

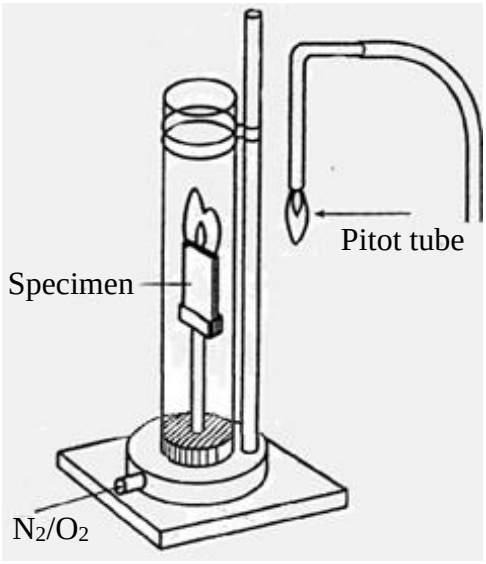

Figure 2.19 Limiting oxygen index test apparatus [56].

In the test, the vertical specimen is put into a chimney, and N_2/O_2 gas mixture is allowed to flow inside the chimney. After burning the top of the specimen, the time is recorded for the continued flame. It is waited for finding the minimum oxygen concentration to ignite and sustain the flame according to the criteria given in ASTM D2863 [57].

If the LOI value is higher than 21 then the material is called as self-extinguishing, if LOI is lower than 21 then it is called as combustible material so it can burn in ambient temperature with an ignition source [2].

2.8.2.2 UL-94 Vertical Burning Test

UL-94 Vertical Burning test is confirmed by the Underwriters Laboratories as a test which is appropriate to determine the flammability of the plastics. The test gives information about the ignition characteristics and flame spread of the vertical test

specimen. As a result of the test, the materials can be classified as V-0, V-1 or V-2 [2].

The schematic drawing of the test apparatus is shown in Figure 2.20.

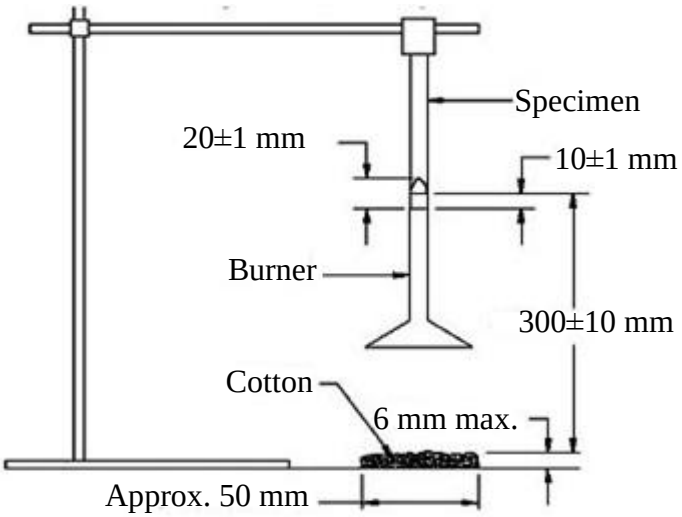

Figure 2.20 UL-94 vertical burning test apparatus [58].

A blue flame with a height of 20 mm is put 10 mm below to the bottom edge of the specimen. After 10 seconds of application of flame to the specimen the burner is removed and time is recorded as afterflame time (t_1) which is the time necessary for flame to extinguish. After this process another 10 seconds of flame is applied to the specimen and the burner is removed again. The afterflame time, t_2 and afterglow time, t_3, which are the times necessary for the fire to glow and extinguish, are recorded. If a burning piece of material falls onto the cotton it must be noted. The classification of the specimen flammability is performed due to the criteria given in Table 2.3.

Table 2.3 The criteria for classification of samples for UL-94 test [58].

Criteria Conditions	**V-0**	**V-1**	**V-2**
Afterflame time for each individual specimen, t_1 or t_2	≤ 10 s	≤ 30 s	≤ 30 s
Total afterflame time for any condition t_1+t_2 for five specimen	≤ 50 s	≤ 250 s	≤ 250 s
Afterflame plus afterglow time for each individual specimen after the second flame application (t_2+t_3)	≤ 30 s	≤ 60 s	≤ 60 s
Afterflame or afterglow of any specimen up to the holding clamp	No	No	No
Cotton indicator ignited by flaming particles or drops	No	No	Yes

2.8.3 Morphological Analysis

2.8.3.1 Scanning Electron Microscopy (SEM)

Scanning electron microscopy deals with the surface analysis of the materials. For this purpose, the conducting surface is scanned with electron beam and the backscattered electrons are collected to provide a signal to display in a cathode ray tube. The scanning electron micrograph on the screen shows the morphology of the specimen. Specimen must be electrically conducted to reflect the electrons and create the image. If the specimen is not conductive, then a very thin surface coating is applied using conducting materials. The magnification of the test is changed from 10 to 50,000 times of the area that is photographed. Additional equipments can be used together with SEM, and qualitative and quantitative analyses can be carried out [11].

2.8.4 X-Ray Spectroscopy (XPS)

X-Ray photoelectron Spectroscopy is a widely used technique to determine lots of analytical information. In general, XPS is utilized to understand the surface properties of a material such as its composition and crystallography. This technique can be applied to gases, liquids and solids.

During the test, the electrons are excited with the interaction of X-ray light and ejected as shown in Figure 2.21. The energy which is absorbed by the material and the number of electrons which are ejected, are recorded during the irradiation process [59].

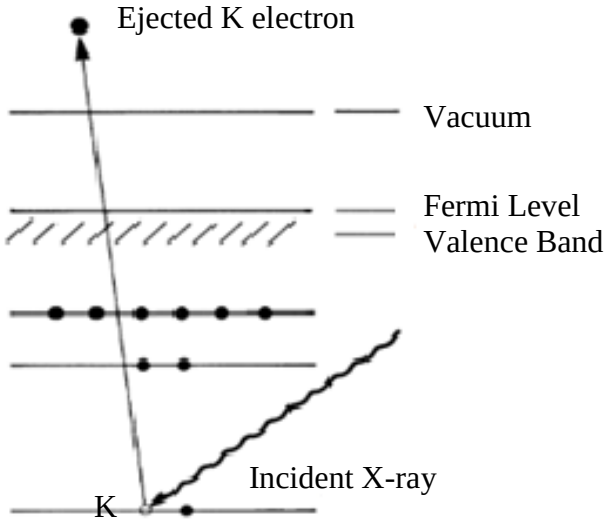

Figure 2.21 Photoemission process [59].

2.8.5 Fourier Transform Infrared (FTIR) Spectroscopy

Fourier transform infrared spectroscopy is basically described as the interaction between the particles of the material and the infrared radiation.

In the analysis IR is passed through the specimen, some of the IR is absorbed and creates vibrations in the bonds of the specimen and remaining light is transmitted. These molecular absorption and transmission are shown by the FTIR spectrum. The same spectrum cannot be produced by two different molecules since each material is composed of different atoms. For this reason FTIR is used to identify unknown materials, identify the functional groups, determine the amount of components in a mixture [60].

2.8.6 X-ray Diffraction (XRD) Analysis

X-ray diffraction method is used for investigation of atoms and molecules due to the interaction between radiation and material. The wavelength of the radiation interferes the arrangements of the atoms or molecules if their sizes are appropriate to the wavelength. X-rays are reflected back only at certain orientations of the material [60].

The diffraction of the X-ray beam can be calculated from Bragg's equation (2.6) which is given below;

$$n\lambda=2d\sin\theta \qquad (2.6)$$

where λ is the wavelength, d is the distance between the planes of the material, θ is the angle of the diffracted light and n is the degree of diffraction [61].

XRD analysis determines the crystallinity of the materials. On the other hand XRD gives information about the proportionality of the crystalline phases in the specimen.

2.8.7 Thermal Characterization

2.8.7.1 Differential Scanning Calorimetry (DSC)

Differential scanning calorimetry is a thermoanalytical measurement which measures amount of heat given or taken from the specimen under heating, cooling or isothermal conditions as a function of specimen temperature.

It is a time-temperature program that controls the temperature of both the specimen and the reference holder with respect to time and temperature together. When heat is applied to the specimen, it undergoes a thermal transition, and data is collected as the heat flow difference between specimen and reference with respect to temperature [60]. Some significant physical and chemical properties of the specimen can be determined due to this collected data. If the specimen is a thermosetting polymer then the glass transition temperature, heat of cure values of the specimen are obtained, and percent curing of the specimen can be calculated [62]. Figure 2.22 shows a typical DSC curve of thermosetting polymers.

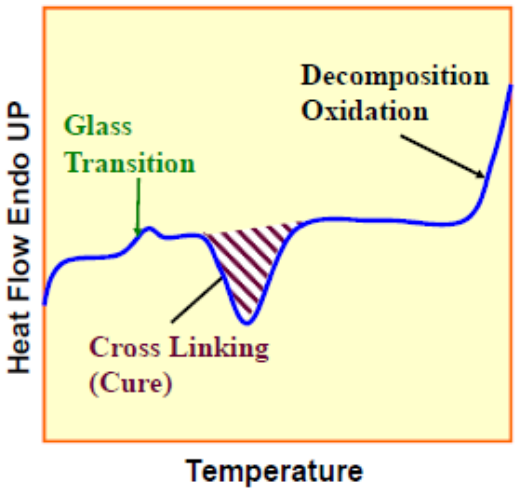

Figure 2.22 Typical DSC curve of a thermoset polymer [63].

It is mentioned that the degree of curing can be calculated using DSC curve. The relation is given in Equation (2.7) to calculate percent curing from heat of cure of cured and uncured specimen [63].

$$\text{Degree of curing } (\%) = \frac{\Delta H_{uncured} - \Delta H_{cured}}{\Delta H_{uncured}} \times 100 \qquad (2.7)$$

In the equation ΔH is the curing enthalpy difference, either for cured or uncured samples, and can be obtained from the area of the curing exotherm which is shown in Figure 2.22.

2.8.7.2 Thermal Gravimetric Analysis (TGA)

Thermal Gravimetric Analysis is a thermal method which measures weight change depending on the time or temperature in a desired atmosphere (N_2 or air).

It gives information about the thermal and oxidative stability. Also decomposition temperature of a specimen can be obtained by the help of TGA. A typical TGA plot is given in Figure 2.23.

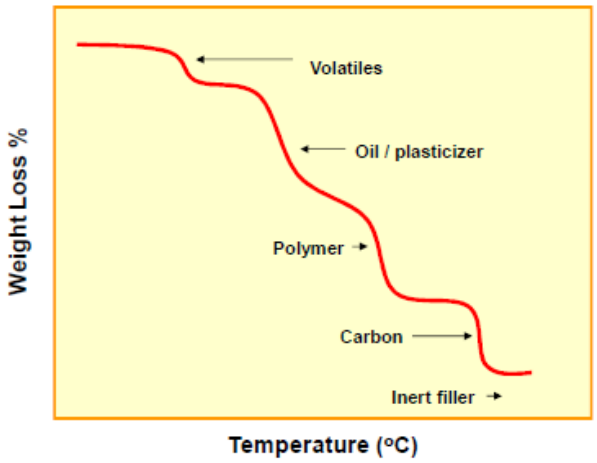

Figure 2.23 TGA plot [63].

The specimen losses its weight and degrades with increasing temperature and time or gains weight due to oxidation and formation of oxides. The residue of the specimen after TGA is generally the inert filler of a composite material [63].

2.8.8 Electrical Characterization

2.8.8.1 Electrical Resistivity Measurement

Electrical resistivity is defined as the resistance to current flow. Conductivity is inversely proportional to electrical resistivity.

In polymeric materials, there is an attention in studying the electrical resistivity because of the promising electrical properties of these materials.

Electrical resistivity measurement using two point probe technique is an elementary method which is usually utilized in samples with high resistivity [64]. The testing apparatus is demonstrated in Figure 2.24.

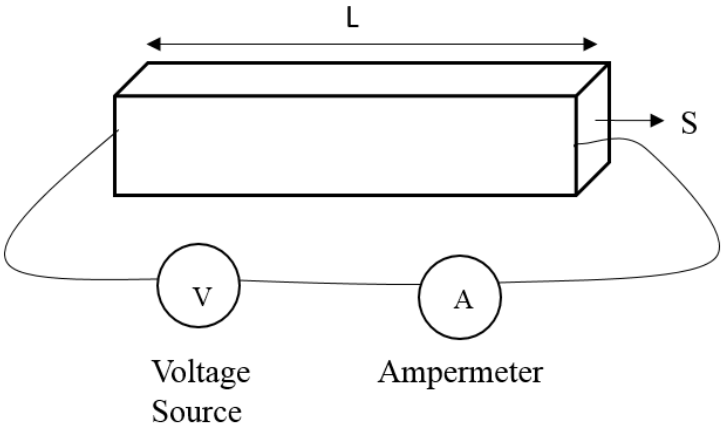

Figure 2.24 Schematic of electrical resistivity measurement [65].

In the test, resistivity of a specimen is calculated from the constant voltage and corresponding current values using Equation (2.8) where ρ is volume resistivity, R is resistance, L is the distance between two probes and S is the cross sectional area of the specimen [64].

$$\rho = \frac{RxS}{L} \tag{2.8}$$

2.9 Previous Studies

In this section, the studies which are related with improving flame retardancy properties of epoxy with the addition of boron containing compounds and the studies which cover the boron carbide and epoxy composites in the literature are reviewed.

2.9.1 Flame Retardancy of Epoxy

Ishii et al. (2006) studied the flame retardancy in epoxy molding compounds with the addition of a boron containing compound, calcium borate to be applied in semiconductor packaging systems. The addition of a small amount of CaB improved the flame retardancy of epoxy, but improvement was not proportional to the additive amount. The decrease in flammability was explained as the cooling effect of CaB which came from the water release from CaB at 376°C and glassy layer formation of boron oxide. Also it was claimed that calcium and calcium oxide have a promoting impact on char formation. The addition of CaB did not affect the moldability since it

was a small amount (5-30 wt.%). Final composites were also said to have better mechanical properties when they were compared with the neat epoxy [66].

Unlu et al. (2014) conducted a research to investigate and compare the effects of boron containing compounds on flame retardancy properties of the composites obtained from epoxy resin and cyloaliphatic polyamine based curing agent. Addition of boric acid and boron oxide increased the flame retardancy properties of epoxy. Best results were achieved with addition of 40% boric acid, and it was claimed that beyond this loading there had been problems in processability. On the other hand, addition of 40% boron oxide reduced the peak heat release rate and total amount of heat evolved. The reasons of improved flame retardancy were announced for boric acid and boron oxide separately. For boron oxide, glassy layer formation and insulating effect of this layer was shown as the reason of improvement in flame retardancy. Endothermic decomposition, fuel dilution via water release and char layer formation in the condensed phase were the beneficial effects of boric acid [41].

Dogan and Unlu (2014) investigated the effect of zinc borate, boric acid and boron oxide on the flame retardant properties and thermal stability of epoxy resin/red phosphorus composites. Addition of boron containing compounds decreased the flammability and heat release rate of epoxy resin. According to the study, boric acid and zinc borate increased the char formation and released water. Moreover zinc borate increased the char formation by the stabilizing effect of produced zinc oxide. When the boron containing additives were compared, zinc borate showed the most beneficial effect on flame retardancy by lowering the heat release rate and total heat evolved [67].

Yürekli (2014) studied the flammability properties of epoxy-based composites containing mainly barium metaborate, zinc borate, calcium borate and melamine phosphate as an intumescent flame retardant additive. 1% addition of barium metaborate increased LOI value of the composites from 19 to 25% O_2 but decreased the mechanical properties. The addition of 10% melamine phosphate increased the LOI value from 19 to 27% O_2. Also the addition of 1%BaM and 10% MP gave the best results with epoxy resin. On the other hand, while improving the flame retardancy properties, mechanical properties of the composites were also taken into account [68].

Chen et al. (2004) synthesized melamine phosphate containing epoxy composites and investigated their flame retardation and thermal properties. It was observed that the addition of melamine phosphate improved the flame retardation properties, increased the LOI value and the char yield. Melamine phosphate was more efficient in reactive mode than the additive mode. Decomposition temperature was decreased at higher contents of melamine phosphate, and it was explained as the formation of a protective layer which prevented further decomposition [69].

Rallini et al. (2013) studied the thermal behavior of an epoxy composite which contained carbon fiber and boron carbide as additives. It was explained that addition of boron carbide did not affect the mechanical properties. Two different concentrations of boron carbide were impregnated into composites, and the effect of amount of boron carbide on flammability was also studied. 5% addition of boron carbide decreased the heat release rate and permitted residue to keep its structural integrity. Besides, addition of boron carbide improved the thermal stability and postponed the thermal oxidation of epoxy composite. The formation of glassy layer of boron oxide prevented the further oxidation and bounded the plies of the composite together [70].

2.9.2 Mechanical Properties of Epoxy

Rodrigues et al. (2013) studied the adhesion between epoxy and boron carbide particles. Since the composites without adhesion led to restricted mechanical properties, silane coupling agent was used as a surface modifier to develop the adhesion. Surface analysis showed that there was B-O bonds so surface modification was succeeded. The improved adhesion between epoxy and boron carbide exhibited increase in mechanical properties. The other mechanical properties such as flexural and tensile strengths also increased [71].

Abenojar et al. (2009) studied the mechanical properties of boron carbide containing epoxy composites. The effect of particle size, addition amount of boron carbide and distribution of the particles were investigated, and it was found that bending strength increased with smaller particles and the boron carbide content. However, the lack of adhesion between particles increased the wear resistance. Glass transition temperature of the composites decreased with the addition of boron carbide [13].

Hsieh et al. (2010) investigated how the addition of silica particles affect the toughness, modulus and glass transition temperature of epoxy matrix. It was claimed that, the addition of silica decreased the glass transition temperature slightly and increased the fracture toughness of the composite. The mechanism of toughening of epoxy was explained as plastic shear-yield bands and debonding between the filler and the matrix [12].

2.10 Motivation of the Study

Flammability is a significant problem which is resulted in deaths and serious injuries. Since epoxy is an important and widely used polymer, the flammability problem of epoxy has to be taken into account in the usage areas especially where heat is applied.

Studies about improving the flame retardation properties of epoxy are valid in the literature [41, 67]. Generally zinc borate, boric acid and boron oxide are used as boron containing flame retardant additives. However, there is only one study in the literature which investigates the effect of boron carbide on the flame retardation properties of epoxy. On the other hand, when considering the synergistic effect between the boron containing compounds there is not any study in the literature which has chosen boron carbide as the main component.

Mechanical properties of epoxy composites are as important as the flame retardant properties. Therefore the mechanical properties should be preserved while improving the flame retardancy of epoxy. In the literature, mechanical properties of epoxy is improved with the addition of various fillers such as carbon nanotubes, graphene, rubber, glass, etc. [72, 73].

To our knowledge, improving the mechanical properties of epoxy with the addition of boron carbide is only studied by a group of scientist. A comprehensive study which investigates the mechanical, flame retardation, thermal, electrical properties and morphologies of epoxy/boron carbide composites is not available in the literature. For this reason the main objective of this study is to investigate the effects of boron carbide addition on the properties of epoxy-based composites. It is also aimed to extent the use of different types of boron containing compounds and melamine phosphate in order to study their synergistic effect together with B_4C.

CHAPTER 3

EXPERIMENTAL

3.1 Materials

3.1.1 Epoxy Resin

The epoxy resin (Polires 188) was purchased from Polikem Kimyevi Maddeler San. Tic. Ltd. Şti. This prepolymer is a liquid, and synthesized from unmodified bisphenol A [$(CH_3)_2C(C_6H_4OH)_2$] and epichlorohydrin [C_3H_5ClO]. Also it is one of the most standard liquid resin which can be cured with a various types of curing agents.

Table 3.1 gives the properties of epoxy resin which was taken from the manufacturers' technical data sheet.

Table 3.1 The properties of Polires 188 [74].

Property	**Value**
Weight per epoxy equivalent, g/eq	182–192
Viscosity at 25°C, mPa.s	11000–15000
Color, (APHA)	<30
Specific gravity	1.15 –1.18
Nonvolatile, minimum wt%	99.7
Chlorine, ppm	<1000

3.1.2 Curing Agent

The curing agent (Cetepox 1393 H) which is a modified stabilised cycloaliphatic polyamine hardener was purchased from Polikem Kimyevi Maddeler San. Tic. Ltd. Şti. Table 3.2 gives the properties of Cetepox 1393 H which was obtained from the manufacturer.

Table 3.2 The properties of Cetepox 1393 H [75].

Property	**Value**
Hydrogen active equivalent weight, g/eq	93
Viscosity at 23°C, mPa.s	190
Color, Gardner scale	< 2
Density at 23°C, g/m^3	1.03
Flash point, °C	> 100
Initial viscosity at 23°C, s	105
Pot life, min	23

3.1.3 Boron Carbide

Boron carbide, which was procured from Boroptik Engineering who mentioned that the B_4C was produced using carbothermal synthesis of boric acid. Table 3.3 gives the properties of B_4C, and Table 3.4 shows the chemical analysis data of B_4C which was given by the supplier.

Table 3.3 The properties of B_4C [76].

Property	**Value**
Molecular formula	B_4C
Density, g/cm^3	2.4
Particle size, μm	3.4
Specific surface area, m^2/g	1.22
Purity, %	>96
Form	Black powder

Table 3.4 Chemical analysis data of B_4C [77].

Compounds	**Amount, wt. %**
Free boron + B_2O_3	0.47
Free C	1.60
Fe compounds	0.31
Boron carbide	96.81

3.1.4 Zinc Borate (ZnB)

Zinc borate was used as boron containing compound which is expected to improve the flame retardancy of epoxy composites. It was ordered from Great Lakes. The properties of ZnB are given in Table 3.5.

Table 3.5 The properties of ZnB [78].

Property	**Value**
Molecular formula	$2ZnO{\cdot}3B_2O_3{\cdot}3.5H_2O$
Particle size, μm	5
Form	White powder

3.1.5 Boric Acid (BA)

Boric acid, which was used as one of the alternative to boron contaning compounds was procured from ETI Mine Works. The properties of BA was given in Table 3.6.

Table 3.6 The properties of BA [79].

Property	**Value**
Molecular formula	H_3BO_3
Molecular weight, g/mol	61.83
Density, g/cm^3	1.44
Form	White powder

3.1.6 Calcium Borate (CaB)

Calcium borate, was used as an alternative flame retardant additive in boron containing compounds, and ordered from Portaflame. The properties of CaB are shown in Table 3.7.

Table 3.7 The properties of CaB.

Property	**Value**
Molecular formula	$Ca_3(BO_3)_2$
Density, g/cm^3	2.4
Particle size, μm	4.3
Form	White powder

3.1.7 Melamine Phosphate (MP)

Melamine phosphate is a halogen free melamine-based flame retardant additive which was used as an alternative additive for enhancing the flame retardancy of epoxy-based composites in the present study. It was supplied by BASF. Table 3.8 gives the properties of MP.

Table 3.8 The properties of MP [80].

Property	**Value**
Molecular formula	$C_3H_9N_6O_4P$
Specific gravity, g/cm^3	1.74
Molecular weight, g/mol	224.12
Particle size, μm	116
Form	White powder

3.1.8 Solvent (Acetone)

Acetone, was used as solvent in the preparation of the neat epoxy and the composites. It was purchased from Sigma Aldrich, and some information from the supplier is given in Table 3.9.

Table 3.9 The properties of acetone [81].

Property	**Value**
Molecular formula	$(CH_3)_2CO$
Density at 20 °C, g/mL	0.790-0.792
Melting point at 1 atm, °C	−94
Boiling point at 1 atm, °C	56
Purity, % (GC)	≥99
Vapor pressure at 20 °C, mmHg	184

3.2 Preparation of Epoxy Polymer and Epoxy-based Composites

3.2.1 Preparation of Neat Epoxy

Figure 3.1 shows the neat epoxy preparation in block diagram form. In the first step epoxy resin was put into an oven and degassed at 80 °C under vacuum for 3 hours to remove the air bubbles in the epoxy resin. At the same time the acetone was put into an ultrasonication bath, and ultrasonication was applied for 1 hour. After keeping the epoxy 3 hours in the vacuum oven, it was taken out of the oven and mixed with the same amount of acetone in ultrasonication for another 30 minutes. Next, the mixture was mixed with a mechanical stirrer at 60 rpm and 80 °C for 2 hours while the ultrasonication was continued to be applied. Curing agent and the mixture of acetone and epoxy were separately put into the oven and degassed at 70°C under vacuum for 1 hour. Later, the epoxy and the curing agent were separately kept at room temperature. After 30 minutes of cooling they were mechanically stirred at 40 rpm for 25 minutes with a mixing ratio (epoxy/curing agent) of 100:54 by weight. The molds were pretreated with teflon spray and waited at least 40 minutes before the molding. The mixture was poured into aluminum mold and it was waited for 30 minutes to initiate curing at room temperature. Then, the mold was put into oven and the mixture was subjected to further curing at 90°C for 17 hours and to postcuring at 130 °C for 3 hours. The production of neat epoxy and composites was the modified version of the production method in Elif Yürekli's master thesis [68].

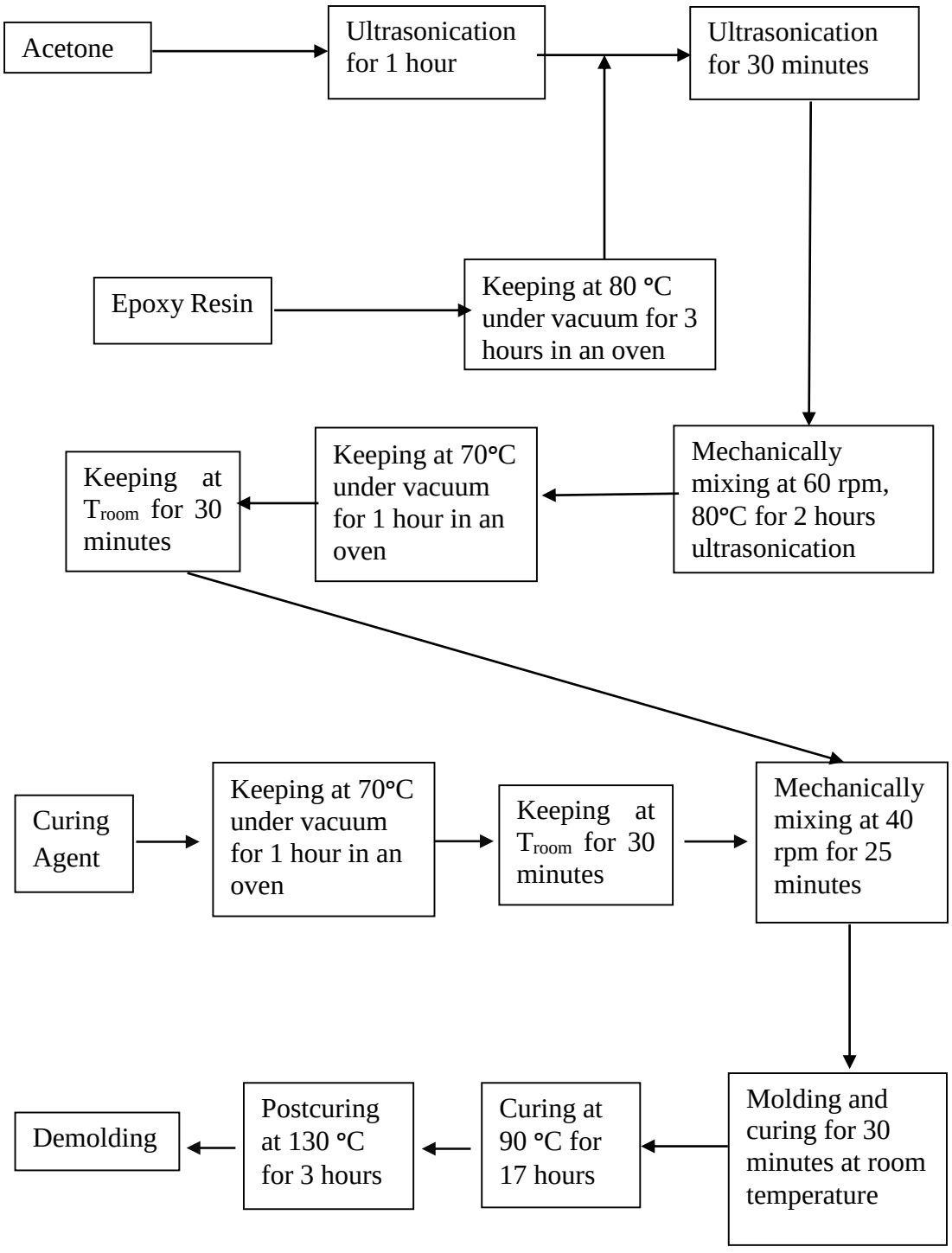

Figure 3.1 Block diagram for the neat epoxy preparation.

3.2.2 Preparation of Epoxy-based Composites

Figure 3.2 shows the preparation steps of the epoxy-based composites in which both the epoxy and an additive are introduced as shown in the flowchart. All the additives, were dried at 100°C for 4 hours as a pretreatment. Apart from the addition step of the additive, the preparations of the neat epoxy and composites were the same. At the beginning epoxy was kept in the oven at 80°C under vacuum for 2 hours, and the ultrasonication was applied for 1 hour to the mixture of the additive and acetone together. After the epoxy was taken out of the oven, it was mixed with the additive-acetone mixture, and ultrasonication was applied to this mixture for another 30 minutes to create a more homogeneous dispersion. The rest of the steps was the same as the preparation steps of neat epoxy samples as mentioned before.

Neat epoxy was prepared with an amount of 100 g epoxy and 54 g curing agent which was taken as basis. The compositions of epoxy boron carbide and the other boron containing compounds were varied during the experiments. The percentages of the additives for the composites containing epoxy and boron carbide are given in Table 3.10, and the ones with other boron containing additions and MP are shown in Table 3.11. Numbers in the sample codes show the weight percent addition of the related additive.

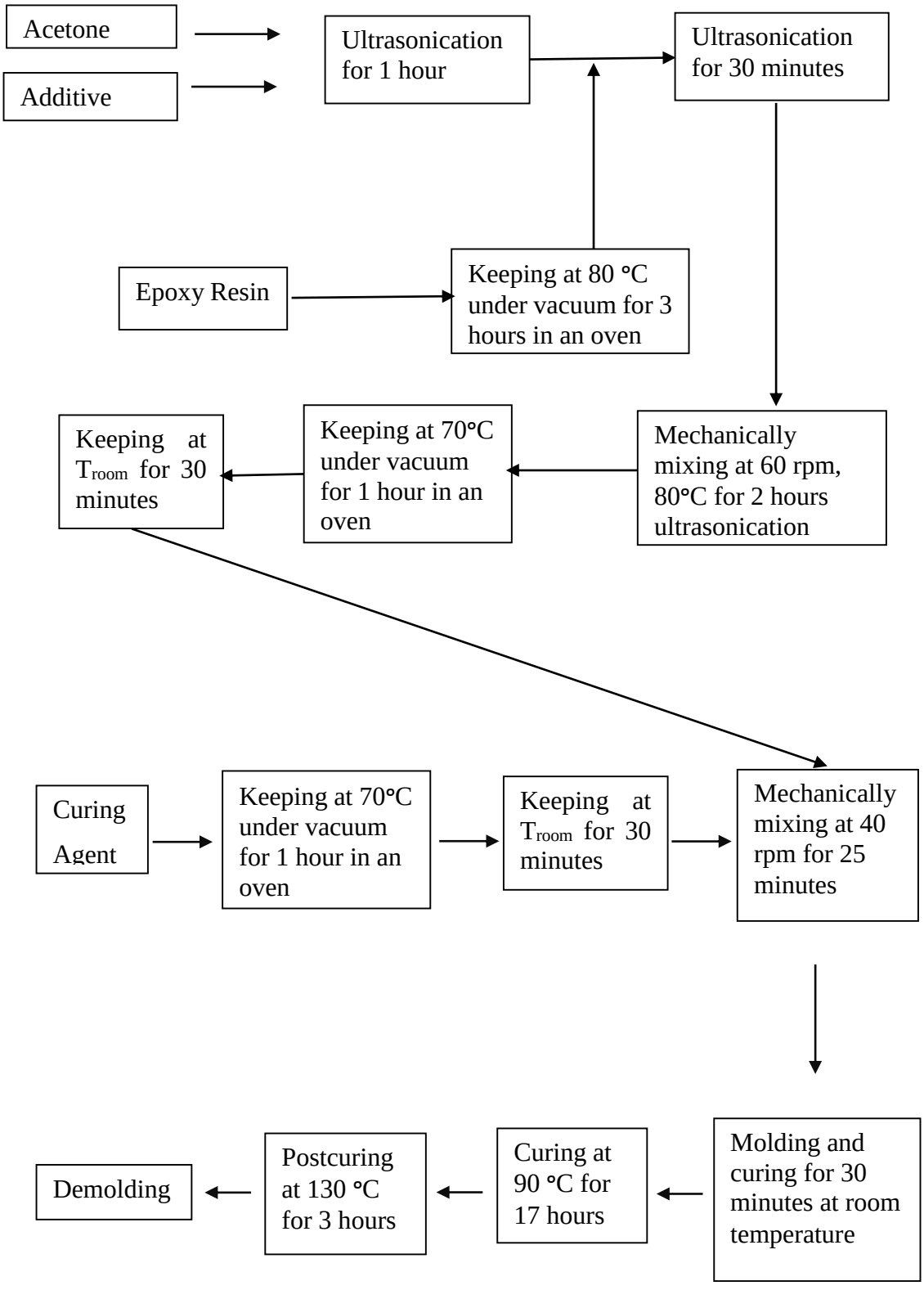

Figure 3.2 Block diagram for the preparation of epoxy composites containing flame retardant additive.

Table 3.10 The compositions of epoxy/boron carbide composites.

Sample Code	Composition, wt.%	
	EP	**B_4C**
Neat EP	100	-
EP/0.5B_4C	99.5	0.5
EP/1 B_4C	99	1
EP/3 B_4C	97	3
EP/5 B_4C	95	5
EP/8 B_4C	92	8

Table 3.11 The compositions of epoxy/boron containing compounds composites.

Sample Code	Composition, wt.%					
	EP	**B_4C**	**BA**	**ZnB**	**CaB**	**MP**
EP/1ZnB	99	-	-	1	-	-
EP/1BA	99	-	1	-	-	-
EP/1CaB	99	-	-	-	1	-
EP/3B_4C/1ZnB	96	3	-	1	-	-
EP/3B_4C/1 BA	96	3	1	-	-	-
EP/3B_4C/1CaB	96	3	-	-	1	-
EP/10MP	90	-	-	-	-	10
EP/10MP/3B_4C	87	3	-	-	-	10
EP/10MP/3B_4C /1ZnB	86	3	-	1	-	10

3.3 Characterization Methods

3.3.1 X-Ray Diffraction (XRD)

The crystalline phases of boron carbide and EP-based composites were obtained using a Rigaku Ultima IV X-Ray Diffractometer with a $CuK\alpha_1$ radiation source. Boron carbide powder was scanned from 5º to 90º with a rate of 2 º/min. Neat epoxy samples and EP-based composites were scanned within Bragg angles from 5º to 50º with a rate of 2º/min. The voltage and current of the analysis were 40 kV and 40 mA, respectively.

3.3.2 Scanning Electron Microscopy (SEM)

Quanta 400 F Field Emission Scanning Electron Microscope was utilized to analyze the surface morphology of as-received boron carbide particles and EP-based composites. Since boron carbide and EP-based composites are not conductive materials, the samples were coated with gold-palladium alloy to prevent charging and to create electrically conductive surfaces.

3.3.3 X-Ray Photoelectron Spectroscopy (XPS)

SPECS EA 300 was used to determine the content of elements in bulk boron carbide. Monochromatic Al Kα radiation with a power of 600 Watt was employed as an X-ray source.

3.3.4 Thermal Gravimetric Analysis (TGA)

The thermal stability of boron carbide particles and the thermal degradation temperatures, thermal stability and char yield of epoxy-based composites were determined with a Shimadzu DTG-60/60H. These samples were heated in a temperature range from 25°C to 800°C with a heating rate of 10°C/min under nitrogen atmosphere with a flow rate of 70 ml/min for EP-based composites and under both nitrogen and air atmospheres for boron carbide with a flow rate of 70 ml/min.

3.3.5 Fourier Transformed Infrared (FTIR) Spectroscopy

Chemical structure of boron carbide was obtained with FTIR Spectroscopy using a Shimadzu IR Prestige21 with attenuated total reflectance apparatus (ATR) between

wavenumbers from 700 cm^{-1} to 3500 cm^{-1}. Before the experiment, potassium bromide (KBr) pellets were prepared with the addition of 0.1% B_4C to KBr. The dispersion of the B_4C into KBr was achieved in a muller and then this mixture was pelletized using a cold press at 60 bar for 4 minutes.

FTIR Spectroscopy analysis was also performed to determine the chemical compositions of epoxy, curing agent, neat epoxy samples and epoxy-based composites. Transmittance versus wavenumber graphs were plotted between wavenumbers from 500 cm^{-1} to 4000 cm^{-1}. Perkin Elmer UATR Two was used for FTIR analysis.

3.3.6 Mechanical Characterization of EP-based Composites

3.3.6.1 Tensile Test

The tensile measurements of the samples were carried out with a Shimadzu Autograph AG-100 KNIS MS universal tensile testing instrument. Figure 3.3 shows a photograph of the tensile testing instrument.

Figure 3.3 Shimadzu Autograph AG-100 KNIS MS universal tensile testing instrument.

The dog bone shape tensile test specimens were produced according to ASTM D638-10 standard. Dimensions of the dog bone shape specimens are given in Table 3.12. In testing machine the crosshead speed was selected as 4 mm/min. Tensile stress, tensile modulus and elongation at break values were calculated. Five samples of each compositions were tested with tensile testing machine. The average value and its standard deviation were calculated for five different samples.

Table 3.12 Dimensions of the dog bone shape sample.

Property	**Value**
Length, mm	115
Gauge length, mm	65
Width, mm	6
Thickness, mm	4

3.3.6.2 Impact Test

The impact measurements of the samples were carried out with a Ceast Resil Impactor 6967. The pendulum was selected as 7.5 J. The impact test equipment is illustrated in Figure 3.4.

Figure 3.4 Ceast Resil Impactor 6967 instrument.

.

The specimen which was used in impact testing instrument was produced according to ISO 179 standard. Dimensions of the bar shape specimen is given in Table 3.13. The impact area which the material was exposed to impact load was measured, and the impact energy was recorded from the device. Impact stregth was determined by dividing impact energy with the area.

Table 3.13 Dimensions of the impact test sample.

Property	**Value**
Length, mm	80
Width, mm	10
Thickness, mm	4

Five samples of each compositions were tested with impact testing instrument. Their average values and standard deviations were also calculated.

3.3.6.3 Shore D Hardness Test

Shore D Hardness test was applied to the tensile specimens according to ASTM D 2240 standards. Average of five analyses which were applied to five different specimens was taken as the Shore D value.

3.3.7 Flame Retardancy Characterization of EP-based Composites

3.3.7.1 Limiting Oxygen Index Test (LOI)

Fire retardancy behaviour of the neat epoxy sample and epoxy-based composites was determined using a Dynisco Polymer LOI test instrument. Test was performed according to ASTM D2863 standard. Figure 3.5 shows a photograph of LOI test apparatus. The specimen which was used for LOI test was the same as impact test specimen. Therefore the dimensions of the specimen were the same as in Table 3.13. The test was repeated for the same oxygen concentration maximum two times for some composites.

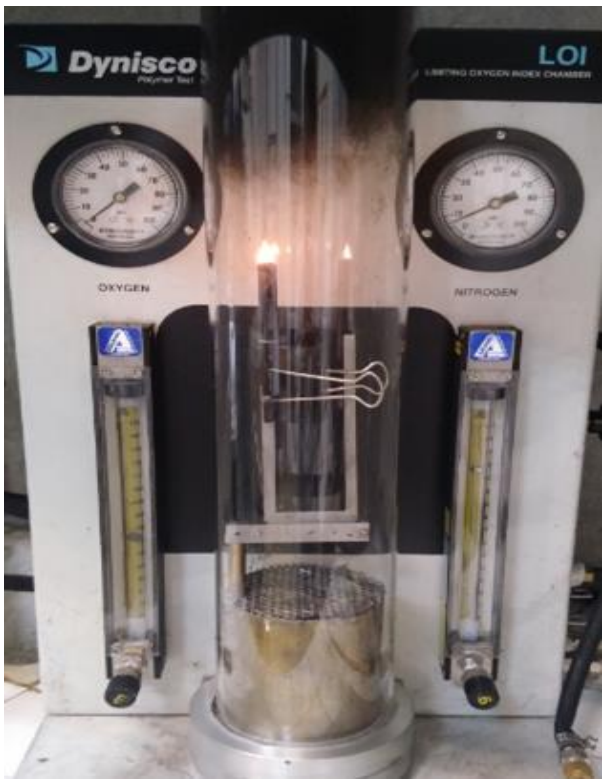

Figure 3.5 Dynisco Polymer LOI test instrument.

3.3.7.2 UL-94 Vertical Burning Test

UL-94 Vertical Burning Test was applied to the specimen according to the ASTM 3801 to characterize the flame retardation properties of the composite. The dimensions of the sample were the same as the ones for the impact test.

3.3.8 Differential Scanning Calorimetry (DSC)

Glass transition temperature and heat of cure for the epoxy specimen were determined using a Shimadzu DSC-60 differential scanning calorimeter. The specimen was heated in a temperature range from 25°C to 200°C with a heating rate of 10°C/min. After the first run, it was cooled to room temperature and was heated with the same conditions again in nitrogen atmosphere with a flow rate of 70 ml/min.

3.3.9 Electrical Characterization of EP/B_4C Composites

Two Point Probe Electrical Resistivity Measuring Method was applied to sintered boron carbide, neat epoxy and epoxy-based composites containing B_4C because B_4C is a semiconducting material. Keithley 2400 SourceMeter was utilized as the current

source. Two probes were placed between two ends of the impact specimen of which the dimensions are given in Table 3.13. The constant voltage which was set as 20 V from DC source was applied, and corresponding current values were measured and recorded by the device during the analysis. The resistance of the specimen was calculated according to ASTM F43 standards. The measurement was done using 5 different specimens, and each specimen was subjected to this test five times to reach the highest accuracy. Figure 3.6 shows a photograph of the measuring device.

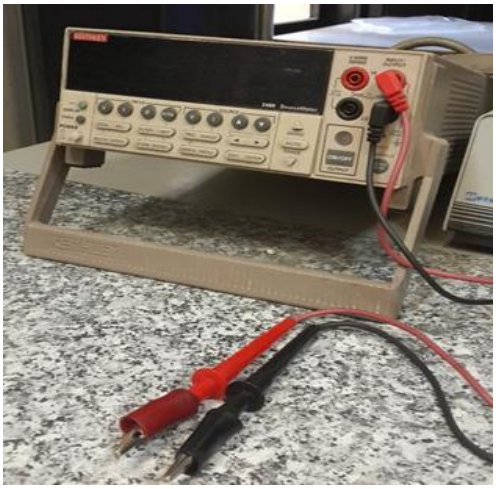

Figure 3.6 Two Probe measurement device, Keithley 2400 SourceMeter.

CHAPTER 4

RESULTS AND DISCUSSION

Results and discussion section contains mainly three parts. First part includes the results of the studies which are performed to obtain information about the materials that we bought. Hence structural, thermal and electrical properties and morphology of as-received boron carbide material were characterized. After that, the characterization of epoxy resin, curing agent and cured epoxy was performed with FTIR analysis. The percent curing of prepared neat epoxy sample was calculated by the help of DSC analysis.

In the second part, the characterizations of epoxy/boron carbide composites are first given in terms of mechanical, flame retardation, thermal, electrical properties and morphologies. The final boron carbide percentage, which was necessary amount to be added into the epoxy/boron containing compound composites, was decided according to these characterizations. Subsequently, the characterization of epoxy/boron containing compound composites is given in terms of flame retardation, mechanical and thermal properties, and morphologies.

As mentioned above, the as-received boron carbide particles have been subjected to many characterization tests to have information about the nature of the material that we have. The XRD pattern of as-received material is shown in Figure 4.1. XRD data of as-received material is given in Appendix A.

As it is seen in Figure 4.1, in the XRD pattern of material peaks at 2θ values of 37.85°, 35.02°, 23.52°, 31.8°, 22.14° and 19.78° are observed. Those peaks belong to the

characteristic peaks of boron carbide. The peaks at 2θ value of 32.20° and 35.64° correspond to Fe_2O_3. The peaks at 2θ values of 35.45°, 62.57° and 56.99° are the peaks of Fe_3O_4. Boron peak can be observed at 2θ value of 22.06°. There is also carbon peak at 2θ value of 26.53°. Detailed data for the XRD patterns of compounds is tabulated in Appendix A.

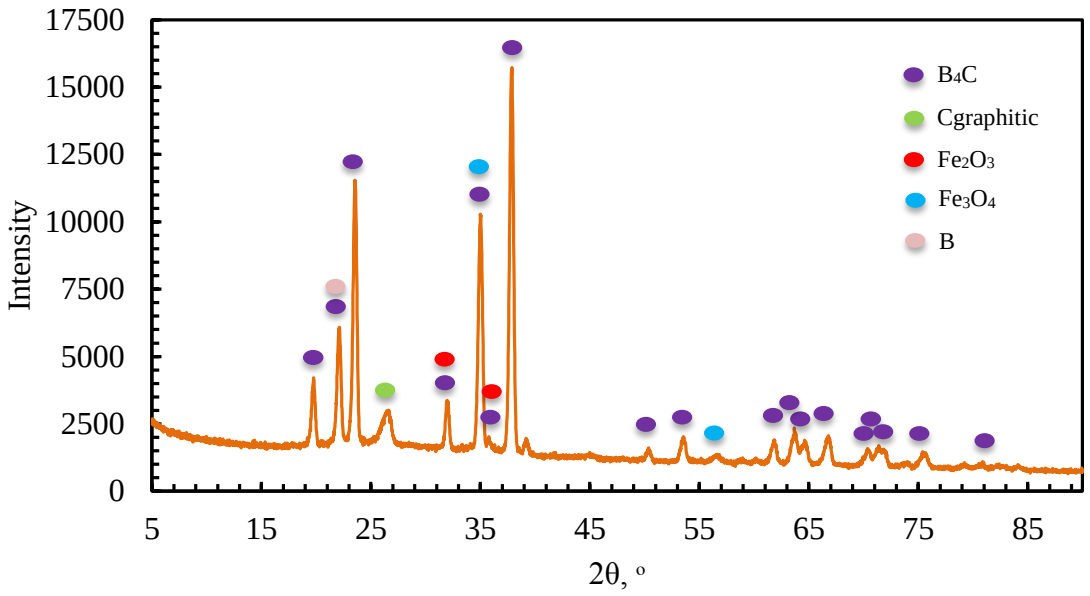

Figure 4.1 XRD pattern of as-received boron carbide.

XRD results showed that the as-received material contained mainly boron carbide. Besides, since the XRD pattern of as-received material had the peaks for iron compounds, amorphous boron and carbon as impurities, the XRD analysis verified the data in Table 3.4, which had been given by the manufacturer.

Heat treatments of boron carbide under argon and air atmospheres were performed to determine the thermal stability, possible reactions and products from these reactions.

Boron carbide was heated from room temperature to 800°C with a heating rate of 10°C/min and then the temperature was kept constant at 800°C for 2 hours for all atmospheres. After the heat treatments, the samples were characterized using XRD analysis. Figure 4.2 shows the XRD patterns of heat treated boron carbide under argon and air atmospheres.

In Figure 4.2, the characteristic peaks of boron carbide are seen. A decrease in the main characteristic peak for the as-received boron carbide at 2θ value of 37.85° was observed under both argon and air atmosphere. It is also seen from the XRD patterns that, the intensities of peaks at 2θ values of 26.6° for heat treated boron carbide under argon and air are increased when they are compared with the as-received boron carbide.

Under air atmosphere, in addition to increase in carbon peak, new two peaks are observed at 2θ values of 14.64° and 27.92° which correspond to B_2O_3. The increase in intensity of carbon peak and formation of new peaks for boron oxide may be due to the formation of carbon because of the reaction of B_4C with air to yield carbon and boron oxide in the environment of air [82, 83]. XRD pattern showed that there was formation of boron oxide (B_2O_3) in air atmosphere. Besides, there is a wide amorphous peak between the 2θ values of 15° and 30° which again may prove the formation of glassy boron oxide layer [84]. There are also boron peaks at 2θ values of 22.06°, 35.51° and 21.19° in the XRD pattern of heat treated boron carbide in air.

Under argon atmosphere, boron peaks are observed at 2θ values of 35.51° and 21.19° in the XRD pattern. In addition to boron and boron carbide peaks, boron oxide peaks were observed at 2θ values of 27.77° and 14.56°. This boron oxide, which was not observed in XRD pattern of as-received material, came from the material. For the XRD analysis a small amount of material was used. Therefore, this small amount of material may not reflect the whole material.

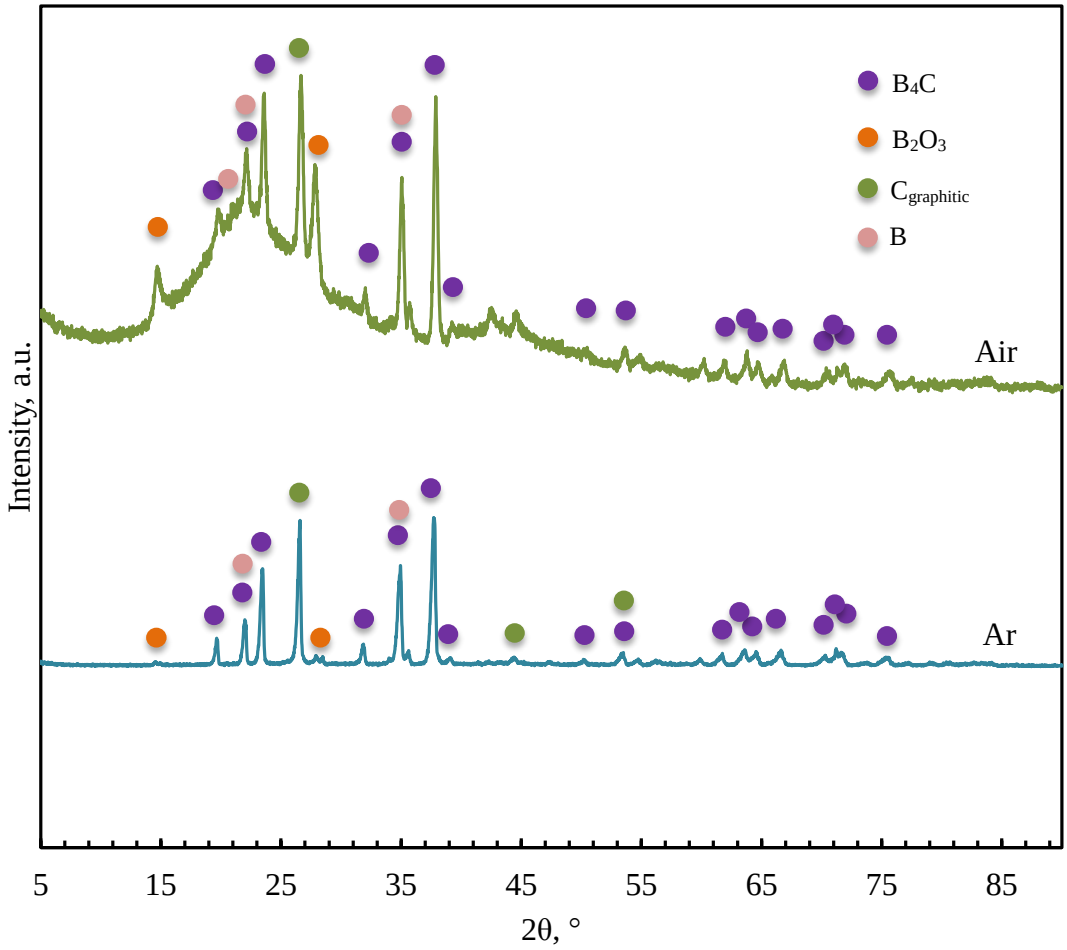

Figure 4.2 XRD pattern of boron carbide after heat treatment under different atmospheres: Air, Ar.

In addition to XRD analysis, boron carbide material was characterized using a Scanning Electron Microscope to observe their particle sizes and shapes.

SEM micrographs of boron carbide particles are given in Figure 4.3. These photographs show the characteristic polygonal shapes of boron carbide with different magnifications. As it is seen from Figure 4.3b, particles with sizes of 8 μm, 4.8 μm, 2.7 μm and 5.3 μm were observed in the as-received material. SEM results revealed that the shapes and sizes of B_4C particles were irregular. Their particle sizes are mostly in the range of 3-8 microns. This results agree with the size and shape in the technical data sheet given by the supplier.

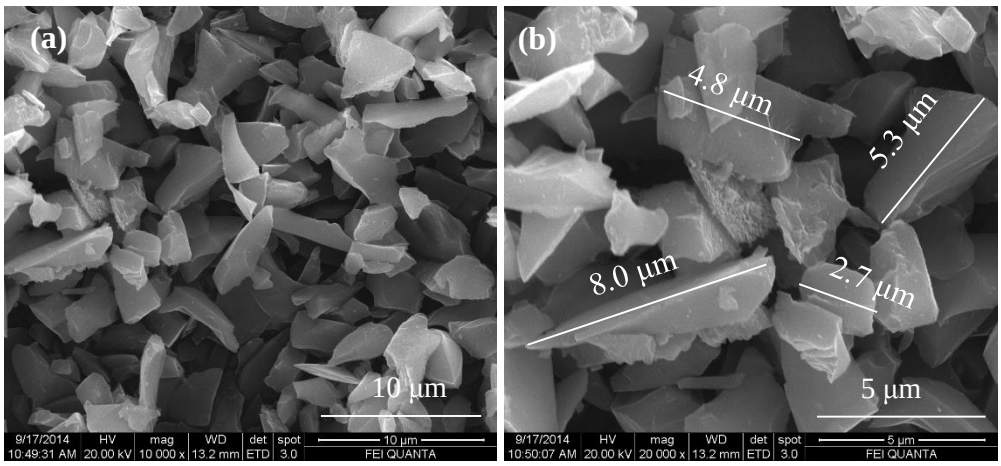

Figure 4.3 SEM Micrographs of boron carbide particles (a) 10,000x magnification, (b) 20,000x magnification.

Figure 4.4 shows the XPS spectrum of the as-received boron carbide material. XPS results revealed the existence of B, C, O, Fe elements in the material. The B1s peak at 187.2 eV and C1s peak at 285 eV represent B_4C. The O1s peak at 532.2 eV can represent the oxygen element in B_2O_3 [85]. Fe2p3 peak at 725.7 eV corresponds to Fe_2O_3 [86]. The peak at 215 eV corresponds to the satellite peak which is not related with the material being analyzed. XPS results showed the presence of impurities (Fe_2O_3, B_2O_3) in the material.

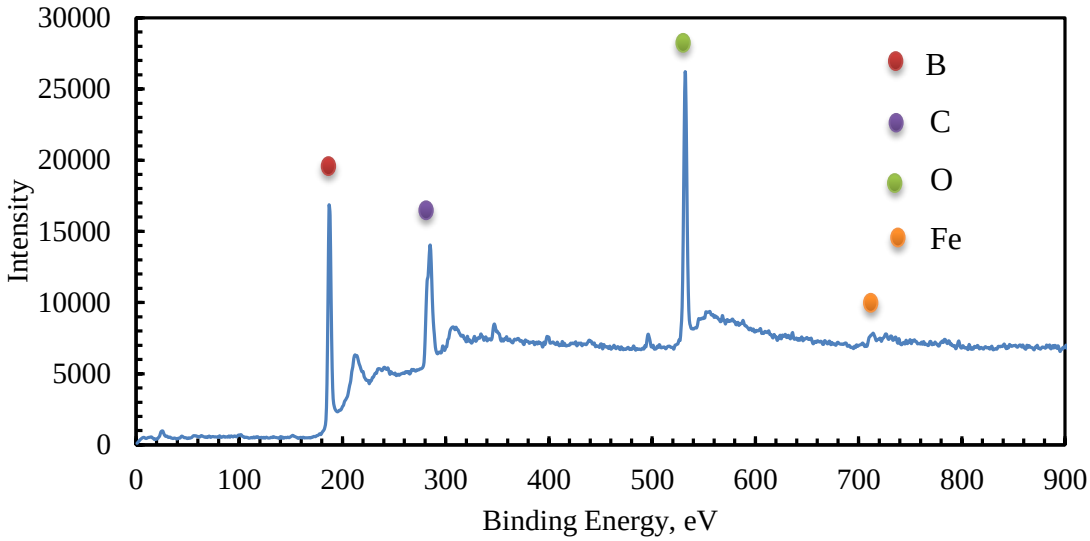

Figure 4.4 XPS spectrum of boron carbide.

The atomic elemental percentage of boron and carbon in the as-received boron carbide is given in Table 4.1. The atomic ratio of C to B was approximately 0.52. According to the stoichiometry of B_4C, the atomic ratio of C to B is 0.25 [22]. The atomic ratio of the material was higher than the stoichiometric ratio. This situation may be due to the presence of free carbon in the material. XPS results are consistent with the XRD results.

Table 4.1 Atomic amount of boron and carbon in the as-received boron carbide.

Element	**Percentage, at.%**
Boron	53.0
Carbon	27.4

TGA analyses in different atmospheres are given in Figure 4.5. It was observed that boron carbide gained weight in temperature range between 550-800°C. Even though nitrogen provides an inert environment, there is still 12 wt.% gain in boron carbide until 800 °C. However, under air atmosphere, 63.4 wt.% increase in the weight of boron carbide was obtained. There is boron oxide layer formation at temperatures like 600°C. Therefore the temperature range of increasing weight gives information about the product of this heat treatment. In the XRD pattern which was shown in Figure 4.2, it was observed that there was formation of B_2O_3 and carbon due to the reaction of B_4C in air and this can be the explanation of increase in the weight of boron carbide in air atmosphere.

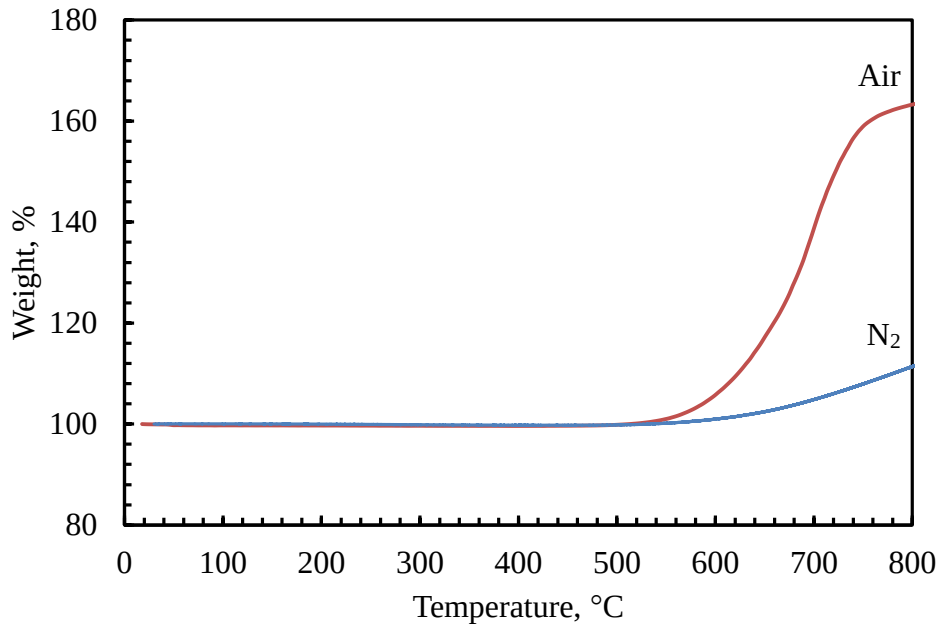

Figure 4.5 TGA plots of boron carbide under different atmospheres.

TGA analysis as a function of time was performed under nitrogen atmosphere at 800°C. After reaching 800°C, temperature was kept constant and the analysis was continued to understand how the weight of boron carbide changes in isothermal conditions for 2 hours. It was observed (Figure 4.6) that 51% of increase in weight of boron carbide was obtained at 800°C after 2 hours. The reason of this increment is thought to be formation of carbon and boron.

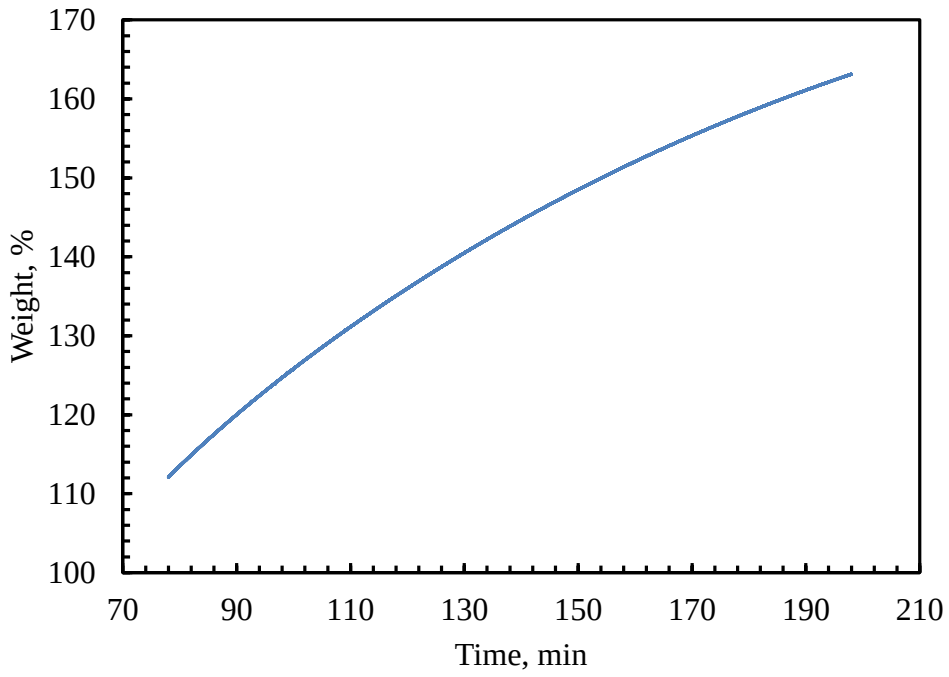

Figure 4.6 Time-dependent weight gain of boron carbide under nitrogen atmosphere.

FTIR spectrum of boron carbide is given in Figure 4.7. In this spectrum, the peak at wavenumber of 837 cm^{-1} shows the B–B–B–C bond in boron carbide structure. Peak at 1068 cm^{-1} corresponds to B–B bonds which indicates the boron content in material. Peak at 1373 cm^{-1} shows the disordered graphite structure. The peak at wavenumber of 1557 cm^{-1} can be attributed to existence of free carbon in the boron carbide structure or the linear C–B–B chains which combine the icosahedra [87, 88]. FTIR analysis showed that as-received B_4C has boron and graphitic carbon content.

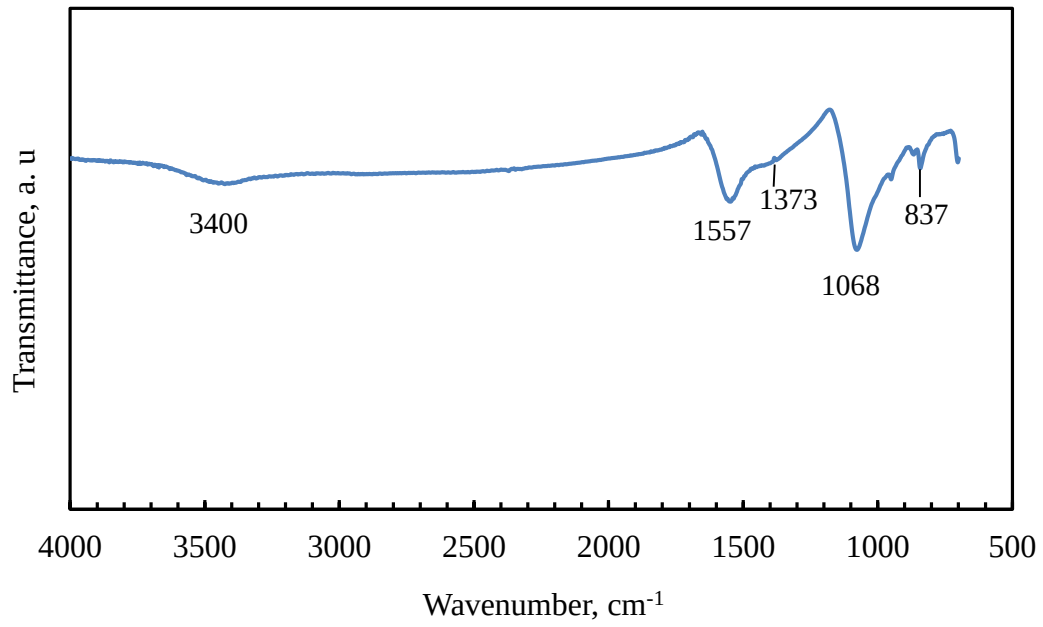

Figure 4.7 FTIR spectrum of boron carbide.

In order to reflect the actual characteristics of the epoxy polymer that is produced, the curing reaction between the epoxy resin and the curing agent has to be completed. FTIR and DSC analyses were performed to prove the existence of interaction between epoxy resin and the curing agent. DSC was also used to calculate the degree of curing of epoxy sample.

Figure 4.8 shows the curing mechanism of epoxy and amine based curing agent. In a curing reaction of epoxy and curing agent, the oxirane ring (C-O-C) opens and C links with the nitrogen of the amine curing agent. O-H and C-N bonds are formed during the curing reaction as it is shown in Figure 4.8. Therefore, the peak which represents the deformation of C-O-C bond should disappear, C-N and O-H bonds should be observed in FTIR spectrum of a cured epoxy.

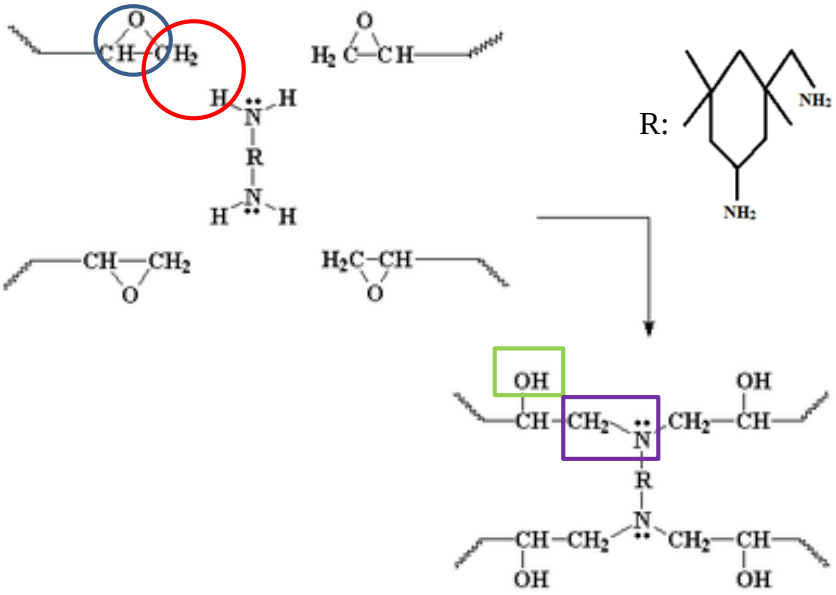

Figure 4.8 Curing mechanism of epoxy [68].

FTIR spectra of epoxy resin, curing agent and cured epoxy sample are shown in Figure 4.9. In Figure 4.9 for the cured epoxy sample, the peaks between 2959-2869 cm^{-1} refer to the methylene groups. Peaks at 1606 and 1508 cm^{-1} belong to the C=C and the C-C stretching of aromatic band, respectively. C-N bonds which are coming from the cycloaliphatic amines of curing agent, are detected at a wavenumber of 695 cm^{-1} and 1182 cm^{-1}. C-O-C stretching of ethers can be observed with the peak at 1032 cm^{-1} and C-O-C bond for oxirane group can be seen with the peak at 827 cm^{-1} [89].

Throughout the curing reaction between diglycidyl ether of bisphenol A based epoxy resin and cyloaliphatic polyamine based curing agent, C-O-C bond in the epoxy resin breaks, and O-H and C-N bonds are observed as stated in Figure 4.8. As it is seen in Figure 4.9, epoxy resin has peak at wavenumber of 915 cm^{-1} which represents the presence of C-O deformation band which is shown with red circle in Figure 4.8. Since this band deforms to give reaction with curing agent, the cured epoxy does not have peak at wavelength of 915 cm^{-1}. Hence, it is one of the proof that the curing reaction took place between epoxy resin and the curing agent. Since epoxy resin does not have nitrogen content, there cannot be seen any peaks at wavelength of 695 cm^{-1} which correspond to C-N bonds. However, after curing reaction, the cured epoxy has peak at 695 cm^{-1} that comes from the nitrogen of curing agent. This situation also show the

occurrence of curing reaction. The peak at wavelength of 3300 cm^{-1} shows the existence of O-H bonds.

FTIR analysis showed that the curing reaction between epoxy resin and curing agent was completed.

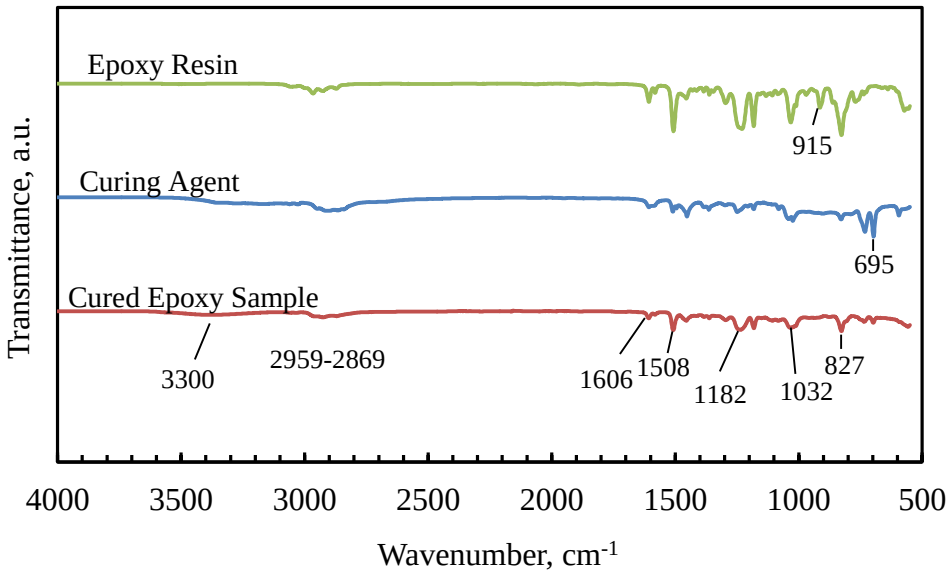

Figure 4.9 FTIR spectra of epoxy resin, curing agent and cured epoxy sample.

Another method for determination of the degree of curing is DSC analysis. It is a suitable analysis to calculate the percentage of curing according to the data which is taken first for the uncured epoxy polymer and then cured epoxy polymer samples. By measuring the peak area of curing exotherms of both plots, the curing degree of the epoxy samples was calculated according to Equation (2.7). A large exotherm peak is seen in the DSC plot of uncured epoxy sample. 99% of curing was obtained since there was a small exotherm peak in DSC plot of cured epoxy samples. The DSC plots of uncured and cured epoxy samples and the calculations for the curing degree are given in Appendix B. It can be said that FTIR and DSC results are in good agreement with each other which shows the curing reaction was completed.

4.1 FTIR Results of Epoxy/Boron Carbide Composites

Figure 4.10 shows the FTIR spectra of the neat epoxy sample and the EP/B_4C composites with 0.5, 1, 3, 5 and 8% of boron carbide content. FTIR spectrum of as-received boron carbide powder was given in Figure 4.7 with the characteristic peaks of boron carbide at wavenumbers of 837, 1068, 1373, 1557, 3400 cm^{-1}. Figure 4.10 shows that FTIR spectra of neat epoxy and EP/B_4C composites are the same. It can be said that, there is no change in chemical structures of the composites with the addition of boron carbide. Boron carbide acts as an additive only in the epoxy matrix which means no reaction takes place between B_4C and epoxy matrix.

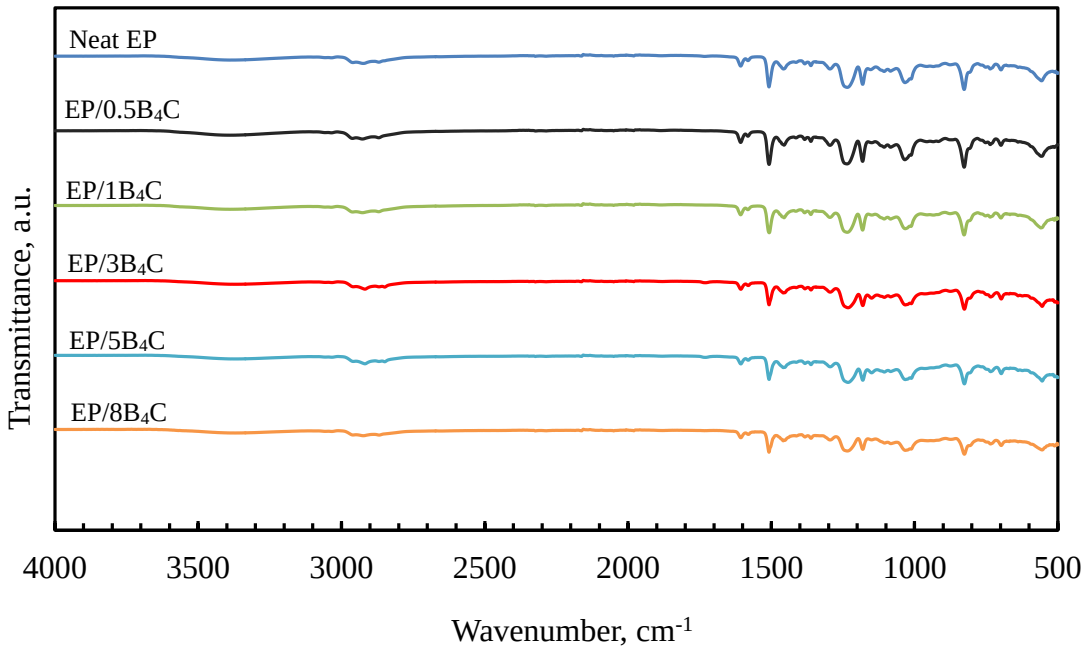

Figure 4.10 FTIR spectra of neat epoxy and epoxy/boron carbide composites.

4.2 XRD Analysis of Epoxy/Boron Carbide Composites

XRD analysis is a reasonable way to understand whether or not boron carbide remains as an additive in the polymer composites. XRD analyses were performed between 2θ values of 5° and 50° for the neat epoxy and EP/B_4C composites.

Figure 4.11 represents the XRD patterns of neat epoxy sample and epoxy composites with different boron carbide contents. Epoxy composites show peaks at 2θ values of 37.7°, 34.8° and 23.6°. Those peaks which belong to boron carbide increase with an increase in boron carbide content in the epoxy composites. The presence of these peaks shows that boron carbide cannot be distributed well or boron carbide particles remain as a separate phase in the epoxy matrix. On the other hand, XRD pattern of epoxy composite has a broad and unique characteristic peak of epoxy polymer at 2θ values of 18° which appoints the amorphous structure of epoxy matrix as mentioned in the literature [90].

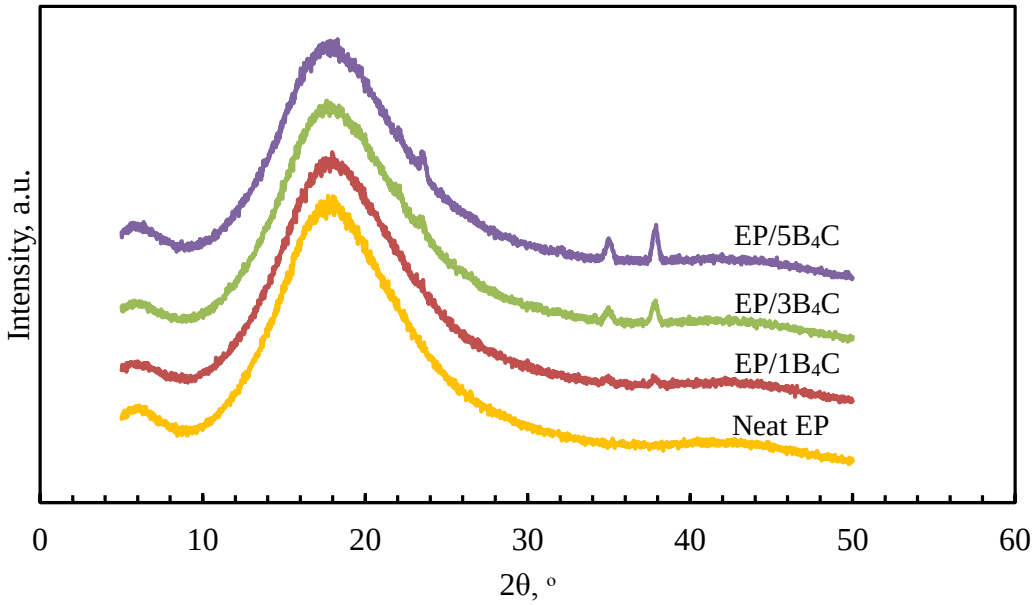

Figure 4.11 XRD patterns of EP/B_4C composites.

4.3 Scanning Electron Microscopy (SEM) Analysis

SEM analysis is used to observe the surface fractures of the composites and distribution of the filler into the epoxy matrix. Impact and some tensile samples were used to obtain the morphologies of the neat epoxy and the EP-based composites.

4.3.1 SEM Analysis of EP/B_4C Composites

The SEM micrographs of the neat epoxy composites and EP/B_4C composites with 0.5, 1, 3, 5 and 8% addition of boron carbide are given at 1,000, 5,000, 10,000 and 20,000 magnifications in Figures 4.12- 4.20.

Impact and/or tensile fractured surfaces of neat epoxy and epoxy-based composites were used for the SEM analyses.

Figure 4.12 shows the SEM images of impact fractured neat epoxy samples at four different magnifications. It is observed that neat epoxy sample has a smooth surface which appoints the brittle fracture. Sharp propagation lines in the figure are due to the brittle nature of the epoxy.

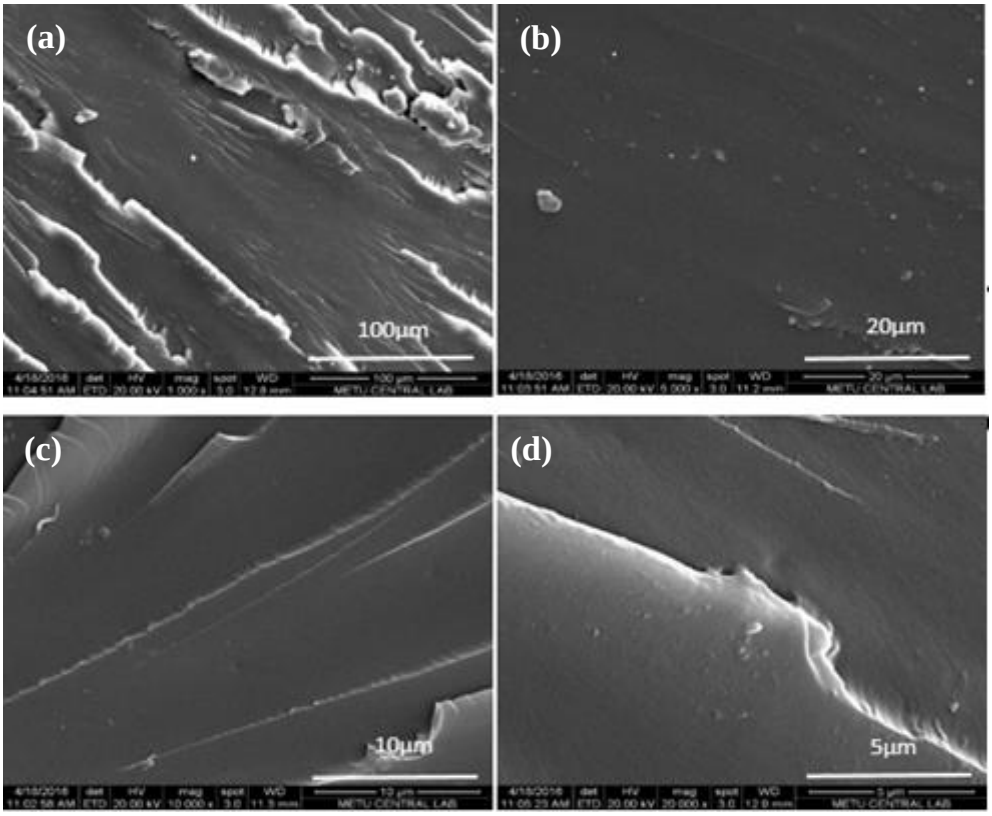

Figure 4.12 SEM images of Neat EP (a) 1,000x magnification, (b) 5,000x magnification, (c) 10,000x magnification, and (d) 20,000x magnification.

Figure 4.13 shows the SEM analysis results for impact fractured EP/0.5B_4C composite. The fracture surface is rougher than that of neat epoxy sample. The addition of B_4C to the epoxy matrix imparts surface roughness which can be seen through the tortuous lines on the fractured surfaces.

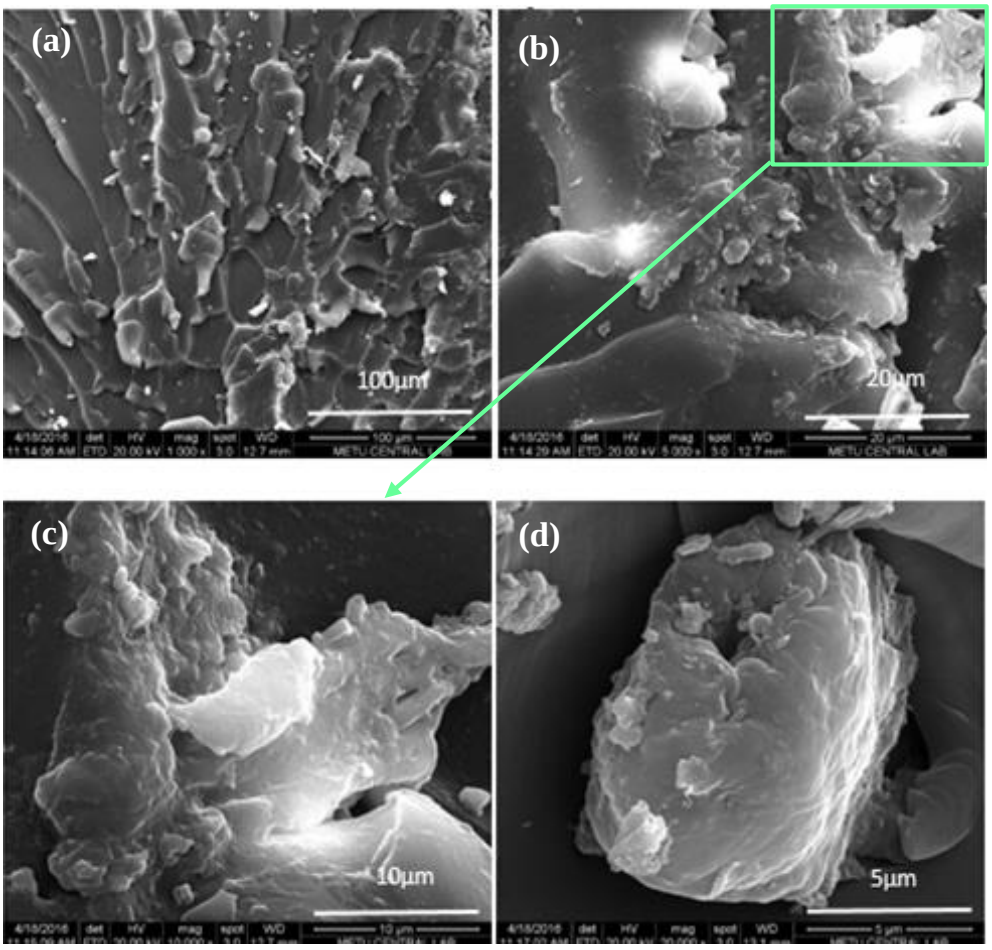

Figure 4.13 SEM images of EP/0.5B_4C composites (a) 1,000x magnification, (b) 5,000x magnification, (c) 10,000x magnification, and (d) 20,000x magnification.

SEM micrographs of tensile fractured EP/0.5B_4C composites are shown in Figure 4.14. The boron carbide particles are circled in the figure. On the other hand, high void content, which are produced with trapping air during mixing process of boron carbide and epoxy resin, can be seen in Figure 4.14a and b. The debonding between boron carbide particles and the epoxy matrix which is observed from Figure 4.14, creates a porous structure throughout the composite. It was mentioned that boron carbide has the irregular shape and size as seen in Figure 4.3. Therefore, the depths

and sizes of the voids which surround the B_4C particles depend on the each particle. Both existence of voids and irregular sizes of the particles should be responsible for the decrease in the tensile strength of the neat epoxy sample with the addition of 0.5% boron carbide. On the other hand, the fracture mechanism of tensile test samples is totally different from the impact test ones. In tensile test the samples are clamped from the top and the bottom of the specimen and pulled out. Therefore the fracture occurs from the weakest point throughout the sample. In the impact test, a pendulum hits the sample which causes breakage of the sample from this impact point. Nature of both tensile and impact tests causes the differences between the SEM images of tensile fractured and impact fractured EP/0.5B_4C composites.

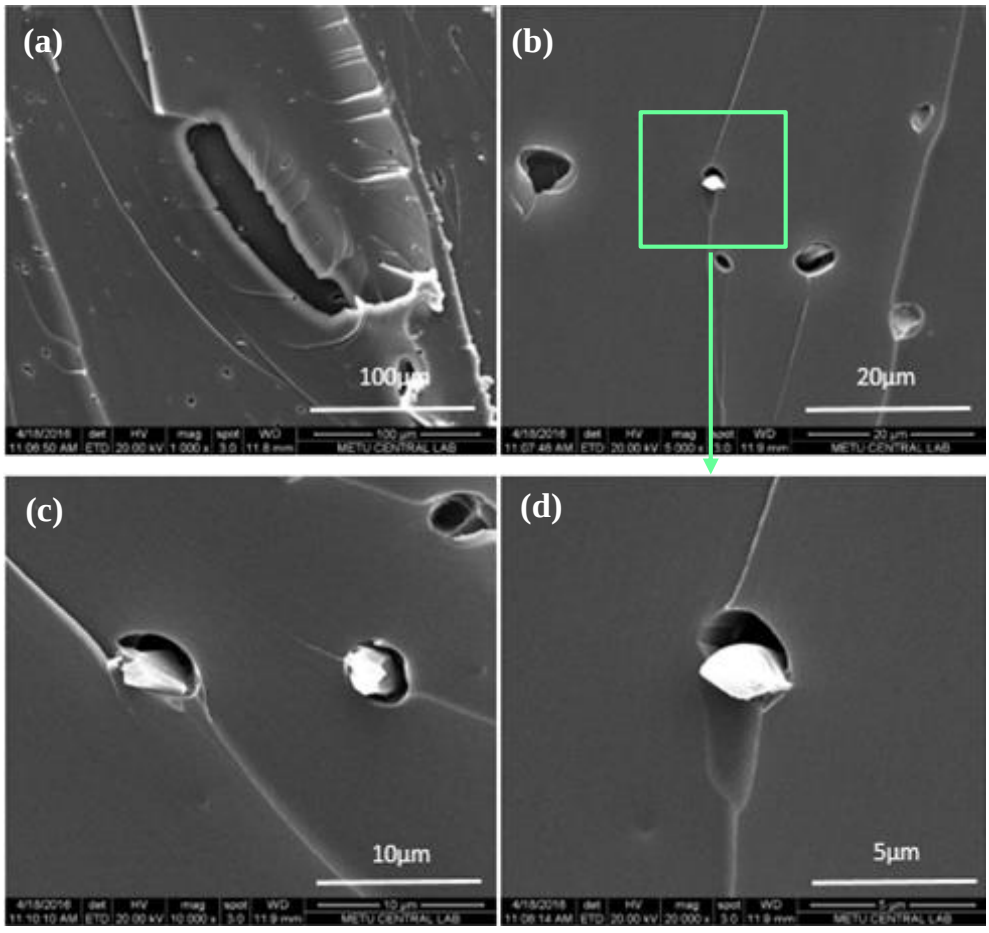

Figure 4.14 SEM images of tensile samples of EP/0.5B_4C composites (a) 1,000x magnification, (b) 5,000x magnification, (c) 10,000x magnification, and (d) 20,0000x magnification.

Figure 4.15 represents the SEM photographs of impact fractured EP/1B_4C composites. Similar to EP/0.5B_4C composites, the rougher surfaces of the composite are obtained with the addition of B_4C to the epoxy matrix. The B_4C particles in the matrix are shown in white circles. There exists some lack of adhesion between B_4C and the epoxy matrix.

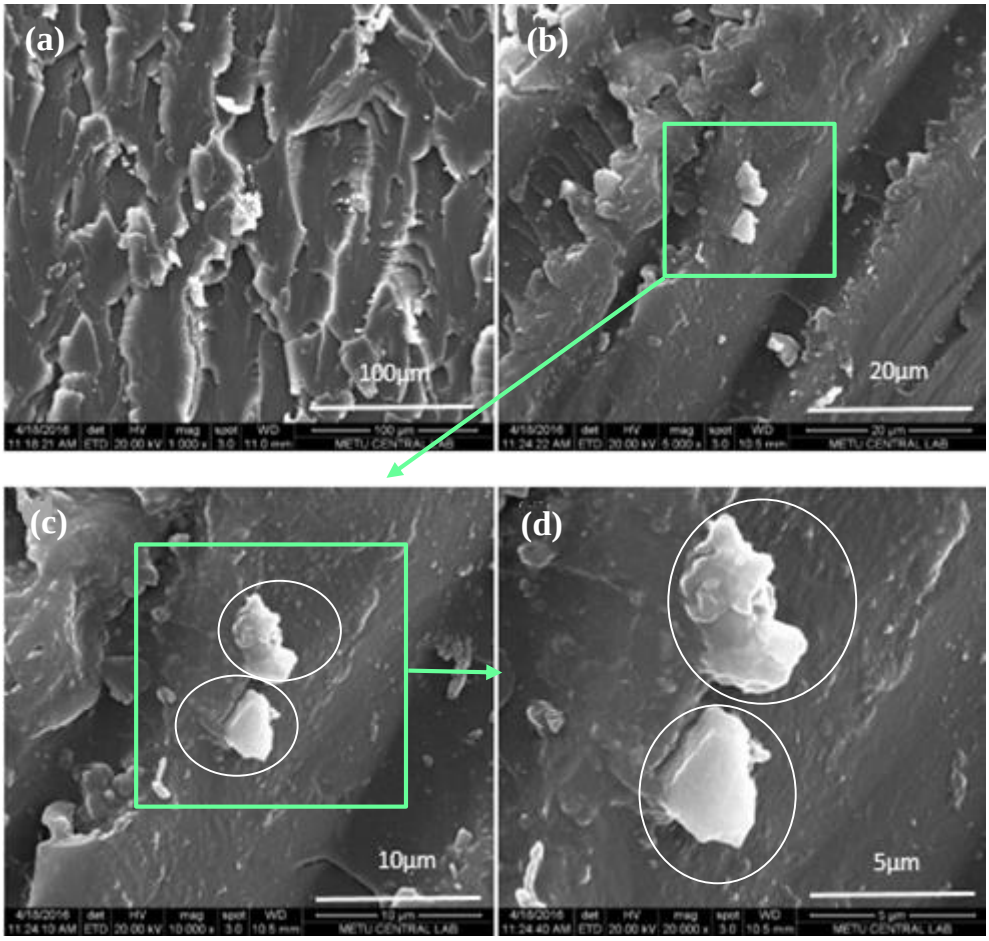

Figure 4.15 SEM images of EP/1B_4C composites (a) 1,000x magnification, (b) 5,000x magnification, (c) 10,000x magnification, and (d) 20,000x magnification.

Figure 4.16 shows the SEM images of the impact fractured EP/3B_4C composites. Boron carbide particles are circled on the SEM images. It can be said that the surface roughness of the neat epoxy increased with the addition of 3 wt.% boron carbide. The brittleness of the materials are expected to decrease due to the discontinuity in the crack propagation lines.

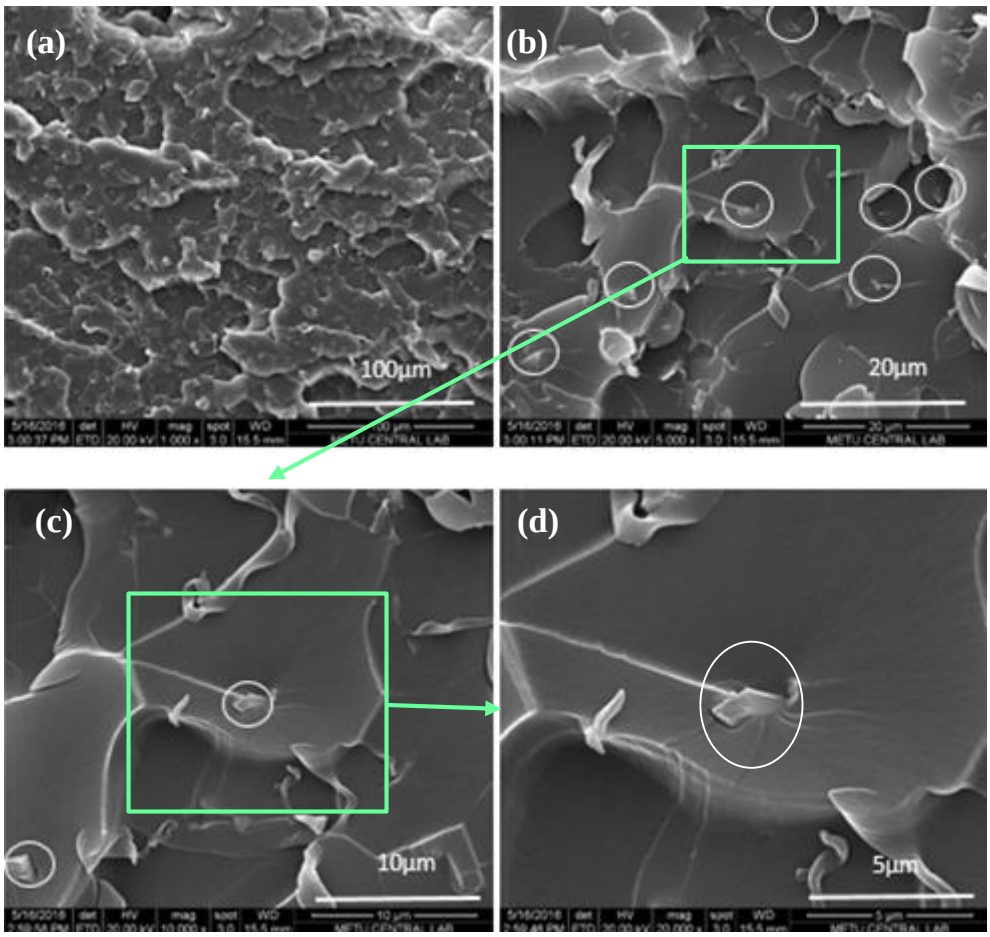

Figure 4.16 SEM images of EP/3B_4C composites (a) 1,000x magnification, (b) 5,000x magnification, (c) 10,000x magnification, and (d) 20,000x magnification.

Figure 4.17 shows the SEM images of the tensile fractured EP/3B_4C composites. The white circles in the SEM images show the boron carbide particles especially in lower magnifications (Figure 4.17b).

It is seen from Figures 4.16 and 4.17 that the boron carbide particles are separated from each other. On the other hand, these two figures have different fracture mechanisms since the fracture occurs from the weakest point in tensile test, and fracture occurs from the place that the pendulum hits the sample in impact test. Because of this difference in fracture surfaces, there is not seen any voids in Figure 4.16 but there are voids between boron carbide particles and the epoxy matrix in Figure 4.17c and d. It can be said that the distribution of B_4C particles is provided well.

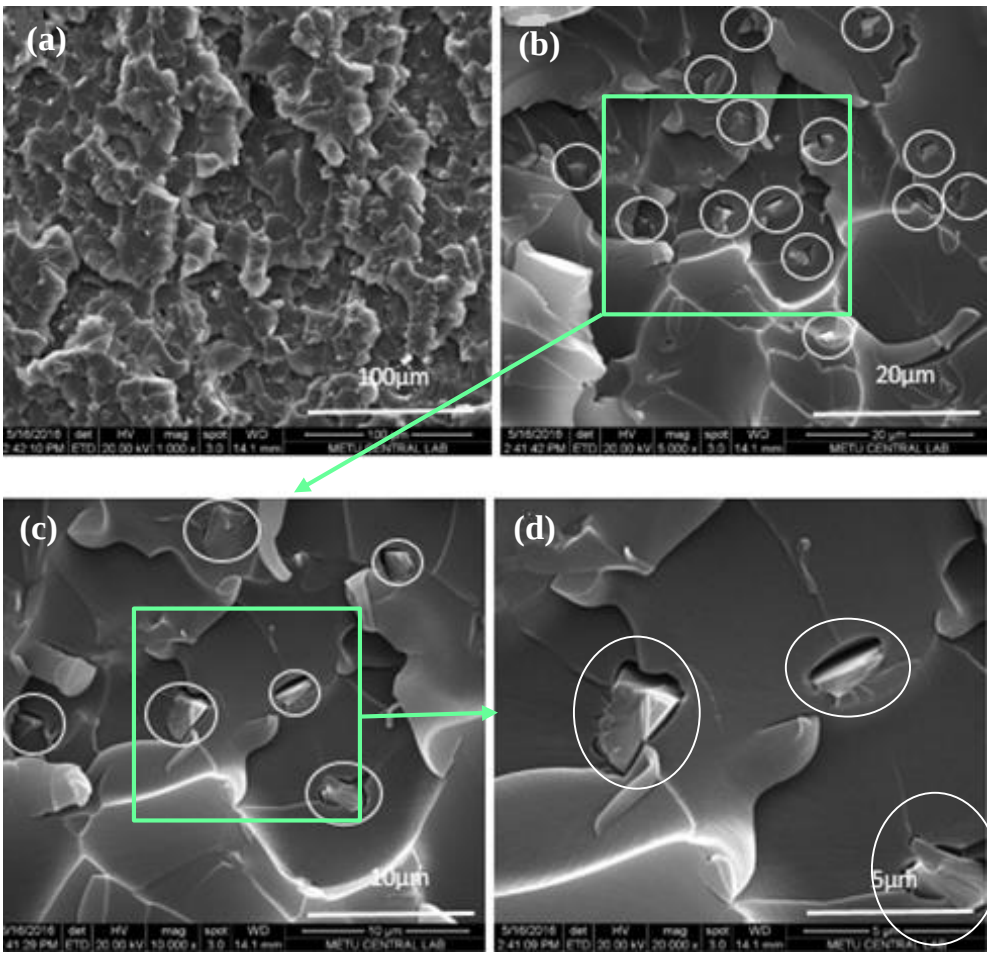

Figure 4.17 SEM images of tensile samples of EP/3B_4C composites (a) 1,000x magnification, (b) 5,000x magnification, (c) 10,000x magnification, and (d) 20,000x magnification.

SEM images of impact fractured EP/5B_4C composites were obtained as in Figure 4.18. SEM results revealed that boron carbide particles are embedded into epoxy matrix and not agglomerated. Besides, a few voids can be seen in the EP/5B_4C composite structure. It was stated before that the presence of the boron carbide peaks in Figure 4.11 indicated that boron carbide particles remained as a separate phase in the epoxy matrix. The distribution of the particles in the matrix seems to be well in the areas focused on the SEM analyses.

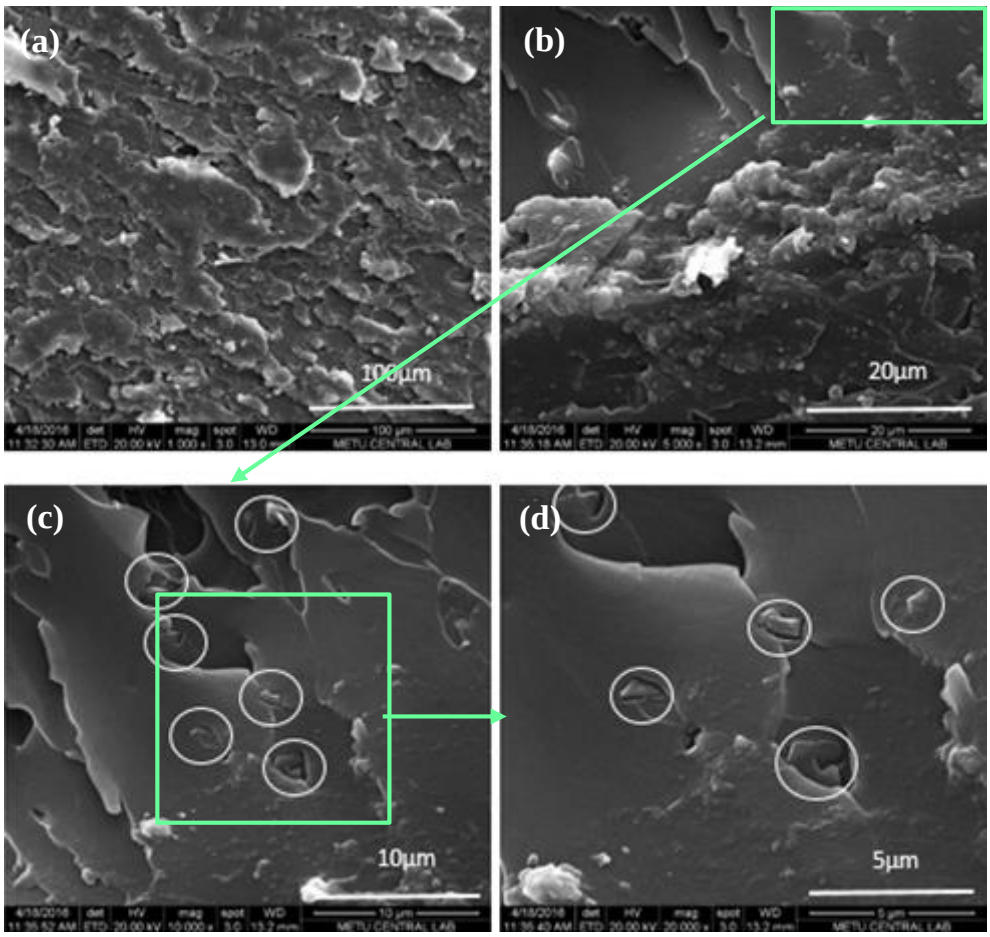

Figure 4.18 SEM images of EP/5B_4C composites (a) 1,000x magnification, (b) 5,000x magnification, (c) 10,000x magnification, and (d) 20,000x magnification.

SEM micrographs of impact fractured EP/8B_4C composites are represented in Figure 4.19. The irregular shape and size of voids can be seen from the SEM images. The voids do not have any particles in them as seen from one side of the fractured surface. There are also agglomerations of B_4C which are shown in Figure 4.19a as white circles.

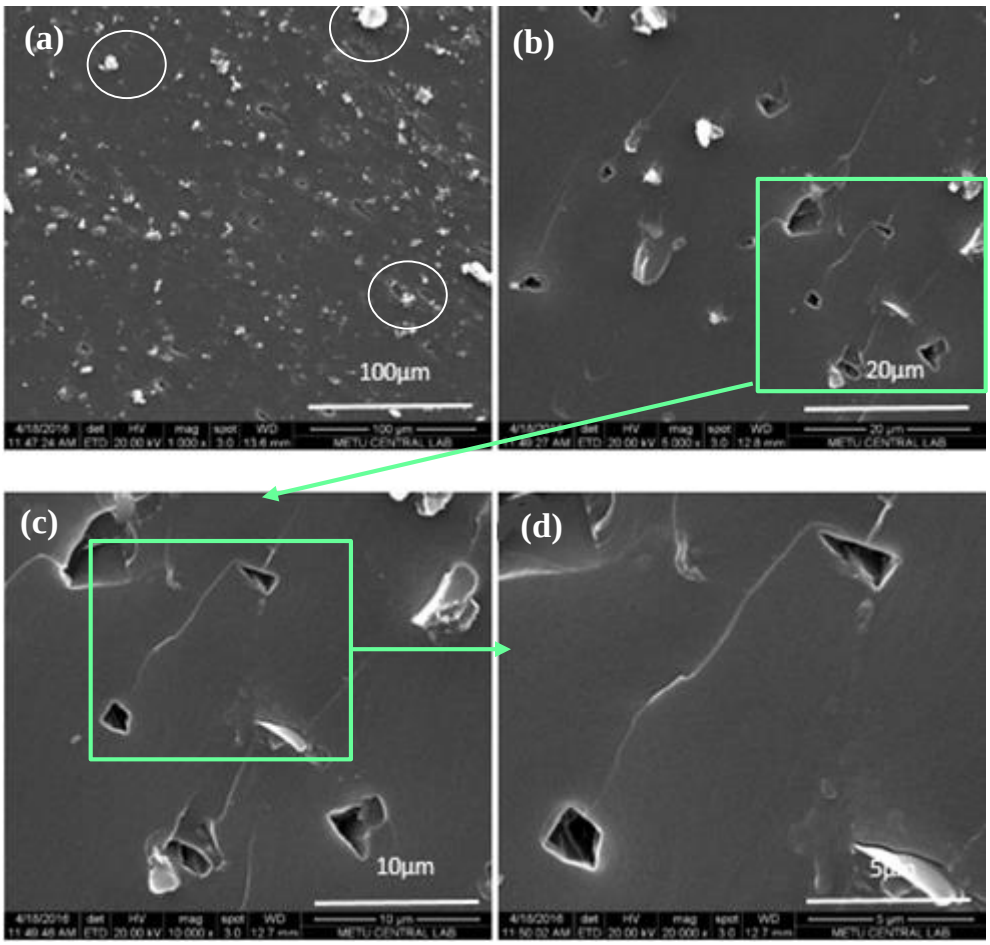

Figure 4.19 SEM images of EP/8B_4C composites (a) 1,000x magnification, (b) 5,000x magnification, (c) 10,000x magnification, and (d) 20,000x magnification.

Figure 4.20 shows the SEM images of EP/8B_4C composites. Since the content of boron carbide particles increased, B_4C agglomerations occurred in the structure of the composite (Figure 4.20b). These agglomerates act as stress concentrated regions which are responsible for the breakage of the sample under impact forces.

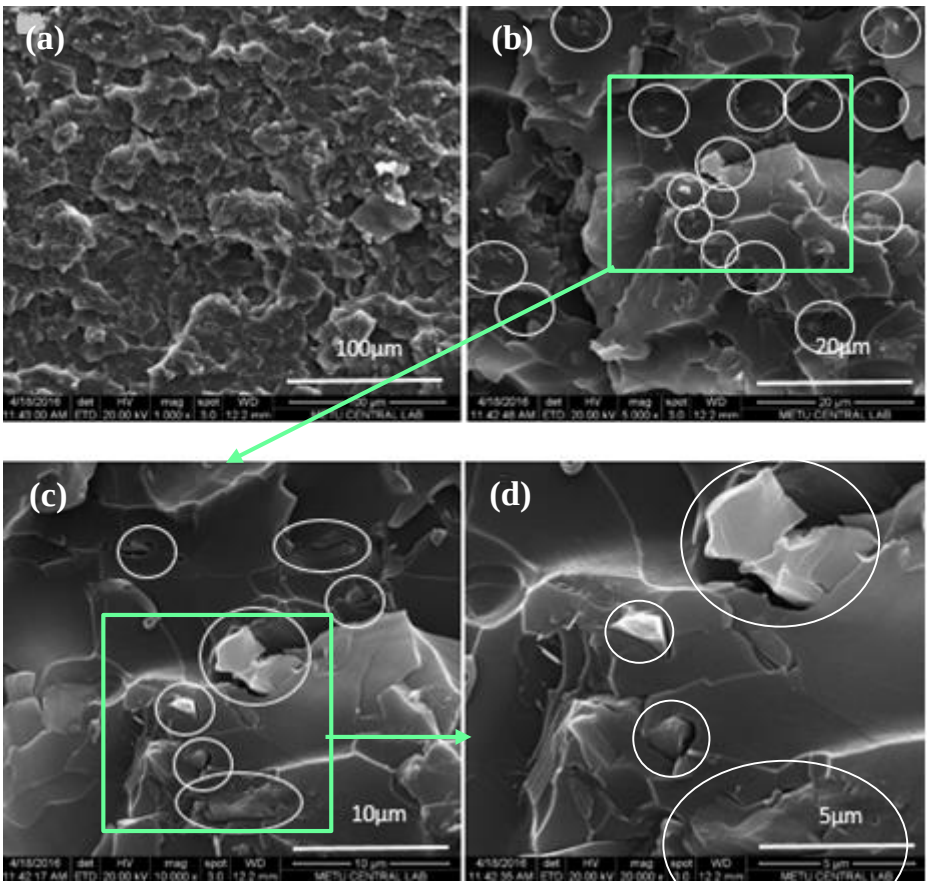

Figure 4.20 SEM images of tensile samples of EP/8B_4C composites (a) 1,000x magnification, (b) 5,000x magnification, (c) 10,000x magnification, and (d) 20,000x magnification.

4.3.2. SEM Analysis of Epoxy/Boron Containing Compound Composites and Epoxy/Melamine Phosphate Composites

The SEM micrographs of EP-based composites with boron containing compounds and melamine phosphate are given at 1000 and 5000 magnifications in the following Figures 4.21-4.22 and 4.24. Impact fractured composites were used for the SEM analyses.

Figure 4.21 shows the SEM micrographs of EP/1ZnB, EP/1BA and EP/1CaB composites at different magnitudes. The ZnB particles could not be observed in Figure 4.21a and b presumably due to the lower amount of addition. Also the BA particles could not be seen in Figure 4.21c and d, since BA is dissolved in the epoxy matrix during material preparation step. On the other hand, the CaB particles in Figure 4.21e and f can be observed which are circled in white color. There exists a small void between the interface of the particle and the matrix which may be the indication of a poor adhesion among them.

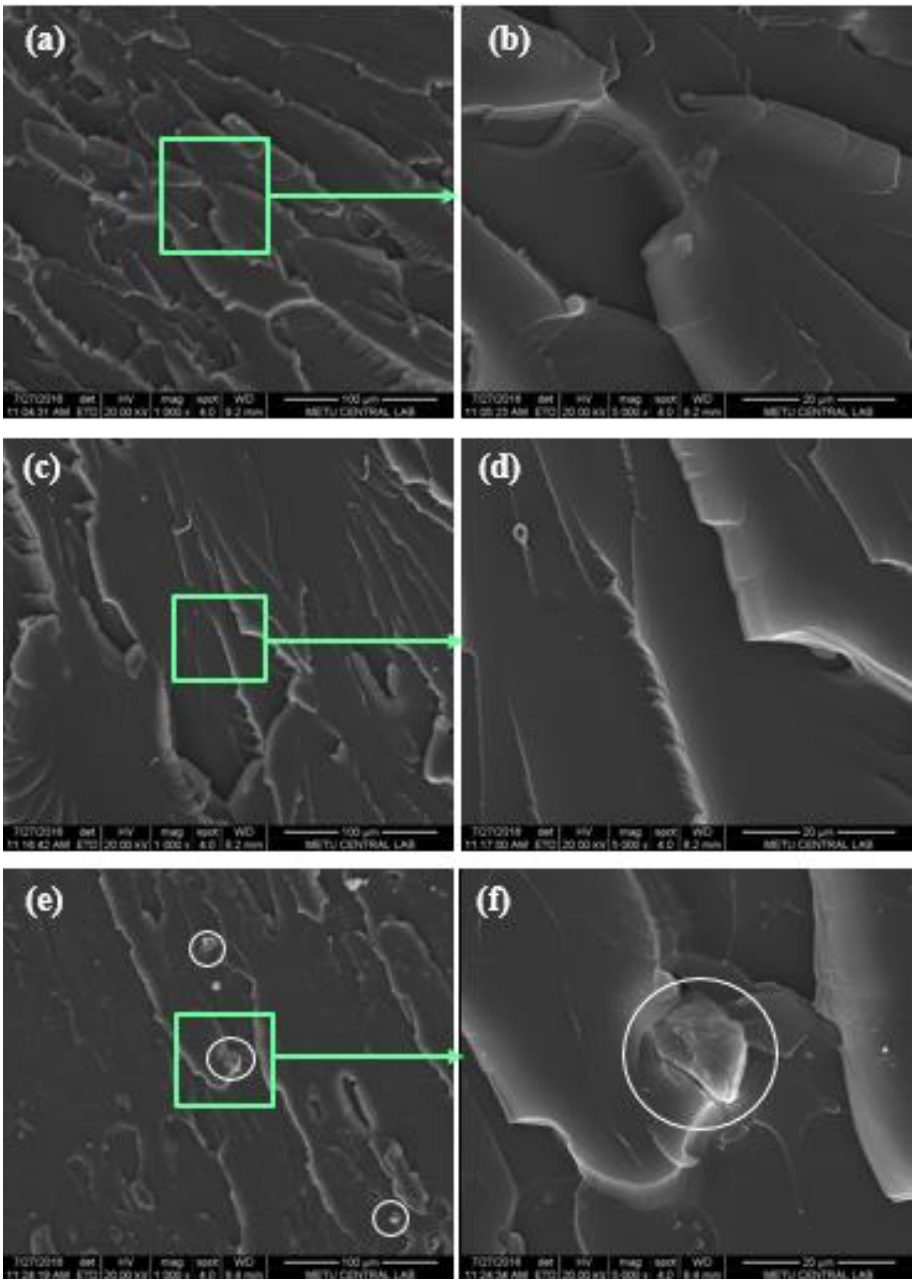

Figure 4.21 SEM images of samples of (a) EP/1ZnB at 1,000x magnification, (b) EP/1ZnB at 5,000x magnification, (c) EP/1BA at 1,000x magnification, (d) EP/1BA at 5,000x magnification, (e) EP/1CaB at 1,000x magnification, and (f) EP/1CaB at 5,000x magnification.

The SEM micrographs of EP/3B_4C/1ZnB, EP/3B_4C/1BA and EP/3B_4C/1CaB composites at different magnitudes are shown in Figure 4.22. The roughness of the fracture surface of these ternary composites increased due to higher amount of additives, when they were compared with the neat epoxy and EP/1ZnB, EP/1BA and EP/1CaB composites. Since BA was soluble in the epoxy matrix, the surface of the fracture was smoother than the other types of additions.

B_4C and ZnB particles can be seen in Figure 4.22b in white circles and yellow circle, respectively. In Figure 4.22d, B_4C particle was shown in white circle and no BA particles can be seen. CaB particles in yellow circles and B_4C particles in white circles were shown in Figure 4.22f. No agglomerations were observed according to the areas which are focused on the SEM images.

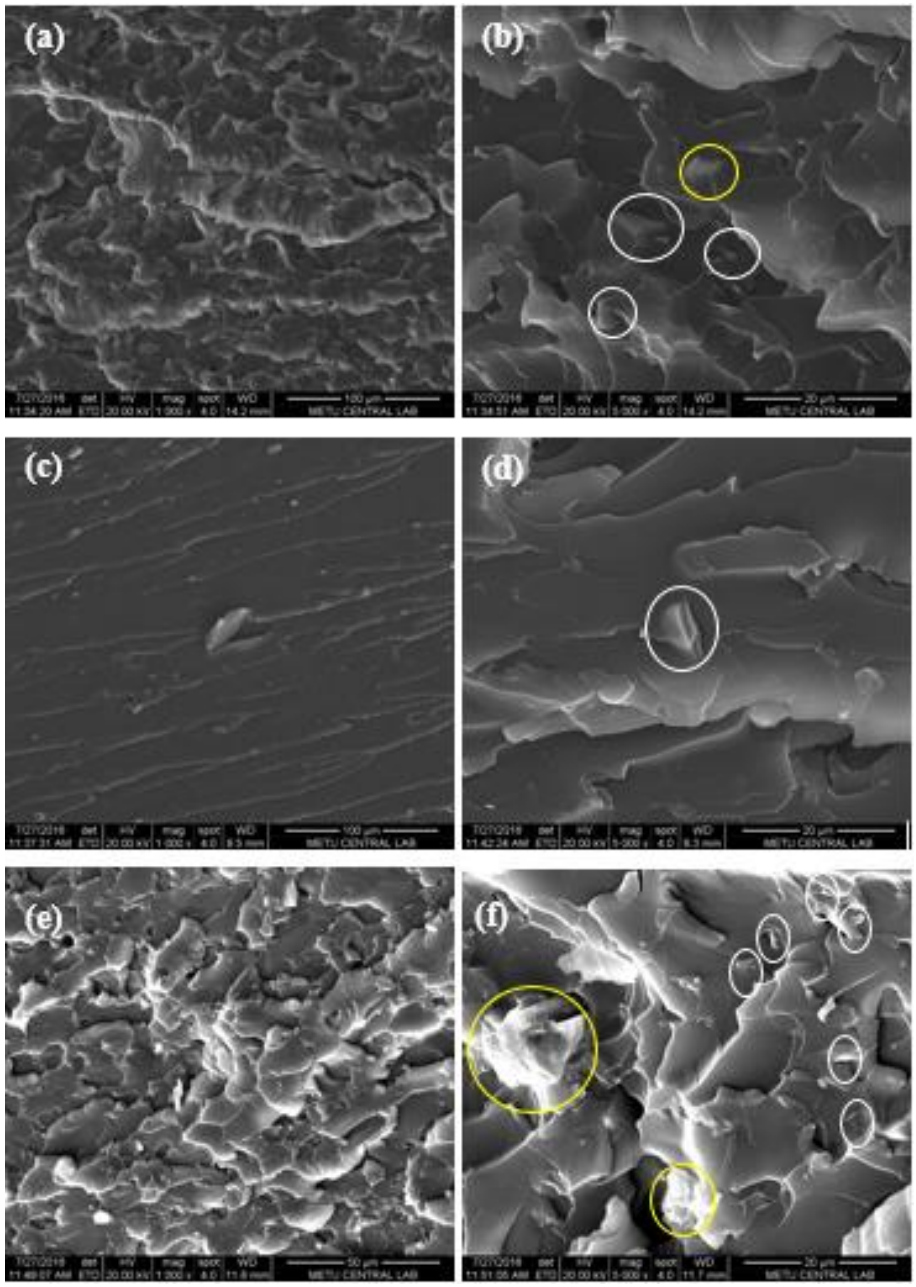

Figure 4.22 SEM images of samples of (a) EP/3B_4C/1ZnB at 1,000x magnification, (b) EP/3B_4C/1ZnB at 5,000x magnification, (c) EP/3B_4C/1BA at 1,000x magnification, (d) EP/3B_4C/1BA at 5,000x magnification, (e) EP/3B_4C/1CaB at 1,000x magnification, and (f) EP/3B_4C/1CaB at 5,000x magnification.

Figure 4.23 shows the EDX spectra of SEM images of EP/1CaB (Figure 21f), EP/3B_4C/1ZnB (Figure 22b), and EP/3B_4C/1CaB (Figure 22f). Ca and Zn came from CaB and ZnB. Therefore, the existence of CaB and ZnB in the corresponding composite structure was verified based on the EDX results. In addition, gold-palladium alloy coated on the surface of the EP/1CaB can be seen from Figure 4.23a.

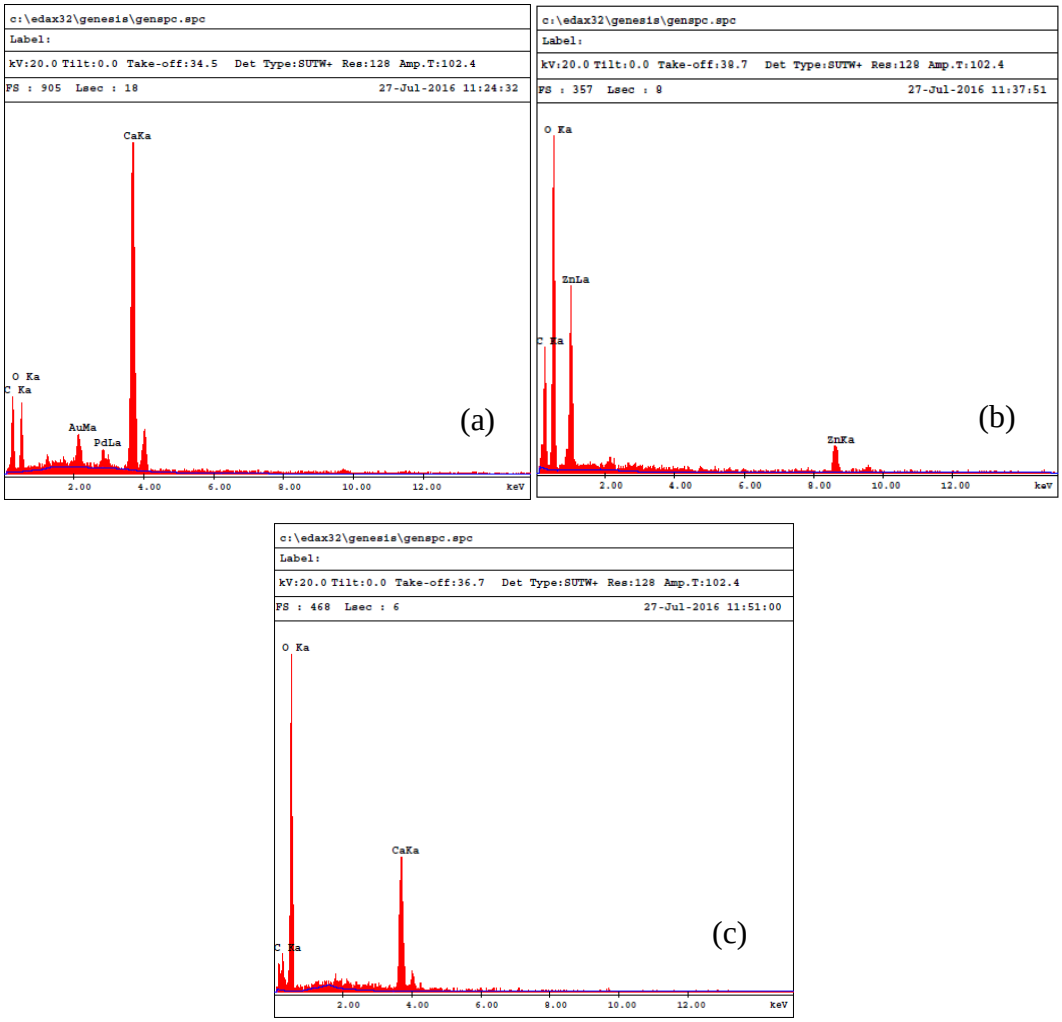

Figure 4.23 EDX spectra of (a) EP/1CaB, (b)EP/3B_4C/1ZnB, and (c) EP/3B_4C/1CaB composites.

SEM micrographs of EP/10MP, EP/10MP/3B_4C and EP/10MP/3B_4C/1ZnB are represented in Figure 4.24. The fracture surface of EP/MP composites showed the roughest surfaces since their addition amounts were higher than all the other composites which were prepared throughout this study. MP and B_4C particles were shown in green and white circles, respectively. Agglomerations among the MP particles were observed for EP/10MP, EP/10MP/3B_4C and EP/10MP/3B_4C/1ZnB composites according to Figure 4.24.

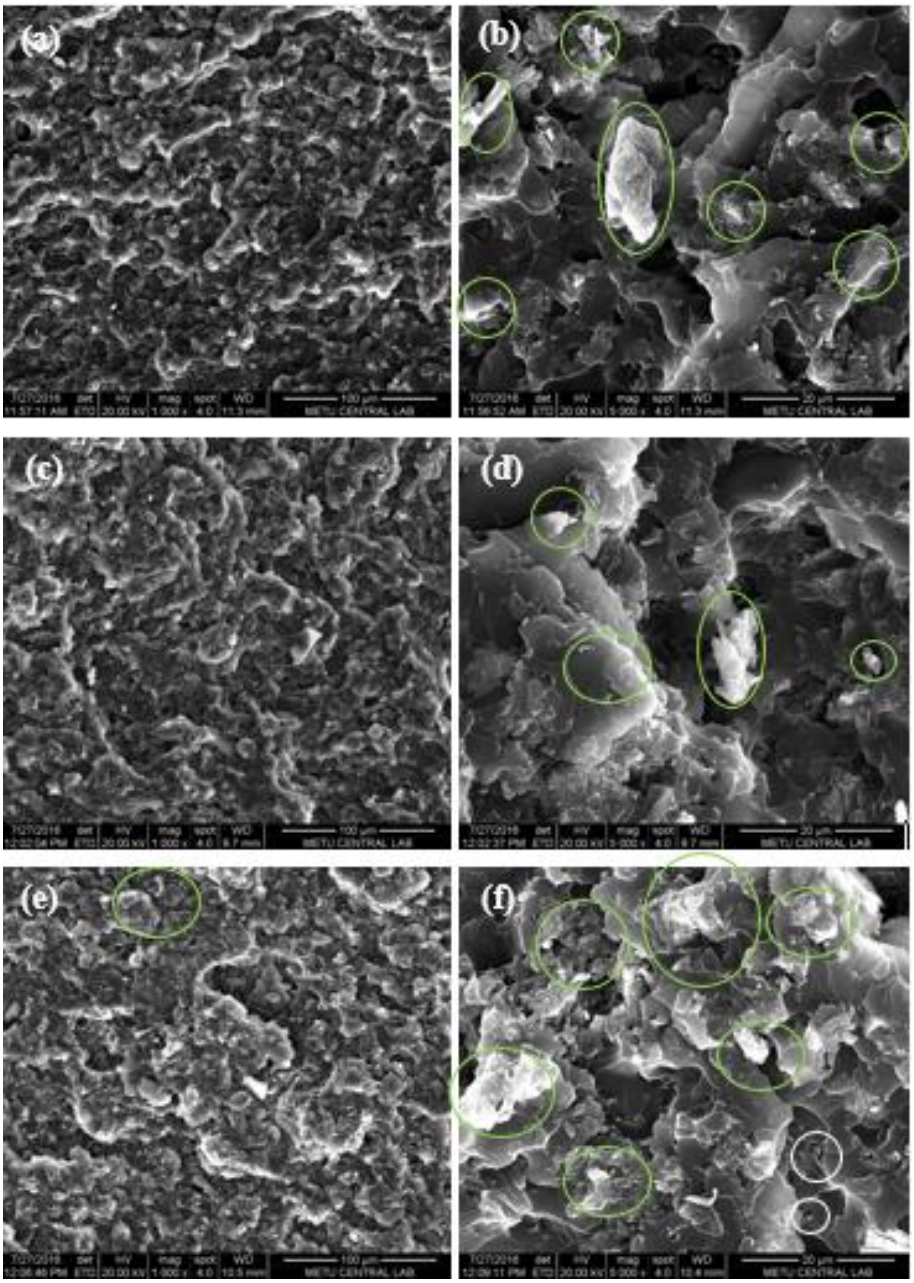

Figure 4.24 SEM images of samples of (a) EP/10MP at 1,000x magnification, (b) EP/10MP at 5,000x magnification, (c) EP/10MP/3B_4C at 1,000x magnification, (d) EP/10MP/3B_4C at 5,000x magnification, (e) EP/10MP/3B_4C/1ZnB at 1,000x magnification, and (f) EP/10MP/3B_4C/1ZnB at 5,000x magnification.

4.4 Mechanical Analysis of Epoxy-Based Composites

4.4.1 Mechanical Properties of Epoxy/Boron Carbide Composites

Tensile, impact and Shore D hardness tests were carried out to understand the effect of addition of boron carbide on the mechanical properties of epoxy-based composites. The aim of the study was to improve both mechanical and flame retardant properties of epoxy. Tensile and impact tests results are tabulated in Appendix C.

Figure 4.25 represents the tensile test results of EP/B_4C composites. This figure shows the effect of boron carbide amounts on the tensile strength values.

Neat epoxy sample had a tensile strength value of 48 MPa. The addition of 0.5% and 1% boron carbide decreased the tensile strength of the neat epoxy. In SEM analysis, the existence of voids and irregular B_4C particle sizes was observed (Figure 4.14). These voids and irregular particle sizes might cause a decrease in the tensile strength. There was not any interaction between boron carbide and epoxy. While the epoxy was curing, the voids were formed between the boron carbide and the epoxy resin.

Further addition of boron carbide slightly increased the tensile strength, and finally for the 8% addition of boron carbide the tensile strength was 50 MPa which was very similar to that of the epoxy. There are competing effects of B_4C and the preparation technique of the composite. Similar tensile strength values of EP/8B_4C and neat epoxy may be attributed to the voids and irregular sizes of the particles, agglomerations from insufficient distribution at 8wt.% B_4C loading and also effect of B_4C particles on the degree of curing of epoxy composites.

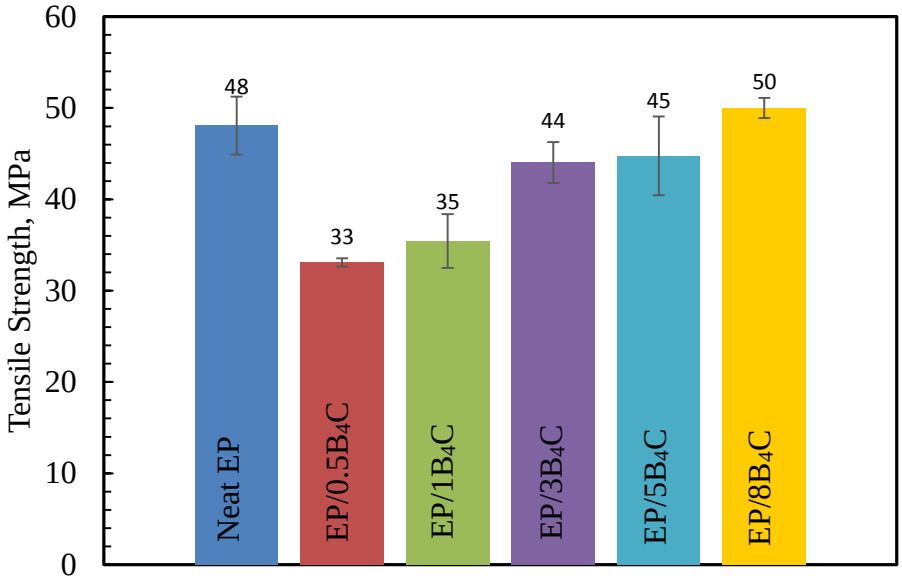

Figure 4.25 Tensile strengths of neat epoxy and epoxy/boron carbide composites.

Elastic moduli of neat epoxy samples and EP/B_4C composites are shown in Figure 4.26. Neat epoxy sample had an elastic modulus value of 2815 MPa. As it is seen from the figure, the same trend as the tensile strength values were observed for the elastic moduli of the neat epoxy samples and the composites. Even though B_4C particle is known to have very high modulus and hardness, it did not increase the elastic modulus of the EP-based composites as expected. This is mainly due to the defects and voids coming from the preparation technique and insufficient adhesion among the constituents. Also, the amount of B_4C which was used may not be sufficient to increase the elastic modulus values.

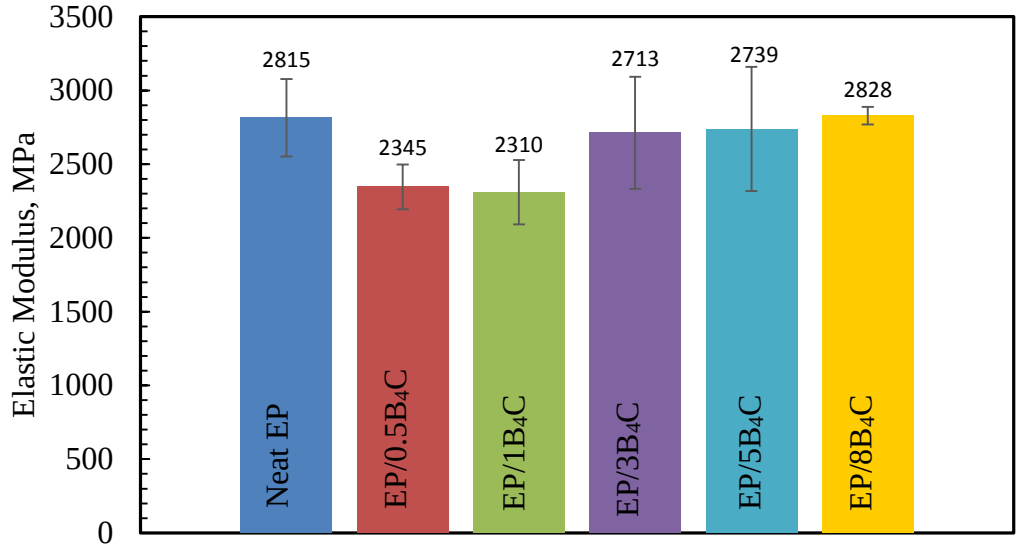

Figure 4.26 Elastic moduli of neat epoxy and epoxy/boron carbide composites.

Figure 4.27 represents the results for the elongation at break values of neat epoxy sample and the composites. The elongation at break of neat epoxy was 3.9%. It can be said that the elongation at break values are in the range of brittle material. SEM images showed the presence of agglomerations in the EP/8B_4C composite (Figure 4.19a). The increase in the elongation at break value of neat epoxy with the addition of 8% B_4C may arise from the voids in the composite structure which were formed during the preparation of the composites. These voids were the indication of low degree of crosslinking in the composite structure. Another reason may be the sliding of B_4C particles in the agglomerates at this high loading which may lead to the highest elongation at break value for EP/8B_4C composite.

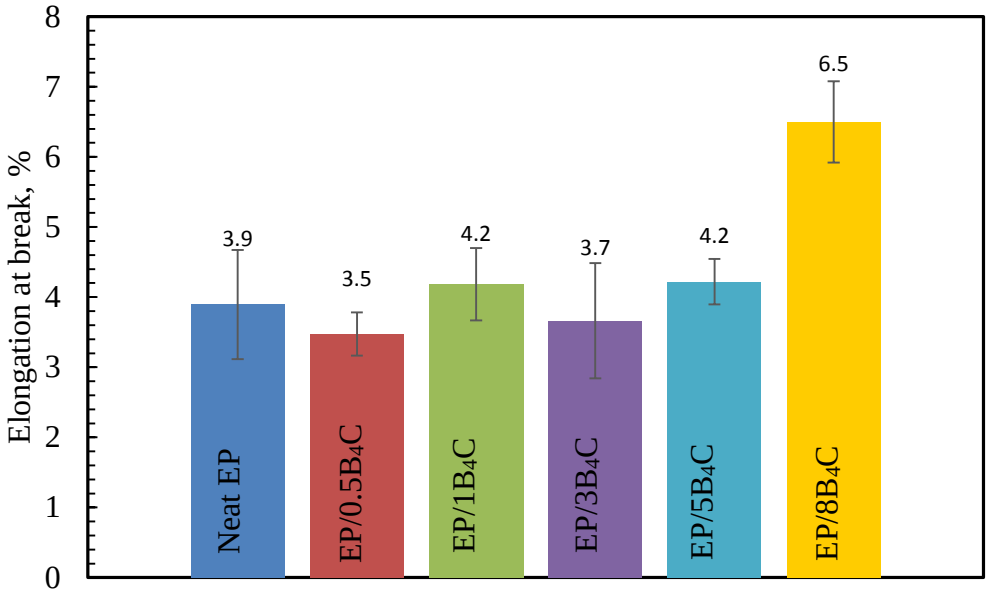

Figure 4.27 Elongation at break of neat epoxy and epoxy/boron carbide composites.

Impact strength values of neat epoxy and the EP/B_4C composites are given in Figure 4.28. The impact strength of neat epoxy was 11 kJ/m^2. The impact strength values of the composites increased with an increase in boron carbide content. As boron carbide is hard and rigid filler, it acted as toughening agent in the epoxy matrix and created debonding between matrix and the filler. Therefore further addition of boron carbide increased the capability of energy absorption which means the increase in the impact strength of the composites. The impact strength for the EP/$8B_4C$ composite decreased when it was compared with EP/$5B_4C$, because there might be agglomerations for further additions of B_4C (more than 5wt.% B_4C addition).

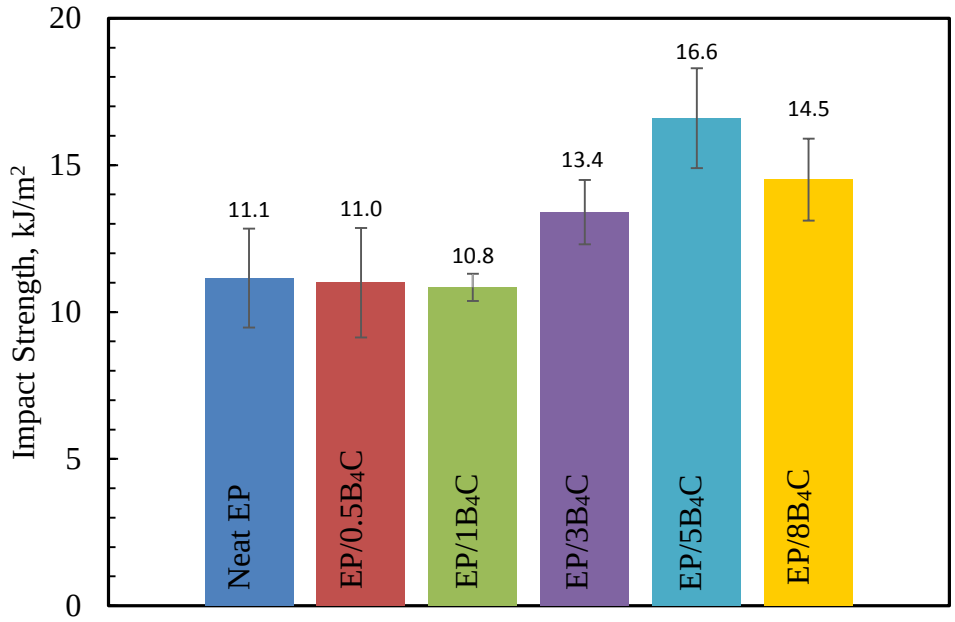

Figure 4.28 Impact strengths of neat epoxy and epoxy/boron carbide composites.

Shore D hardness test, which defines a range of hardness, was carried out for neat epoxy, EP/B_4C and epoxy-based composites to measure how hard the sample surface is.

Table 4.2 shows the data of the Shore D hardness values of neat epoxy and EP/B_4C composites. It is seen from the table that neat epoxy has a Shore D hardness value of 83.2 which is close to the value for hardness of DGEBA-based epoxy polymer [91]. The addition of boron carbide to the neat epoxy slightly increased the hardness of the composites. Boron carbide could not show its extreme hardness on the composites because of the lower amounts of B_4C.

After mechanical and flame retardancy tests which will be given in following subsections, the preparation of the epoxy composites were continued with the 3% addition of B_4C. EP/3B_4C system can be considered as a promising composite when combined with other boron containing compounds and melamine phosphate in order to obtain a potential improvement for its properties.

Table 4.2 Shore D hardness values of neat epoxy and EP/B_4C composites.

Sample Code	**Shore D Hardness**
Neat EP	83.2 ± 1.1
EP/0.5B_4C	85 ± 0.7
EP/1 B_4C	85.2 ± 0.4
EP/3 B_4C	86 ± 0
EP/5 B_4C	87 ± 0
EP/8 B_4C	86.5 ± 0.5

Shore D hardness values of epoxy-based composites are shown in Table 4.3. As it is seen from the table, all the composites exhibited higher hardness behavior when compared with neat epoxy except EP/1BA and EP/3B_4C/1BA composites. The decrease in hardness values of the composites containing BA may arise from the solubility of BA in acetone during the composite preparation step as stated before. It can be said that, this solubility problem caused a general decrease in mechanical properties of the composites containing BA. The maximum hardness value in Table 4.3 was observed with the addition of 10% MP and 3% B_4C to the neat epoxy. This might be because of the high hardness value of B_4C. Also it can be mentioned that EP/10MP/3B_4C composite exhibited slightly higher hardness than EP/3B_4C composite (Table 4.2) owing to higher hardness of EP/10MP with respect to the neat epoxy.

Table 4.3 Shore D hardness values of epoxy-boron containing compound composites and epoxy/melamine phosphate composites.

Sample Code	Shore D Hardness
Neat EP	83.2 ± 1.1
EP/1ZnB	83.8±0.8
EP/1BA	70.8±1.3
EP/1CaB	85±0
EP/3B_4C/1ZnB	85.6±0.5
EP/3B_4C/1BA	81±1.4
EP/3B_4C/1CaB	85±0.7
EP/10MP	85.4±0.5
EP/10MP/3B_4C	86.8±0.4
EP/10MP/3B_4C/1ZnB	85.8±0.4

4.4.2 Mechanical Properties of Epoxy/Boron Containing Compound Composites and Epoxy/Melamine Phosphate Composites

Tensile and impact tests were performed to determine the effects of the different additives on the mechanical properties of epoxy and epoxy/boron carbide composites. Boron containing flame retardants which are ZnB, BA and CaB and also an intumescent fire retardant MP were added to the epoxy resin. The existence of the synergistic effect between the boron carbide and the other flame retardants were also investigated through the characterization tests. Detailed data of tensile and impact tests for the epoxy-based composites are tabulated in Appendix C.

Tensile test data of epoxy-based composites is given in Figure 4.29. Tensile strength values for neat epoxy sample and EP/3B_4C composites were 48 and 44 MPa, respectively.

The addition of 1% of ZnB, BA and CaB slightly decreased the tensile strength of epoxy when they are compared with the neat epoxy. The addition of boron carbide to these composites strengthened the composites except for EP/3B_4C/1BA composites.

Boric acid is soluble in acetone on the contrary the other additives are not soluble. When BA was introduced with boron carbide, the solubility changed throughout the polymer solution in a visible way during the preparation of the composites. Also BA increased the speed of the curing in a noticeable way. The composites with BA even cured before they were put into the oven. Low curing temperature and inhomogeneous solubility in the preparation step caused to decrease in the tensile strength of EP/3B_4C/1BA. Addition of MP to the neat epoxy and EP/3B_4C composites lowered the tensile strength. Another composite was developed with ZnB addition to EP/10MP/3B_4C composite due to the promising properties of the constituents of the composites to investigate their combined effect in the composite. Addition of ZnB to MP/B_4C containing epoxy-based system decreased the tensile strength further. Because the addition of MP in higher contents resulted in agglomerations of the particles in the epoxy matrix. In general, it can be said that the increasing content of the additives with insufficient interfacial adhesion may be the result of the decrease in tensile strength values.

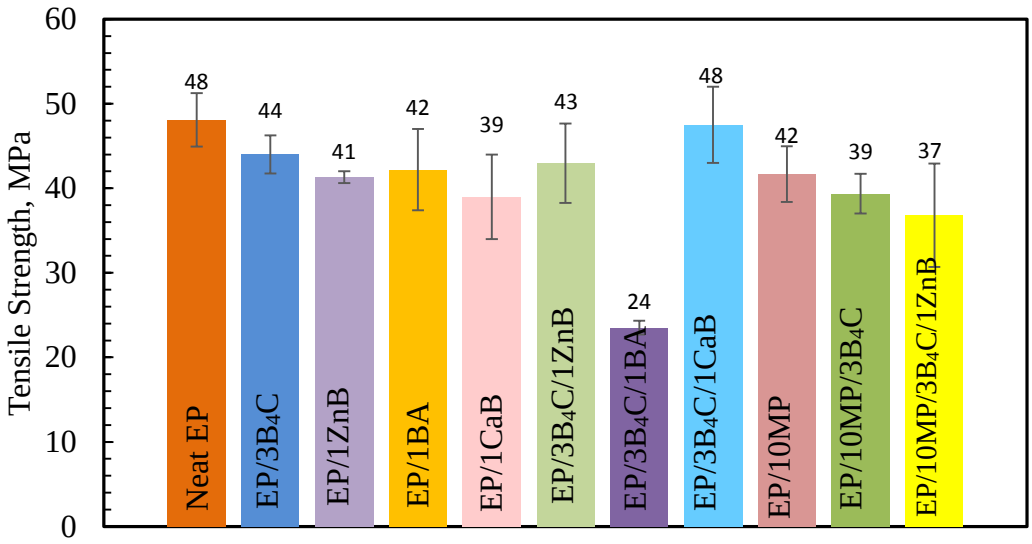

Figure 4.29 Tensile strengths of epoxy/boron containing compound composites and epoxy/melamine phosphate composites.

Elastic moduli of epoxy-based composites are shown in Figure 4.30. Elastic modulus values for neat epoxy sample and EP/3B_4C composites were 2815 and 2713 MPa, respectively.

All of the composites had lower elastic moduli (i.e. stiffness) than that of the neat epoxy. Poor adhesion and debonding between the particles and the epoxy matrix led to decrease in load transfer and decreased the elastic modulus. Addition of MP to the neat epoxy and EP/3B_4C composites decreased the elastic moduli, which may be due to a lower degree of crosslinking in the presence of the high amounts of additives in the epoxy-based composites. The reasons for decrease in stiffness may also come from the competing factors such as the inhomogeneous preparation conditions and the incompatibility of the constituents with each other. On the other hand, the increase in the elastic modulus of EP/10MP/3B_4C/1ZnB showed that ZnB and B_4C are compatible to each other.

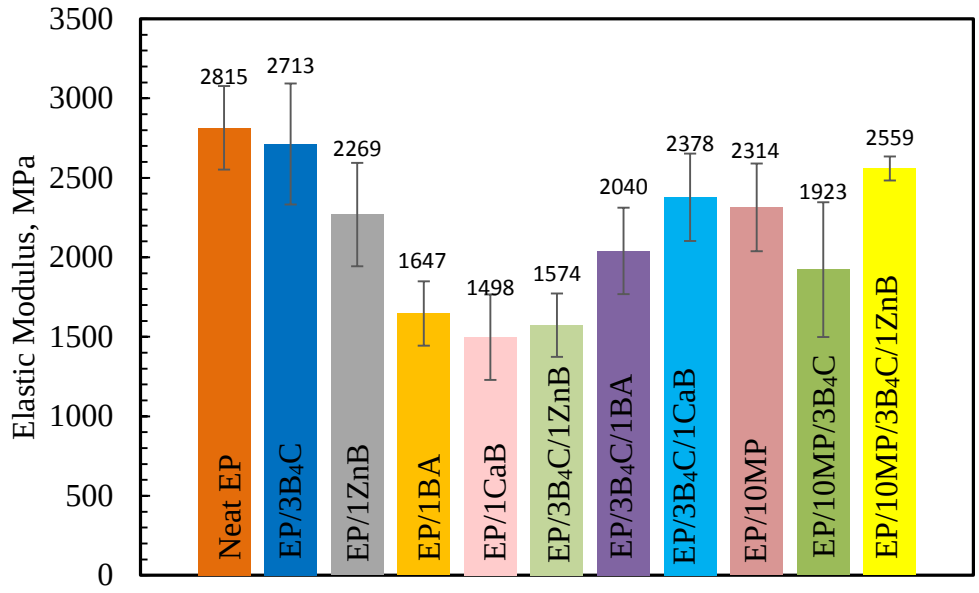

Figure 4.30 Elastic moduli of epoxy/boron containing compound composites and epoxy/melamine phosphate composites.

Figure 4.31 shows the elongation at break values for epoxy-based composites. Elongation at break values of neat epoxy sample and EP/3B_4C composites were 3.9% and 3.7%, respectively.

EP/3B_4C/1BA composites has the lowest elongation at break value among the materials studied in this thesis. This result can be explained with Figure 4.22. SEM analysis of impact fractured EP/3B_4C/1BA composite showed that there is a brittle fracture due to the smooth fracture surface of the composite. The solubility of BA in acetone changed the crosslinking conditions within the epoxy matrix, therefore,

inhomogeneous crosslinking occurred, and this might have lowered the elongation at break values. The addition of 10% MP to the epoxy increased the elongation at break value when it was compared with the neat epoxy. This can be attributed to the increase in debonding between matrix and MP particles. EP/10MP/3B_4C and EP/10MP/3B_4C/1ZnB composites have relatively lower elongation at break values than EP/10MP, this may be because of the formation of agglomerates which may form some stress concentrated areas in the composites, and those areas may decrease the elongation at break values of the composites.

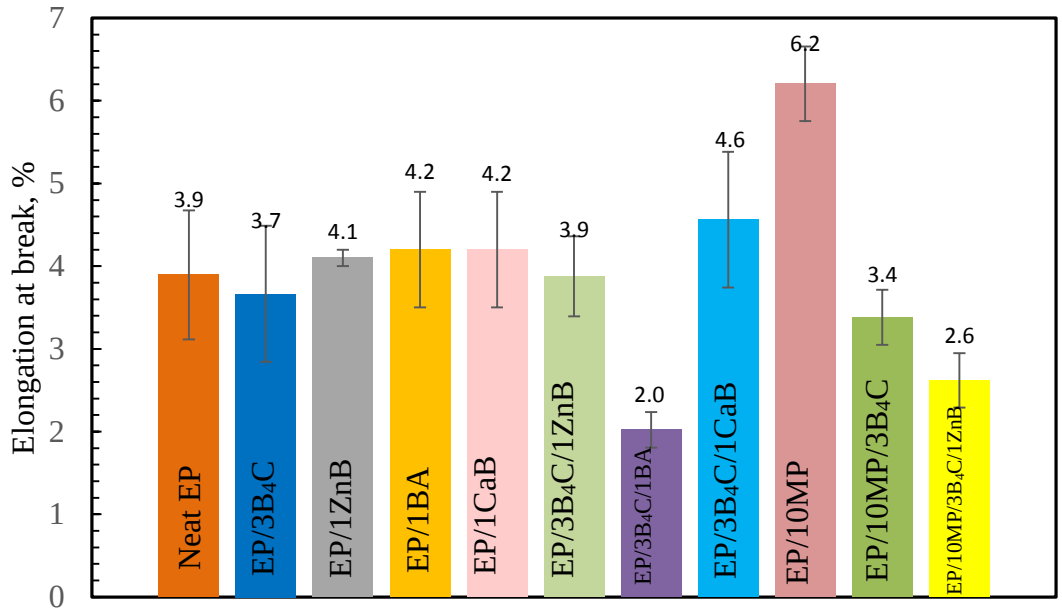

Figure 4.31 Elongation at break of epoxy/boron containing compound composites and epoxy/melamine phosphate composites.

The impact strength values for epoxy-based composites are represented in Figure 4.32. Impact strength values for neat epoxy sample and EP/3B_4C composites were 11.1 and 13.4 kJ/m^2, respectively.

Except for EP/3B_4C composite, all of the other ones had lower impact strength values than the neat epoxy. This may be due to the fact that flexibility of the polymer chains of the composites is reduced with the addition of the fillers. Among the epoxy-based composites, EP/3B_4C had the highest impact strength value since boron carbide is the hardest additive among the ones used in this study. Boron carbide increased the toughness of the composites which also indicated the increase in the impact

resistance. The addition of ZnB and CaB to the neat epoxy decreased the impact strength value. As the hardness of B_4C was greater than ZnB and CaB, the addition of B_4C to the EP/1ZnB and EP/1CaB increased the impact strength of the ternary composites of these components.

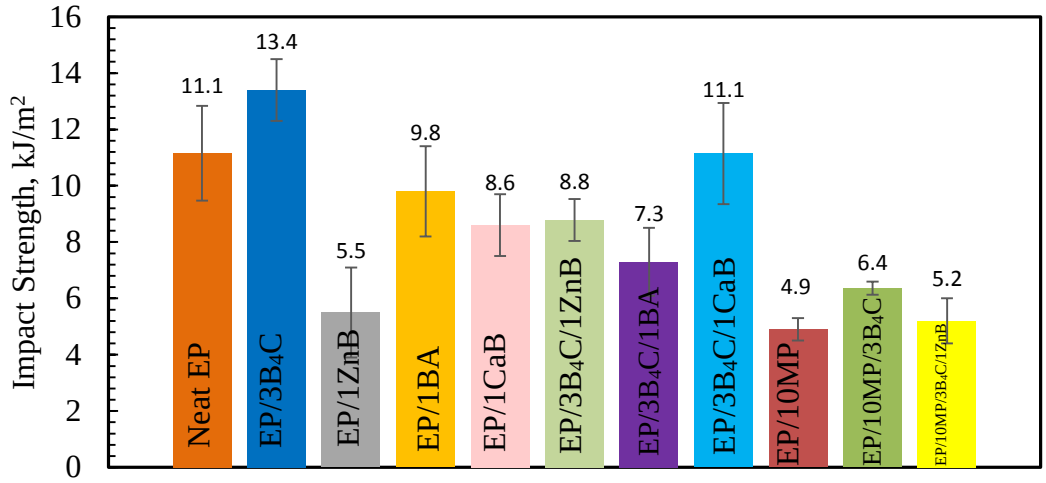

Figure 4.32 Impact strengths of epoxy/boron containing compound composites and epoxy/melamine phosphate composites.

4.5 Flammability Analysis of Epoxy-Based Composites

Flammability properties of EP/B_4C, EP/BCC and EP/MP-based composites were characterized through Limiting Oxygen Index (LOI) and UL-94 tests.

4.5.1 Flammability Properties of Epoxy/Boron Carbide Composites

In this part of the study, the flame retardant properties of neat epoxy sample and EP/B_4C composites with different amounts of boron carbide were characterized using LOI and UL-94 tests to understand whether B_4C has an effect on the flame retardancy of the epoxy resin. The flame retardancy mechanism of B_4C was also investigated.

The flammability test results from LOI and UL-94 tests for the neat epoxy and the EP/B_4C composites are listed in Table 4.4. Neat epoxy sample had a LOI value of 20% and it could not pass the UL-94 test. Since the LOI value is below 21%, neat epoxy can be called as combustible material which can burn in the ambient temperature in the existence of an ignition source [2].

In Table 4.4, it is seen that the LOI values of the composites increased with the increasing content of boron carbide. Boron carbide has an effect on improving flame retardancy of epoxy. Since it is a boron containing compound, when EP/B_4C composites are subjected to fire, there is a formation of B_2O_3 on the surface of the composites in the presence of air which has been previously proven in Figure 4.2. B_2O_3 formation starts at approximately 600°C which is lower than flame temperature of a natural gas burning. B_2O_3 acts as a barrier between epoxy surface and flame, protects the surface from flame, and prevents the further oxidation [2].

EP/B_4C composites could not pass the UL-94 tests. One of the reason might be the time to ignition values of the composites. It was observed from LOI and UL-94 tests that boron carbide did not have any effect on the time to ignition value so the EP/B_4C composites ignited in 10s.

According to the mechanical and flammability tests, the appropriate boron carbide content was selected as 3%. Further compositions were developed by taking this 3% of boron carbide as the basis.

Table 4.4 The flammability test results of neat epoxy and epoxy/boron carbide composites.

Sample Code	**LOI, O_2%**	**UL-94**
Neat EP	20	No Rating
EP/0.5B_4C	21	No Rating
EP/1 B_4C	22	No Rating
EP/3 B_4C	23	No Rating
EP/5 B_4C	23	No Rating
EP/8 B_4C	24	No Rating

Figure 4.33 shows the photographs of the neat epoxy sample and the EP/B_4C composites after applying LOI test. As it is seen from the photographs, the residue content increased as B_4C content in the epoxy matrix increased. Since B_4C is a thermally stable material it remains as char after burning.

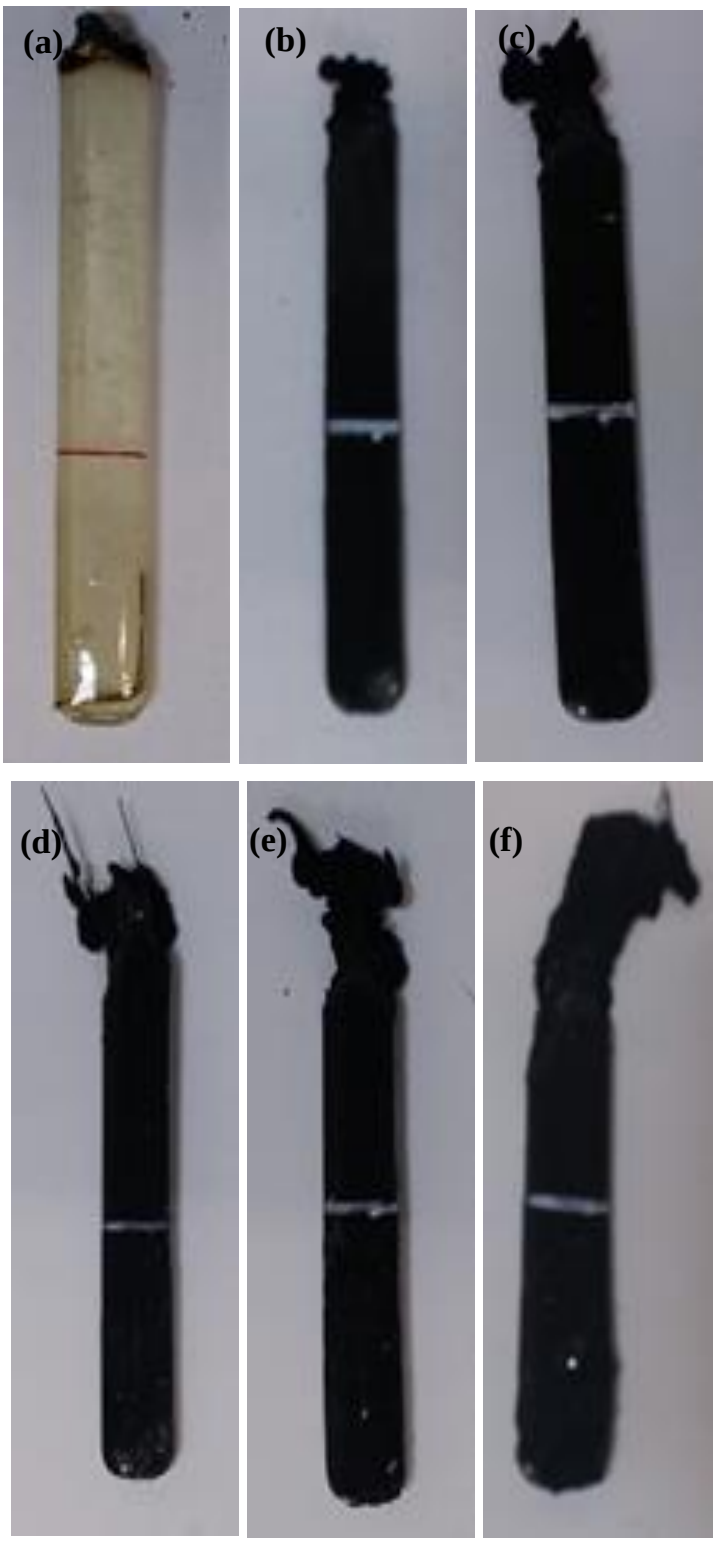

Figure 4.33 Photographs of the burned samples after LOI test a) Neat EP, b) EP/0.5B_4C, c) EP/1B_4C, d) EP/3B_4C, e) EP/5B_4C, f) EP/8B_4C.

4.5.2 Flammability Properties of Epoxy/Boron Containing Compound Composites and Epoxy/Melamine Phosphate Composites

In this part of the study, it is aimed to improve the flame retardancy properties of epoxy and EP/3B_4C composites by developing compositions with the commonly used flame retardant additives. For this purpose, ZnB, BA and CaB flame retardants were added to epoxy composite system as boron containing flame retardants, and MP was added as intumescent fire retardant additive. The synergism in flame retardancy between boron carbide and the flame retardant additive was also studied. LOI and UL-94 tests were performed to characterize the composites in terms of flame retardancy properties, and the results of the tests are given in Table 4.5.

Table 4.5 The flammability test results of epoxy/boron containing compound composites and epoxy/melamine phosphate composites.

Sample Code	**LOI, O_2%**	**UL-94**
Neat EP	20	No Rating
EP/3B_4C	23	No Rating
EP/1ZnB	24	No Rating
EP/1BA	22	No Rating
EP/1CaB	23	No Rating
EP/3B_4C/1ZnB	26	No Rating
EP/3B_4C/1BA	25	No Rating
EP/3B_4C/1CaB	24	No Rating
EP/10MP	27	V-0
EP/10MP/3B_4C	27.5	V-0
EP/10MP/3B_4C/1ZnB	27	V-0

The LOI value of neat epoxy and EP/3B_4C were found as 20% and 23%, respectively. The addition of 1% ZnB, BA and CaB flame retardants increased the flame retardancy of neat epoxy. Among these boron containing flame retardants, ZnB has the highest effect on flame retardancy of neat epoxy by considering the LOI results. This may be attributed to release of crystalline water of ZnB at high temperatures, which might lower the temperature during burning.

Figure 4.34 shows the photographs of neat epoxy, EP/1ZnB, EP/1BA and EP/1CaB composites which were obtained after they were burned in LOI test. It is seen from the photographs that ZnB addition creates char formation since ZnB acts as char promoter in flame retardancy systems [42]. Char residue of EP/1BA composites relatively high with respect to EP/1CaB composite as can be seen from the figure.

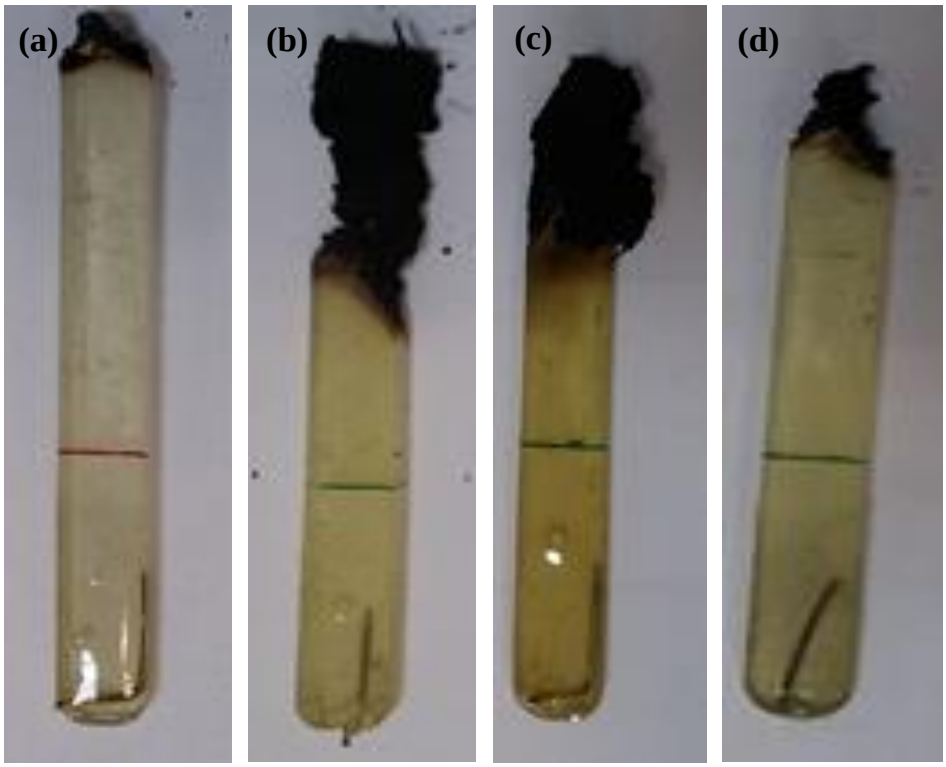

Figure 4.34 Photographs of the burned samples after LOI test a) Neat Epoxy, b) EP/1ZnB, c) EP/1BA, d) EP/1CaB.

The LOI values of EP/1ZnB, EP/1BA, and EP/1CaB composites were 24%, 22% and 23%, respectively. The addition of 3% B_4C to EP/1ZnB, EP/1BA, and EP/1CaB composites increased the LOI values of these composites. The LOI value of EP/1ZnB increased from 24% to 26% with the addition of 3% B_4C. The addition of 3% B_4C to EP/1BA increased the LOI value from 22% to 25%. Finally the LOI value of EP/1CaB increased from 23% to 24% with the addition of 3% B_4C. It is understood from the increase in LOI values that there was a synergism between boron carbide and ZnB, BA, CaB flame retardants. They had higher LOI values when they were used together. EP/3B_4C/1ZnB had higher LOI value (26%) when compared with the composites of EP/3B_4C/1BA and EP/3B_4C/1CaB. When these binary and ternary

composites were considered, ZnB was chosen as the most effective boron containing flame retardant which gave a synergism with boron carbide among the boron containing flame retardants which were used in this part of the study.

Figure 4.35 shows the photographs of burned neat epoxy, EP/3B_4C/1ZnB, EP/3B_4C/1BA and EP/3B_4C/1CaB composites after LOI test. It is seen from the photographs that the composites, which have ZnB as flame retardant additives, have layers on the surfaces of the polymers. ZnB releases its dehydration water after 290°C and dehydration water forms glassy boron oxide layer on the surface of the polymer. Boron oxide layer protects the surface from further burning and insulates the surface from oxygen which is necessary to continue the burning. Also it is known that ZnB has a synergistic effect in flame retardancy [42]. In this part, it is proven that it also has a synergism with boron carbide in flame retardancy of epoxy.

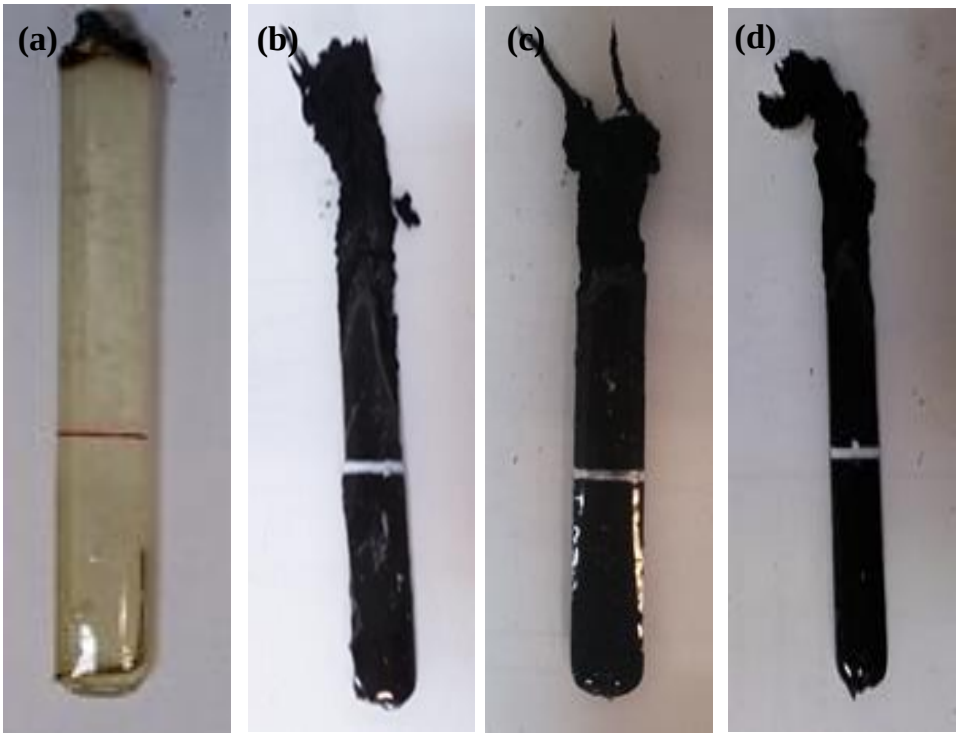

Figure 4.35 Photographs of the burned samples after LOI test a) Neat Epoxy b) EP/3B_4C/1ZnB, c) EP/3B_4C/1BA, d) EP/3B_4C/1CaB.

As seen in Table 4.5, melamine phosphate addition to the neat epoxy increased the LOI value from 20% to 27%. Also the addition of 3% addition of boron carbide to

the EP/10MP composite increased the LOI value from 27% to 27.5%. 1% addition of ZnB to the EP/10MP/3B_4C composite provided a LOI value of 27%. All the composites containing MP passed the UL-94 test with a V-0 rating.

Melamine phosphate is an intumescent flame retardant additive. Intumescent flame retardants start to decompose endothermically with dehydrating, release non-flammable gases and dilute the burning environment. They also swell during burning, cover the surface of the polymer and protect the surface of the material from further burning and in other words it acts as an insulation material and prevents heat transfer [92]. Decomposition of melamine phosphate leads to formation of phosphoric acid and this also contributes to the char formation [35].

Figure 4.36 shows the neat epoxy and the composites containing MP as a fire retardant additive. It is clearly seen that the addition of MP increased the char formation. When these composites were compared with the other composites which did not contain MP, the swelling ratios of the EP/MP-based composites were much higher. It was one of the reasons that the use of MP increased both LOI value, and led the epoxy to pass the UL-94 tests.

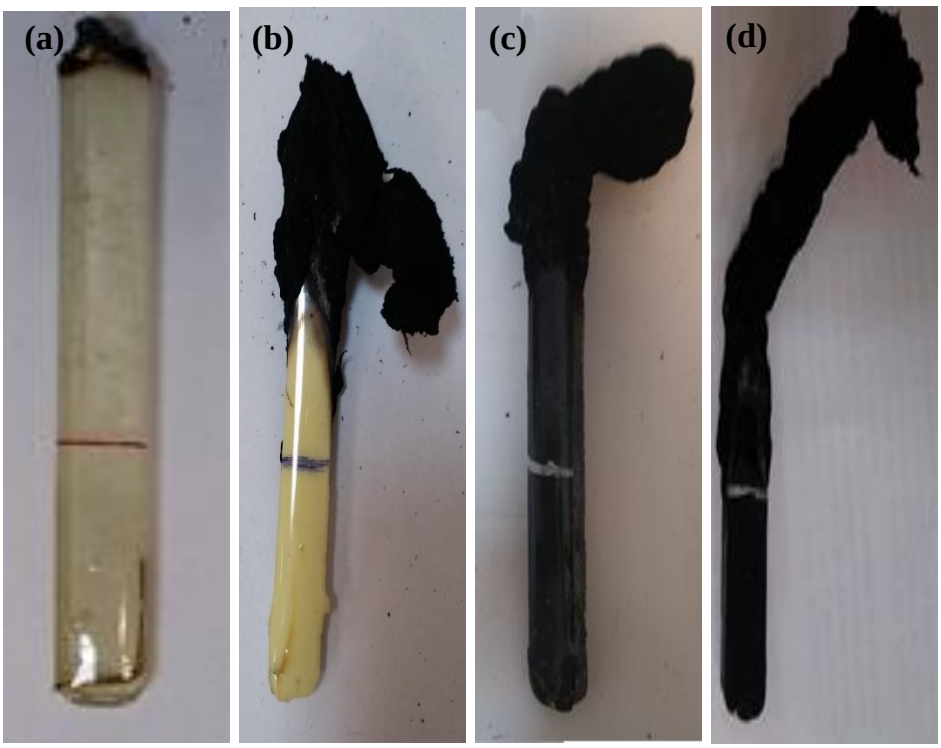

Figure 4.36 Photographs of the burned samples after LOI test a) Neat Epoxy b) EP/10MP, c) EP/10MP/3B_4C, d) EP/10MP/3B_4C/1ZnB.

For the fire retardancy part of the study the best composition is chosen to be EP/10MP/3B_4C with a LOI value of 27.5% and V-0 rating from UL-94 test.

4.6 Thermal Analyses of Epoxy-Based Composites

In order to investigate thermal properties of the composites and neat resin, Differential Scanning Calorimetry (DSC) and Thermal Gravimetric analysis (TGA) techniques were used to determine the glass transition temperature values and thermal stability behavior of the samples, respectively.

4.6.1 Thermal Properties of Epoxy/Boron Carbide Composites

DSC analyses were used to determine the glass transition temperatures (T_g) of neat epoxy sample and EP/B_4C composites. Effect of amount of B_4C on T_g is shown in Figure 4.37. Each sample was subjected to DSC analysis two times and representative DSC plots for the neat epoxy sample and EP/B_4C composites are given in Appendix D.

It is seen from Figure 4.37 that the T_g of neat epoxy sample is 111°C. A decreasing effect on the T_g of the composites was observed with an increase in B_4C loading.

The decreasing trend of the T_g with the addition of boron carbide may be because of the voids between boron carbide and the epoxy matrix which increased the chain mobility and decreased the T_g of the composites [32].

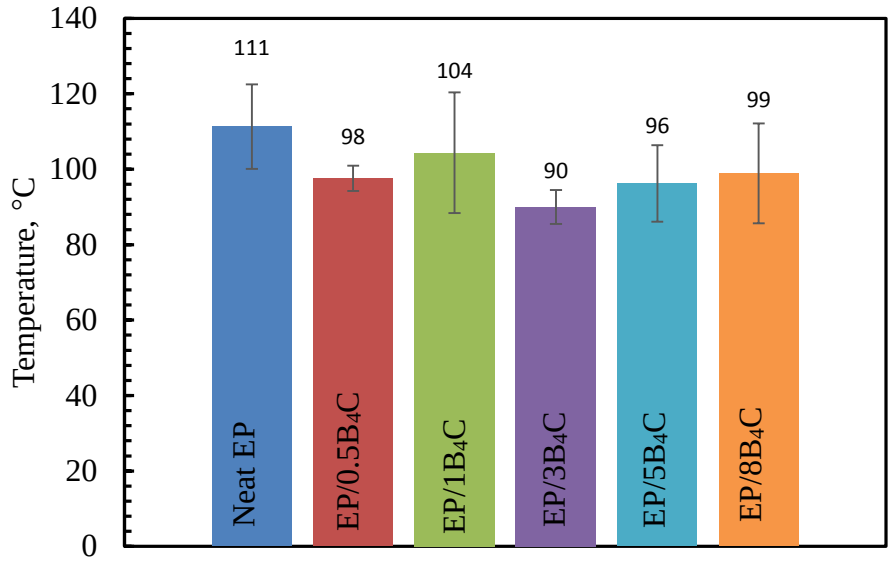

Figure 4.37 Change of T_g with respect to boron carbide addition.

TGA plots of neat epoxy sample and the composites containing boron carbide are given in Figure 4.38.

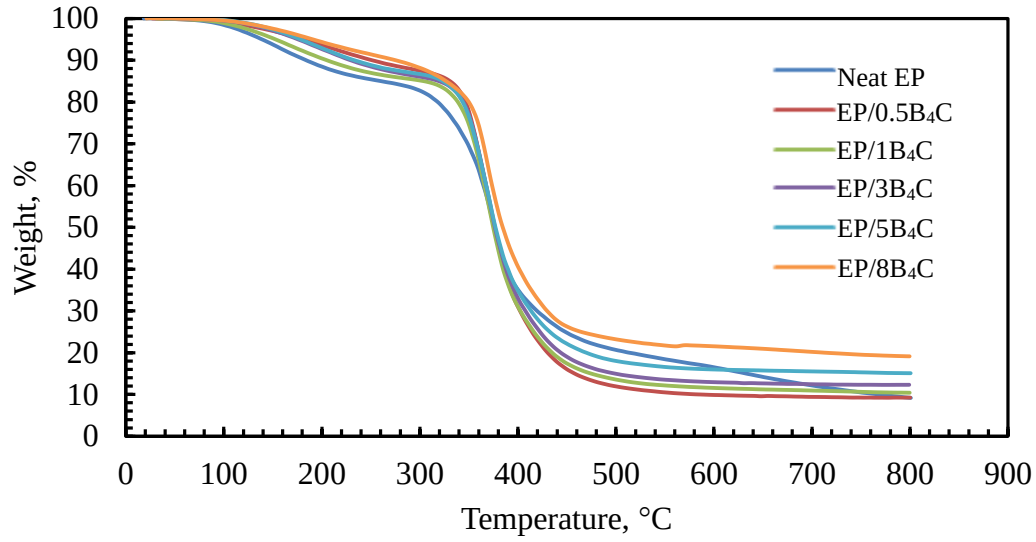

Figure 4.38 TGA plots of neat epoxy and epoxy/boron carbide composites under nitrogen atmosphere.

Table 4.6 shows the degradation temperatures (T_{Peak-1}, T_{Peak-2}), temperatures at 10 wt.% and 50 wt.% weight losses ($T_{10wt\%}$, $T_{50wt\%}$), and char yields at 800°C of the neat epoxy and the epoxy-based composites. The detailed data of TG/DTA plots are presented in Appendix D.

Table 4.6 Thermal degradation temperatures and char yields of neat epoxy and epoxy/boron carbide composites.

Sample Code	**T_{Peak-1}, °C***	**T_{Peak-2}, °C***	**$T_{10wt\%}$,°C**	**$T_{50wt\%}$,°C**	**Char yield at 800°C, wt.%**
Neat EP	158.1	373.6	182.4	377.1	9.1
EP/0.5B_4C	-	370.1	247.8	368.3	9.2
EP/1 B_4C	170.9	370.0	205.4	375.0	10.4
EP/3 B_4C	193.9	370.8	230.1	378.5	12.3
EP/5 B_4C	-	369.8	230.9	376.3	15.1
EP/8 B_4C	224.2	366.1	245.6	379.8	15.4

*T_{Peak-1} and T_{Peak-2} values are directly taken from Dr-TGA.

The neat epoxy had a degradation temperature of 373.6°C and char yield of 9.1% at 800°C. The addition of boron carbide slightly lower the degradation temperature (T_{Peak-2}) of the neat epoxy sample. Char yields of the composites were increased with the addition of B_4C when compared to the neat epoxy since boron carbide is a thermally stable material. This may be attributed to the high thermal stability of B_4C. Nevertheless, TGA graphs (see Figure 4.38) of the neat epoxy and the composites show that the thermal stability of the composites are slightly lower than the neat epoxy. Even though B_4C is a thermally stable material, degradation temperature did not change. This may result from the high thermal conductivity of B_4C with respect to that of the epoxy [93].

4.6.2 Thermal Properties of Epoxy/Boron Containing Compound Composites and Epoxy/Melamine Phosphate Composites

Glass transition temperatures (T_g) of epoxy-based composites are given in Figure 4.39. Each sample was subjected to DSC analysis once and DSC plots for these composites are given in Appendix D.

All the epoxy-based composites had lower T_g values than the neat epoxy (111°C). This may be due to the plasticizing effect of the additives which might increase the flexibility of the chains, therefore lower the T_g of the composites [94].

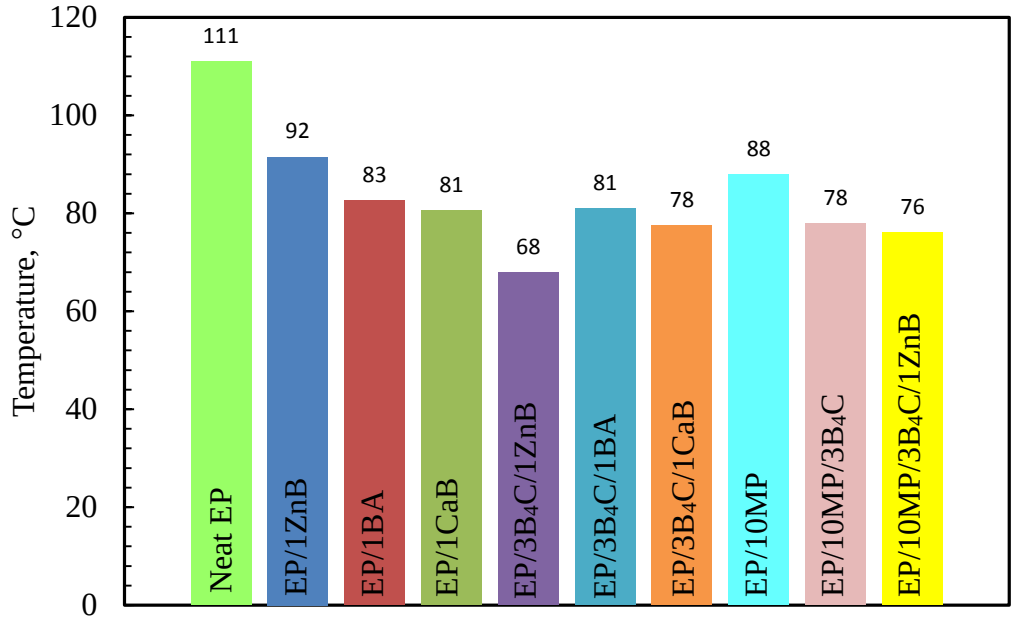

Figure 4.39 T_g values of epoxy-boron containing compound composites and epoxy/melamine phosphate composites.

TGA analyses were applied to epoxy/boron containing compound composites and epoxy/melamine phosphate composites under nitrogen atmosphere. The aim was to determine the effects of addition of flame retardants on the thermal behavior of the neat epoxy. TGA plots of neat epoxy sample and the epoxy-based composites are shown in Figure 4.40.

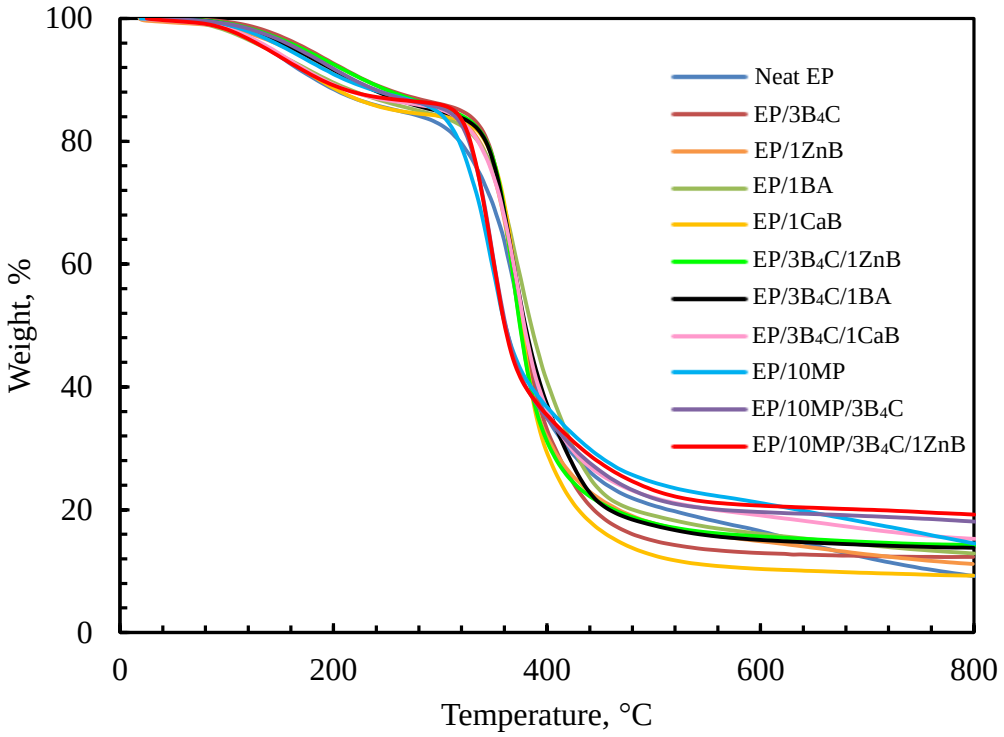

Figure 4.40 TGA plots of epoxy/boron containing compound composites and epoxy/melamine phosphate composites under nitrogen atmosphere.

Degradation temperatures (T_{Peak-1}, T_{Peak-2}), temperatures at 10 wt.% and 50 wt.% weight losses ($T_{10wt\%}$, $T_{50wt\%}$), and char yields at 800°C of the neat epoxy and the epoxy-based composites are given in Table 4.7. The detailed data of TG/DTA plots are presented in Appendix D.

According to Table 4.7 the addition of 1% BA and CaB to the epoxy did not change the thermal degradation temperature of the neat epoxy which was from 373.6°C to 374.1°C and 373.8°C, respectively. On the other hand, incorporation of 1% ZnB to the epoxy slightly decreased the thermal degradation temperature of the neat epoxy from 373.6°C to 369.8°C. When B_4C addition was taken into account, the epoxy-based B_4C containing composites generally had lower thermal degradation temperatures than that of the epoxy. On the other hand, all the composites had higher char yields at 800°C with respect to the epoxy sample. The reasons of the fact that B_4C slightly decreases the degradation temperature but increases the char yield may come from its both high thermal conductivity and high thermal stability with respect to the neat epoxy (Figure 4.40) [68, 93].

MP additions to the neat epoxy and EP/3B_4C composites decreased the thermal stability of epoxy. Since MP is less thermally stable than the neat epoxy, the lowest thermal degradation temperatures were observed in the composites with MP. It decomposes at lower temperatures to give phosphoric acid which might reduce the stability of the composites [2]. Therefore, the composites containing MP had the highest char residues among the other epoxy-based composites of this study.

Table 4.7 Thermal degradation temperatures and char yields of epoxy/boron containing compound composites and epoxy/melamine phosphate composites.

Sample Code	**T_{Peak-1},°C***	**T_{Peak-2},°C***	**$T_{10wt\%}$,°C**	**$T_{50wt\%}$,°C**	**Char yield at 800°C, wt.%**
Neat EP	158.1	373.6	182.4	377.1	9.1
EP/3B_4C	193.9	370.8	230.1	378.5	12.3
EP/1ZnB	-	369.8	216.6	375.0	11.2
EP/1BA	-	374.1	194.4	385.7	12.9
EP/1CaB	-	373.8	183.6	376.3	9.3
EP/3B_4C/1ZnB	-	366.3	229.0	374.6	14.3
EP/3B_4C/1BA	-	366.6	217.4	379.7	13.9
EP/3B_4C/1CaB	158.6	373.4	191.6	219.8	15.3
EP/10MP	-	347.9	212.3	361.0	14.5
EP/10MP/3B_4C	-	347.3	220.1	361.3	18.1
EP/10MP/3B_4C /1ZnB	153.1	351.1	185.4	360.3	19.2

*T_{Peak-1} and T_{Peak-2} values are directly taken from Dr-TGA.

All kinds of flame retardant additives increased the char yield at 800°C since boron containing flame retardants are more stable than neat epoxy [68].

4.7 Electrical Resistivities of Epoxy/Boron Carbide Composites

The electrical resistivities of the neat epoxy and EP/B_4C composites were characterized using a two point probe method for electrical resistivity measurement.

The conductivity measurement was applied to the sintered boron carbide. The sintering procedure is given in detail in Appendix E.

As it is seen from Figure 4.41 boron carbide has a resistivity of $10^{0.56}$ Ω.cm which is in the semiconductor range. On the other hand neat epoxy has a resistivity of $10^{11.5}$ Ω.cm since it is an insulator material. The addition of boron carbide to the epoxy matrix was expected to increase the conductivity of the neat epoxy.

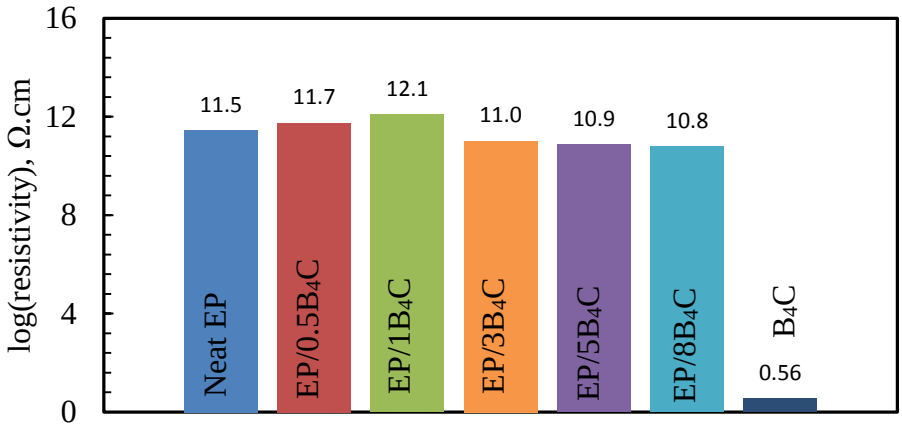

Figure 4.41 log(resistivity) values for neat epoxy, EP/B_4C composites and B_4C.

Figure 4.41 shows that there is not a significant change in the log(resistivity) values of the composites with the addition of boron carbide. The additions of 5% and 8% B_4C slightly decreased the resistivity, in other words increased the conductivity since they have relatively larger amount of B_4C. However, the conductivity is still in the insulator range, it is because of the low amounts of boron carbide in the composite. Electrical charge cannot be travelled through the specimen. Percolation threshold mechanism is expected to obtain at B_4C concentrations which is higher than 8 wt.%.

Figure 4.42 shows the electrical log(resistivity) values of epoxy-based composites. It can be seen that there is not any change in the resistivity with the addition of the different additives to epoxy. All the composites are in insulator range.

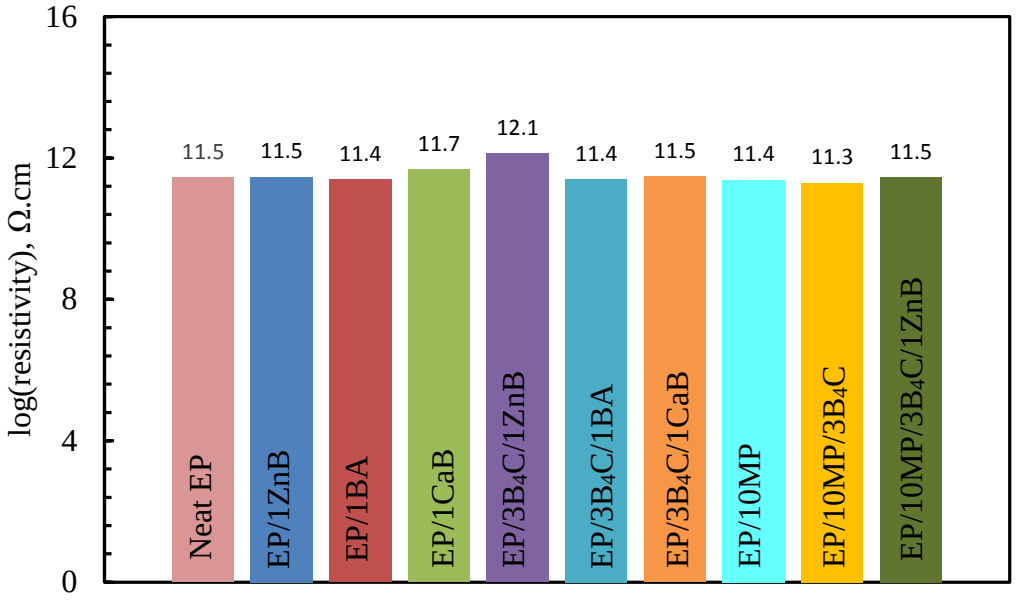

Figure 4.42 log(resistivity) values for epoxy/boron containing compound composites and epoxy/melamine phosphate composites.

CHAPTER 5

CONCLUSIONS

The effect of B_4C addition on the properties of neat epoxy and epoxy-based composites were investigated. Different BCC and flame retardant additives such as ZnB, BA, CaB and MP were also added to the epoxy matrix. Their synergism together with B_4C was examined. Characterization of the composites was performed in terms of their morphologies, and mechanical, flame retardancy, thermal and electrical properties.

The following conclusions can be drawn from the thesis:

- XRD analysis showed that the as-received material contained B_4C with a small amount of impurities. XPS studies revealed that the B_4C was a carbon-rich material with a carbon content of 27%. It was observed from SEM analyses that the size of particles were in the range of 3-8 microns and their shapes were irregular.
- Neat epoxy was successfully prepared using epoxy resin and curing agent. The completeness of curing was analyzed and the percent curing of neat epoxy was found to be 99%. Neat epoxy had 48 MPa tensile strength, 2815 MPa elastic modulus, 3.9% elongation at break value, LOI value of 20%, and electrical resistivity value of $10^{11.5}\,\Omega.cm$.
- EP/B_4C composites were prepared with the additions of 0.5%, 1%, 3%, 5% and 8% of B_4C. The increasing B_4C content generally increased the impact strength values and flame retardancy properties of B_4C. Thermal analysis showed that glass transition temperatures of composites decreased with the

addition of B_4C. Moreover, a slight decrease in decomposition temperature was observed. Electrical conductivity of neat epoxy increased slightly with the addition of B_4C. SEM analysis showed well distributed B_4C in the composites especially at EP/3B_4C composite.

- Epoxy-based composites with BCC and MP were successfully prepared. Addition of ZnB, BA, CaB and MP improved the flame retardancy of epoxy when they were used together with B_4C. Synergistic effect among B_4C, BCC and MP was observed. The highest LOI value of 26% was obtained with the addition of ZnB to EP/B_4C composite among the other BCC/B_4C composites. Mechanical properties of these composites were decreased presumably due to poor adhesion between epoxy and filler, and agglomeration of the particles.
- Addition of 10% MP to the neat epoxy increased the LOI value from 20% to 27% with a V-0 level in UL-94 test. Addition of 3% B_4C to EP/10MP composites increased the LOI value slightly and this composite had a V-0 rating.
- Among the studied composites, EP/10MP/3B_4C had the highest LOI value of 27.5% and "V-0" level from UL-94 test. Mechanical properties of EP/10MP/3B_4C composite was found as 39 MPa in tensile strength, 1923 MPa in elastic modulus, 3.4% elongation at break and 6.4 kJ/m^2 in impact strength.
- In terms of impact strength values, EP/5B_4C had the highest value among all the materials prepared in this thesis.

REFERENCES

[1] A. M. Bagher, Polymer Optic Technology, Optics. 4 (2015) 1-12.

[2] F. Laoutid, L. Bonnaud, M. Alexandre, J.M. Lopez-Cuesta, P. Dubois, New prospects in flame retardant polymer materials: From fundamentals to nanocomposites, Mater. Sci. Eng. R Reports. 63 (2009) 100–125.

[3] A. Toldy, P. Anna, I. Csontos, A. Szabó, G. Marosi, Intrinsically flame retardant epoxy resin - Fire performance and background - Part I, Polym. Degrad. Stab. 92 (2007) 2223–2730.

[4] S.E. Lee, E. Jeong, M.Y. Lee, M.K. Lee, Y.S. Lee, Improvement of the mechanical and thermal properties of polyethersulfone-modified epoxy composites, J. Ind. Eng. Chem. 33 (2015) 73–79.

[5] H. Yang, X. Wang, B. Yu, L. Song, Y. Hu, R.K.K. Yuen, Effect of borates on thermal degradation and flame retardancy of epoxy resins using polyhedral oligomeric silsesquioxane as a curing agent, Thermochim. Acta. 535 (2012).

[6] A.R. Horrocks, D. Price, Fire retardant materials, Woodhead Publishing, England, (2001).

[7] M. Le Bras, S. Bourbigot, G. Camino, R. Delobel, Fire Retardancy of Polymers: The Use of Intumescence, Woodhead Publishing, (1998).

[8] P. Gramatica, S. Cassani, A. Sangion, Are some "safer alternatives " hazardous as PBTs ? The case study of new flame retardants, J. Hazard. Mater. 306 (2016) 237–246.

[9] V. K. Srivastava, P. S. Shembekar, Tensile and Fracture Properties of Epoxy Resin Filled with Flyash Particles, J. Mater. Sci. 25 (1990) 3513-3516.

[10] B. Hulugappa, M. V Achutha, B. Suresha, Effect of Fillers on Mechanical Properties and Fracture Toughness of Glass Fabric Reinforced Epoxy Composites, (2016) 1–14.

[11] D.W. Callister, Materials Science and Engineering: An Introduction, John Wiley & Sons, Inc., USA, (2007).

[12] T.H. Hsieh, A.J. Kinloch, K. Masania, J. Sohn Lee, A.C. Taylor, S. Sprenger, The toughness of epoxy polymers and fibre composites modified with rubber microparticles and silica nanoparticles, J. Mater. Sci. 45 (2010) 1193–1210.

[13] J. Abenojar, M. Martínez, F. Velasco, V. Pascual-Sánchez, J.M. Martín-Martínez, Effect of Boron Carbide Filler on the Curing and Mechanical Properties of an Epoxy Resin, J. Adhes. 85 (2009) 216–238.

[14] V. Domnich, S. Reynaud, R. a. Haber, M. Chhowalla, Boron carbide: Structure, properties, and stability under stress, J. Am. Ceram. Soc. 94 (2011) 3605–3628.

[15] M.A. Meyers, K.K. Chawla, Mechanical Behavior of Materials, Camridge, Second Edition, (2009).

[16] http://www.boren.gov.tr/en/boron/boron-element, Last Visited on: June, 2016

[17] http://www.etimaden.gov.tr/en/page/boron-turkey-history, Last Visited on: June, 2016

[18] O. Yilmaz, Boron in Turkey: Between Myth and Reality, Insight Turkey. 9 (2007) 37–43.

[19] F. Thevenot, A review on boron carbide, Key Engineering Materials, (1991) 59-88.

[20] N. Cho, Processing of Boron Carbide, School of Materials Science and Engineering, Ph.D. Thesis, Georgia Institute of Technology, Georgia, (2006).

[21] A.O. Sezer, J.I. Brand, Chemical vapor deposition of boron carbide, 79 (2001) 191–202.

[22] N. Cho, Z. Bao, R. F. Speyer, Density and Hardness optimized Pressureless Sintered and Post-hot Isostatic Pressed B_4C, 20 (2005) 2110-2116.

[23] A. Alizadeh, E. Taheri-Nassaj, N. Ehsani, H.R. Baharvandi, Production of boron carbide powder by carbothermic reduction from boron oxide and petroleum coke or carbon active, Adv. Appl. Ceram. 105 (2006) 291–296.

[24] A. Alizadeh, E. Taheri-Nassaj, N. Ehsani, Synthesis of boron carbide powder by a carbothermic reduction method, J. Eur. Ceram. Soc. 24 (2004) 3227–3234.

[25] F.L. Jin, X. Li, S.J. Park, Synthesis and application of epoxy resins: A review, J. Ind. Eng. Chem. 29 (2015) 1–11.

[26] F.L. Jin, X. Li, S.J. Park, Journal of Industrial and Engineering Chemistry Synthesis and application of epoxy resins : A review, J. Ind. Eng. Chem. (2015).

[27] D. Ratna, Epoxy Composites: Impact resistance and flame retardancy, Rapra Technology, Report 185, 16, (2005), 3-17.

[28] K.P.Unnikrishnan, Studies on the toughening of epoxy resins, Polymer science and rubber technology Ph.D. Thesis, Cochin University of Science and Technology, India, (2006).

[29] C. Gerard, G. Fontaine, S. Bourbigot, New Trends in Reaction and Resistance to Fire of Fire-retardant Epoxies, materials, 3, (2010) 4476-4499.

[30] G. Levita, S. De Petris, A. Marchetti, A. Lazzeri, Crosslink density and fracture toughness of epoxy resins, J. Mater. Sci. 26 (1991) 2348–2352.

[31] R. Mezzenga, L. Boogh, J.A.E. Månson, A review of dendritic hyperbranched polymer as modifiers in epoxy composites, Compos. Sci. Technol. 61 (2001) 787–795.

[32] B.J. Ash, D.F. Rogers, C.J. Wiegand, L.S. Schadler, R.W. Siegel, B.C. Benicewicz, et al., Mechanical Properties of AI_2O_3 Polymethylmethacrylate Nanocomposites, Polymer (Guildf). 23 (2002).

[33] C.S. Cho, L.W. Chen, Y.S. Chiu, Novel flame retardant epoxy resins, Polym. Bull. 41 (1998) 45–52.

[34] S. V. Levchik, E.D. Weil, Thermal decomposition, combustion and flame-retardancy of epoxy resins - A review of the recent literature, Polym. Int. 53 (2004) 1901–1929.

[35] M. Rakotomalala, S. Wagner, M. Döring, Recent developments in halogen free flame retardants for epoxy resins for electrical and electronic applications, Materials (Basel). 3 (2010) 4300–4327.

[36] C.L. Beyler, M.M. Hirschler, Thermal Decomposition of Polymers, SPE Handb. Fire Prot. Eng. (2001) 110–131.

[37] J.H. Troitzsch, An overview of flame retardants, Chimica Oggi/Chemistry Today, 16 (1998) 19.

[38] K.K. Shen, Polymer Green Flame Retardants: Review of Recent Advances on the Use of Boron-based Flame Retardants, Elsevier B.V., USA, (2014).

[39] A.B. Morgan, C.A. Wilkie, Non-Halogenated Flame Retardant Handbook, Scrivener Publishing, (2014).

[40] S.Y. Lu, I. Hamerton, Recent developments in the chemistry of halogen-free flame retardant polymers, Prog. Polym. Sci. 27 (2002) 1661–1712.

[41] S.M. Unlu, S.D. Dogan, M. Dogan, Comparative study of boron compounds and aluminum trihydroxide as flame retardant additives in epoxy resin, Polym. Adv. Technol. 25 (2014) 769–776.

[42] B. Baltaci, G.Ö. Çakal, G. Bayram, I. Eroglu, S. Özkar, Surfactant modified zinc borate synthesis and its effect on the properties of PET, Powder Technol. 244 (2013) 38–44.

[43] R. Thomas, G.U. Kulkarni, A hydrogen-bonded channel structure formed by a complex of uracil and melamine, Beilstein J. Org. Chem. 3 (2007) 4–7.

[44] P. Lv, Z. Wang, K. Hu, W. Fan, Flammability and thermal degradation of flame retarded polypropylene composites containing melamine phosphate and pentaerythritol derivatives, Polym. Degrad. Stab. 90 (2005) 523–534.

[45] B. Scharte, Phosphorus-based flame retardancy mechanisms-old hat or a starting point for future development?, Materials (Basel). 3 (2010) 4710–4745.

[46] J. Wiley, M. Dekker, F.J. In, Literature Review of Epoxy Toughening, Epoxy. (2005) 154–169.

[47] D. Eiras, L.A. Pessan, Mechanical properties of polypropylene/calcium carbonate nanocomposites, Mater. Res. 12 (2009) 517–522.

[48] Prof. Dr. Rıza Gürbüz, Tension test, Lecture Notes (1998) 1–9. http://users.metu.edu.tr/rgurbuz/Courses/MetE206.htm

[49] http://www2.warwick.ac.uk/fac/sci/wmg/globalcontent/courses/ebm/mant/materials/properties_of_materials Last Visited on: June, 2016.

[50] http://archive.nrc-cnrc.gc.ca/eng/ibp/irc/cbd/building-digest-157.html Last Visited on: June, 2016.

[51] http://wmtr.com/en.impact-testing.html Last Visited on: June, 2016.

[52] http://www.twiglobal.com/technicalknowledge/publishedpapers/theevaluation-of-root-defects-in-fsw-by-through-hole-impact-testingpreliminary-studies -july-2005, Last Visited on: June, 2016.

[53] M. A. Meyers and K. K. Chawla, Mechanical Behavior of Materials, Cambridge University Press, (2009).

[54] http://www.techsil.co.uk/material-properties Last Visited on: June, 2016.

[55] M.W. Chanda, R. Krishna, Selection and Testing of Ballast Stones for Underground Railway Tracks, African Journal of Science and Technology, 4 (2003) 42–50.

[56] http://www.rutlandplastics.co.uk/advice/materials_datasheets_flammability2.html Last Visited on: June, 2016.

[57] ASTM International, Measuring the Minimum Oxygen Concentration to Support Candle- Like Combustion of Plastics, (2008) 2–3.

[58] ASTM International, Standard Test Method for Measuring the Comparative Burning Characteristics of Solid Plastics in a Vertical Position, (2000) 1–5.

[59] J.M. Walls, R. Smith, Surface Science Techniques, Vacuum, 45 (1994) 649-652.

[60] F.W. Billmeyer, Textbook of Polymer Science, John Wiley Interscience, Third Edition, New York (1984).

[61] J. Als-Nielsen, D. McMorrow, Elements of Modern X-ray Physics, Wiley, Second Edition, (2011).

[62] W.J. Sichina, Characterization of Epoxy Resins Using DSC, PerkinElmer Instruments. (2000) 2–5.

[63] K.H. Tan, I. Barshad, Thermal Analysis Techniques, Methods of Soil Analysis: Part 1, 9 (1970) 1–50.

[64] Y. Singh, Electrical Resistivity Measurements: a Review, Int. J. Mod. Phys. Conf. Ser. 22 (2013) 745–756.

[65] F. Ersaraç, Preparation and characterization of shape memory polymer based composite materials for aerospace applications, Chemical Engineering M.Sc. Thesis, Middle East Technical University, Ankara, Turkey, (2012).

[66] T. Ishii, H. Kokaku, A. Nagai, T. Nishita, M. Kakimoto, Calcium borate flame retardation system for epoxy molding compounds, Polym. Eng. Sci. 46 (2006) 799–806.

[67] M. Dogan, S. Murat Unlu, Flame retardant effect of boron compounds on red phosphorus containing epoxy resins, Polym. Degrad. Stab. 99 (2014) 12–17.

[68] E. Yürekli, Preparation of epoxy-based composites containing barium metaborate and their characterization, Chemical Engineering M.Sc. Thesis, Middle East Technical University, Ankara, Turkey, (2014).

[69] W.Y. Chen, Y.Z. Wang, F.C. Chang, Thermal and flame retardation properties of melamine phosphate-modified epoxy resins, J. Polym. Res. 11 (2004) 109–117.

[70] M. Rallini, M. Natali, J.M. Kenny, L. Torre, Effect of boron carbide nanoparticles on the fire reaction and fire resistance of carbon fiber/epoxy composites, Polym. (United Kingdom). 54 (2013) 5154–5165.

[71] D.D. Rodrigues, J.G. Broughton, Silane surface modification of boron carbide in epoxy composites, Int. J. Adhes. Adhes. 46 (2013) 62–73.

[72] F. Wang, L.T. Drzal, Y. Qin, Z. Huang, Enhancement of fracture toughness, mechanical and thermal properties of rubber/epoxy composites by incorporation of graphene nanoplatelets, Compos. Part A Appl. Sci. Manuf. 87 (2016) 10–22.

[73] I. Zaman, T.T. Phan, H.C. Kuan, Q. Meng, L.T. Bao La, L. Luong, et al., Epoxy/graphene platelets nanocomposites with two levels of interface strength, Polymer (Guildf). 52 (2011) 1603–1611.

[74] Polires 188 data sheet, http://www.polikem.com/ Last Visited on: June, 2016.

[75] Cetepox 1393H data sheet, http://www.polikem.com/ Last Visited on: June, 2016.

[76] Boroptik Engineering, boron carbide data sheet, Result : Analysis Report 80 DalianZX F1200-1 Particle Diameter (μm .), (2014).

[77] Boroptik Engineering ANALYSIS REPORT / Chemical Analysis Data (wt .%) Particle Size Distribution (μm), (2014).

[78] http://www.chempoint.com/products/catalog/great-lakes-solutions/great-lakes-solutions- antimony-flame-retardants/great-lakes-solutions-antimony-flame-retardants, Last Visited on: June, 2016

[79] https://us.vwr.com/store/catalog/product.jsp?product_id=4539242, Last Visited on: June, 2016

[80] http://aerospace.basf.com/common/pdfs/BASF_Melapur_Halogenfree_

Flame_Retardants_DS_USL_sfs. pdf Last Visited on: May, 2016

[81] http://www.sigmaaldrich.com/catalog/product/sial/24201?lang=en&region = TR Last Visited on: May, 2016

[82] V. Mitta, Surface Modification of Nanoparticle and Natural Fiber Fillers, Wiley, Switzerland, (2015)

[83] M. Steinbrück, U. Stegmaier, L. Steinbock, Experiments on the Oxidation of Boron Carbide at High Temperatures Experiments on the Oxidation of Boron Carbide, (2004) 127.

[84] A. Atasoy, The aluminothermic reduction of boric acid, Int. J. Refract. Met. Hard Mater. 28 (2010) 616–622.

[85] L.G. Jacobsohn, R.K. Schulze, M.E.H. Maia Da Costa, M. Nastasi, X-ray photoelectron spectroscopy investigation of boron carbide films deposited by sputtering, Surf. Sci. 572 (2004) 418–424.

[86] T. Yamashita, P. Hayes, Analysis of XPS spectra of Fe2+ and Fe3+ ions in oxide materials, Appl. Surf. Sci. 254 (2008) 2441–2449.

[87] S. Kipcak, P. Gurses, E.M. Derun, N. Tugrul, S. Piskin, Characterization of boron carbide particles and its shielding behavior against neutron radiation, Energy Convers. Manag. 72 (2013) 39–44.

[88] D. Ghosh, G. Subhash, C.H. Lee, Y.K. Yap, Strain-induced formation of carbon and boron clusters in boron carbide during dynamic indentation, Appl. Phys. Lett. 91 (2007) 6–8.

[89] M. González, J.C. Cabanelas, J. Baselga, Applications of FTIR on Epoxy Resins - Identification, Monitoring the Curing Process, Phase Separation and Water Uptake, Univ. Carlos III Madrid. 2 (2012) 261–284.

[90] Z. Wang, G. Zhao, Microwave Absorption Properties of Carbon Nanotubes-Epoxy Composites in a Frequency Range of 2 - 20 GHz, Open J. Compos. Mater. 3 (2013) 17–23.

[91] R. Velmurugan, T.P. Mohan, Room temperature processing of epoxy-clay nanocomposites, J. Mater. Sci. 39 (2004) 7333–7339.

[92] Z. Feng, S. Kang, The Application of Halogen-free Intumescent Flame Retardant in Polyolefin, Coating. 1–6.

[93] C. Wood, D. Emin, E. Gray, Thermal conductivity of boron carbide, Phys. Rev. B. 31 (1985) 6811–6814.

[94] F. Laboulfie, M. Hémati, A. Lamure, S. Diguet, Effect of the plasticizer on permeability, mechanical resistance and thermal behaviour of composite coating films, Powder Technol. 238 (2013) 14–19.

APPENDIX A

X-RAY DIFFRACTION DATA

Table A.1 XRD data of trigonal boron.

B **PDF Card No.: 01-085-0702, Trigonal** **Rad:CuKα_1 (λ:1.5406 Å)**			
d	**2θ**	**Intensity, (%)**	**hkl**
4.189	21.19	56.1	003
4.026	22.06	100	101
3.520	25.28	3.6	012
2.526	35.51	56.6	104
2.454	36.59	9.6	110
2.163	41.72	2.9	015
2.117	42.67	3.8	113
2.095	43.14	43.8	006
2.013	44.99	0.7	202
1.760	51.90	0.1	024
1.654	55.53	4.6	107
1.623	56.68	8.7	205
1.594	57.81	8.2	211
1.556	59.33	0.1	122
1.473	63.04	7.0	018
1.430	65.17	16.6	214
1.417	65.87	7.7	300
1.396	66.97	3.9	009
1.371	68.35	8.7	027
1.354	69.37	10.9	125
1.342	70.05	16.6	033
1.263	75.15	12.2	208
1.227	77.77	3	220

Table A.1 (cont'd) XRD data of trigonal boron.

d	2θ	Intensity, (%)	hkl
1.214	78.80	0.1	119
1.205	79.47	0.1	1010
1.197	80.10	0.6	217
1.178	81.71	2.1	223
1.174	82.04	2.9	036
1.159	83.34	0.7	312
1.123	86.61	0.7	128
1.103	88.57	1.2	134
1.082	90.82	0.1	0210
1.067	92.40	0.1	315
1.059	93.37	0.6	226
1.048	94.64	1.1	0012
1.007	99.86	0.9	404
0.994	101.53	2.4	036
0.990	102.20	0.1	2110
0.985	102.84	0.4	137
0.979	103.82	0.1	045
0.972	104.81	0.1	321
0.964	106.15	0.1	232
0.943	109.63	1.4	318
0.931	111.61	7.9	324
0.922	113.39	0.3	229
0.914	114.79	0.1	407
0.909	115.85	0.9	235
0.906	116.56	1.0	143
0.880	122.20	1.2	048
0.878	122.60	0.6	0114
0.860	127.27	0.5	1310
0.857	128.05	2.5	327
0.848	130.52	2.2	416
0.842	132.34	7.1	0312
0.838	133.72	1.2	0015
0.828	136.81	3.4	2113
0.827	137.38	1.7	2014
0.821	139.68	3.9	054
0.818	140.67	3.3	330
0.811	143.38	0.2	4010
0.805	146.10	2.5	505
0.803	147.27	1.2	333

Table A.2 XRD data of rhombohedral boron carbide.

B_4C **35-798, Rhombohedral** **Rad:CuKα_1 (λ:1.5406 Å)**			
d	**2θ**	**Intensity, (%)**	**hkl**
4.499	19.73	14	101
4.033	22.04	21	003
3.783	23.52	49	012
2.803	31.93	11	110
2.565	34.98	64	104
2.377	37.85	100	021
2.300	39.17	4	113
1.891	48.13	1	024
1.813	50.34	4	211
1.712	53.52	11	205
1.626	56.60	2	107
1.567	58.92	1	214
1.500	61.83	9	303
1.460	63.72	13	125
1.442	64.62	10	018
1.399	66.85	12	220
1.337	70.43	8	131
1.323	71.29	7	223
1.313	71.92	8	312
1.282	73.93	2	208
1.260	75.41	3	306
1.257	75.65	6	217
1.211	79.06	1	119
1.206	79.43	1	401

Table A.3 XRD data of B_2O_3.

B_2O_3			
PDF Card No.: 00-006-0297, Hexagonal			
Rad:CuKα1 (λ:1.5406 Å)			
d	**2θ**	**Intensity, (%)**	**hkl**
6.080	14.56	35	
3.210	27.77	100	310
2.920	30.59	12	222
2.600	34.47	10	22
2.490	36.04	10	400
2.260	39.86	14	420
1.980	45.79	8	510
1.880	48.37	6	520
1.680	54.58	4	600
1.600	57.56	4	620
1.410	66.23	4	711
1.070	92.09	4	664
0.946	109.03	6	1032
0.866	125.61	6	103

Table A.4 XRD data of Fe_3O_4.

Fe_3O_4			
19-629			
Rad:CuKα1 (λ:1.5406 Å)			
d	**2θ**	**Intensity, (%)**	**hkl**
4.852	18.28	8	111
2.967	30.12	30	220
2.532	35.45	100	311
2.424	37.08	8	222
2.099	43.09	20	400
1.715	53.44	10	422
1.616	56.99	30	511
1.484	62.57	40	440
1.419	65.80	2	531
1.328	70.99	4	620
1.281	74.02	10	533
1.266	75.03	4	622

Table A.4 (cont'd) XRD data of Fe_3O_4.

d	2θ	Intensity, (%)	hkl
1.212	79.00	2	444
1.122	86.79	4	642
1.093	89.71	12	731
1.050	94.52	6	800
0.990	102.34	2	660
0.969	105.34	6	751
0.963	106.33	4	662
0.939	110.40	4	840
0.895	118.89	2	664
0.880	122.29	6	931
0.857	128.22	8	844
0.823	138.90	4	1020
0.812	143.51	6	951

Table A.5 XRD data of Fe_2O_3.

Fe_2O_3 **33-664** **Rad:CuKα_1 (λ:1.5406 Å)**			
d	**2θ**	**Intensity, (%)**	**hkl**
3.684	24.16	30	012
2.780	32.20	100	104
2.519	35.64	70	110
2.292	39.31	3	006
2.207	40.89	20	113
2.078	43.55	3	202
1.841	49.52	40	024
1.694	54.14	45	116
1.637	56.20	1	211
1.603	57.48	5	122
1.599	57.64	10	018
1.486	62.50	30	214
1.454	64.05	30	300
1.350	69.66	3	208
1.311	72.00	10	1010
1.306	72.33	6	119
1.259	75.50	8	220
1.228	77.80	4	306

Table A.5 (cont'd) XRD data of Fe_2O_3.

d	2θ	Intensity, (%)	hkl
1.214	78.83	2	223
1.190	80.79	5	128
1.163	83.02	5	0210
1.141	85.00	7	134
1.103	88.63	7	226
1.077	91.44	2	042
1.056	93.81	7	2110
1.043	95.34	1	1112
1.039	95.76	3	404
0.989	102.40	4	318
0.971	105.03	1	229
0.961	106.74	5	324
0.958	107.15	4	0114
0.952	108.21	5	410
0.932	111.65	2	413
0.921	113.73	2	048
0.908	116.19	5	1310
0.900	117.91	1	3012
0.895	118.85	3	2014
0.879	122.59	6	416
0.865	126.10	1	238
0.854	128.94	3	4010
0.844	132.08	5	1214
0.839	133.45	3	330

Table A.6 XRD data of graphite.

Carbon- graphite **23-64** **Rad:CuKα$_1$ (λ:1.5406 Å)**			
d	**2θ**	**Intensity, (%)**	**hkl**
3.360	26.53	100	002
2.130	42.44	10	100
2.030	44.64	50	101
1.800	50.72	5	102
1.678	54.70	80	004
1.544	59.90	10	103
1.232	77.47	30	110
1.158	83.47	50	112
1.138	85.28	5	105
1.120	86.99	20	006
1.054	94.01	5	201
0.994	101.71	40	114
0.841	132.88	10	-
0.829	136.84	40	116
0.801	148.48	5	211

Table A.7 XRD data of as-received B_4C.

d	2θ	Intensity, (%)
4.480	19.80	12
4.012	22.14	31
3.770	23.58	70
3.341	26.66	10
2.790	32.06	13
2.559	35.04	62
2.505	35.82	3
2.376	37.84	100
2.287	39.36	5
1.808	50.44	2
1.707	53.64	6
1.621	56.74	1
1.500	61.82	6
1.457	63.82	9
1.439	64.74	6
1.397	66.92	7
1.334	70.52	5
1.319	71.46	52
1.257	75.60	3
1.207	79.34	1
1.186	81.02	1

Table A.8 XRD data of B_4C heated in air atmosphere.

d	2θ	Intensity, (%)
6.046	14.64	17
4.516	19.64	50
4.012	22.14	71
3.776	23.54	79
3.353	26.56	100
3.193	27.92	68
2.784	32.12	26
2.560	35.02	66
2.506	35.80	21
2.372	37.90	82
2.263	39.80	16
2.135	42.30	20
2.012	45.01	21
1.706	53.70	11
1.667	55.04	8
1.534	60.28	5
1.494	62.06	5
1.456	63.86	11
1.418	65.80	8
1.396	67.00	8
1.333	70.60	5
1.307	72.20	8
1.251	76.00	8
1.228	77.70	3

Table A.9 XRD data of B_4C heated in argon atmosphere.

d	2θ	Intensity, (%)
5.676	15.6	1
4.344	20.43	19
3.909	22.73	31
3.837	23.16	65
3.271	27.24	98
3.166	28.16	6
3.063	29.13	5
2.766	32.34	14
2.626	34.11	5
2.550	35.17	68
2.478	36.22	10
2.351	38.25	100
2.300	39.13	5
2.051	44.11	6
1.874	48.53	1
1.794	50.85	4
1.720	53.20	9
1.667	55.05	4
1.621	56.76	2
1.538	60.10	5
1.492	62.18	7
1.449	64.24	10
1.414	66.00	9
1.391	67.24	10
1.340	70.15	7
1.322	71.25	12
1.307	72.21	9
1.250	76.12	6
1.206	79.41	1
1.181	81.45	1

APPENDIX B

RESULTS OF DSC ANALYSIS

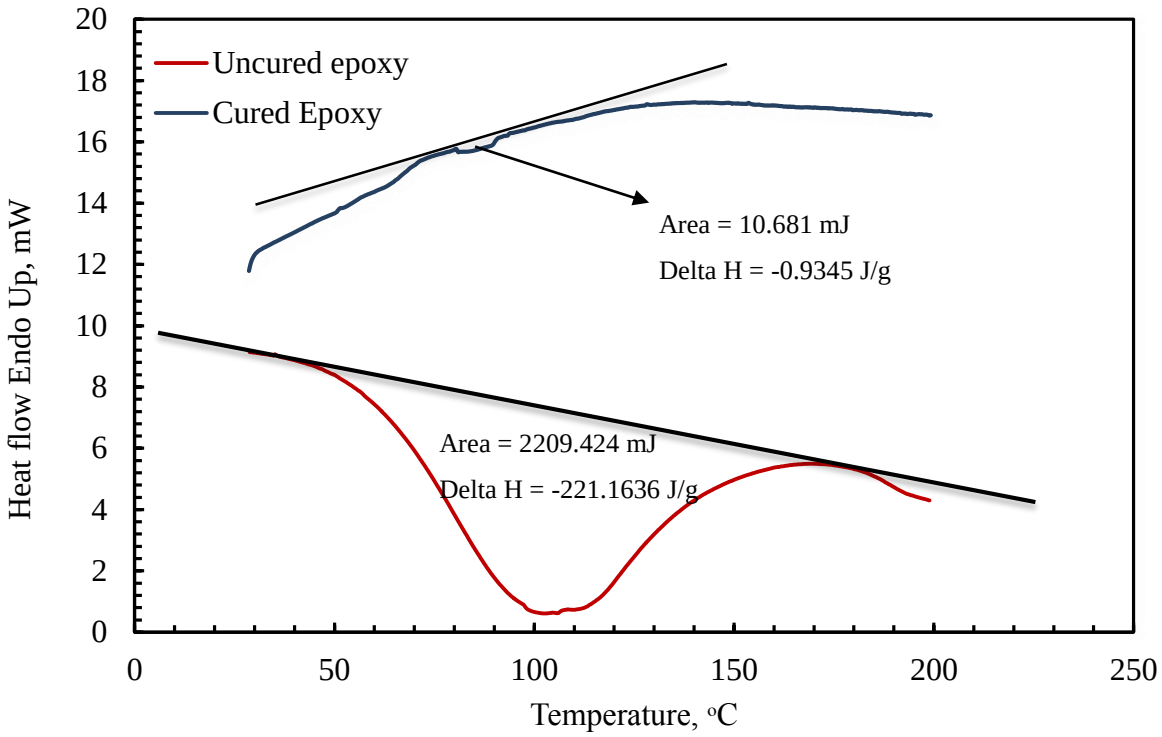

Figure B.1 DSC curve of cured and uncured epoxy sample.

Sample calculation for calculating curing degree of cured epoxy sample, which was calculated using Figure B.1 and Equation 2.7, was shown below:

$$\text{Degree of Curing (\%)} = \frac{221.1636\ \text{J/g} - 0.9345\ \text{J/g}}{221.1636\ \text{J/g}} \text{x} 100$$

$$= 99$$

APPENDIX C

RESULTS OF MECHANICAL ANALYSIS

Table C.1 Tensile test data of neat epoxy and EP/B_4C composites.

Sample Code	Tensile Strength, MPa	Elastic Modulus, Mpa	Elongation at break, %
Neat EP	48±3.0	2815±262	3.9±0.8
EP/0.5B_4C	33±0.5	2345±152	3.5±0.3
EP/1B_4C	35±3.0	2310±217	4.2±0.5
EP/3B_4C	44±2.0	2713±380	3.7±0.8
EP/5B_4C	45±4.0	2739±283	4.2±0.3
EP/8B_4C	50±1.1	2828±60	6.5±0.6

Table C.2 Impact test data of neat epoxy and EP/B_4C composites.

Sample Code	Impact Strength, kJ/m^2
Neat EP	11.1±1.7
EP/0.5B_4C	11.0±1.9
EP/1B_4C	10.8±0.5
EP/3B_4C	13.4±1.1
EP/5B_4C	16.6±1.7
EP/8B_4C	14.5±1.4

Table C.3 Tensile test data of epoxy/boron containing compound composites and epoxy/melamine phosphate composites.

Sample Code	Tensile Strength, MPa	Elastic Modulus, MPa	Elongation at break, %
EP/1ZnB	41±0.7	2269±325	4.1±0.1
EP/1BA	42±4.8	1647±202	4.2±0.7
EP/1CaB	39±5.0	1498±269	4.2±0.7
EP/3B_4C/1ZnB	43±4.7	1574±199	3.9±0.5
EP/3B_4C/1BA	24±0.8	2040±271	2.0±0.22
EP/3B_4C/1CaB	48±4.5	2378±275	4.6±0.8
EP/10MP	42±3.3	2314±276	6.2±0.5
EP/10MP/3B_4C	39±2.3	1923±423	3.4±0.3
EP/10MP/3B_4C /1ZnB	37±6.1	2559±75	2.6±0.3

Table C.4 Impact test data of epoxy/boron containing compound composites and epoxy/melamine phosphate composites.

Sample Code	Impact Strength, kJ/m^2
EP/1ZnB	5.5±1.6
EP/1BA	9.8±1.6
EP/1CaB	8.6±1.1
EP/3B_4C/1ZnB	8.8±0.7
EP/3B_4C/1BA	7.3±1.2
EP/3B_4C/1CaB	11.1±1.8
EP/10MP	4.9±0.4
EP/10MP/3B_4C	6.4±0.2
EP/10MP/3B_4C /1ZnB	5.2±0.8

APPENDIX D

RESULTS OF DSC AND TGA ANALYSES OF EPOXY-BASED COMPOSITES

Figures D.1-D.15 show DSC results, the other figures (Figure D.16-D.30) represent TGA results.

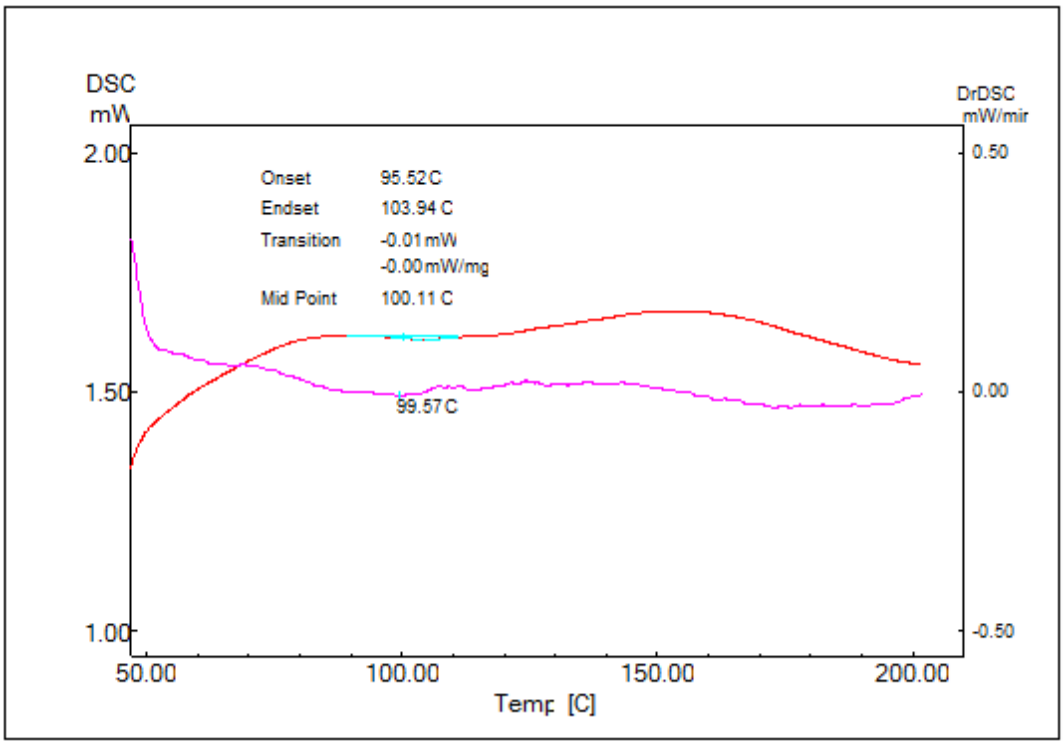

Figure D.1 DSC Thermogram of Neat EP.

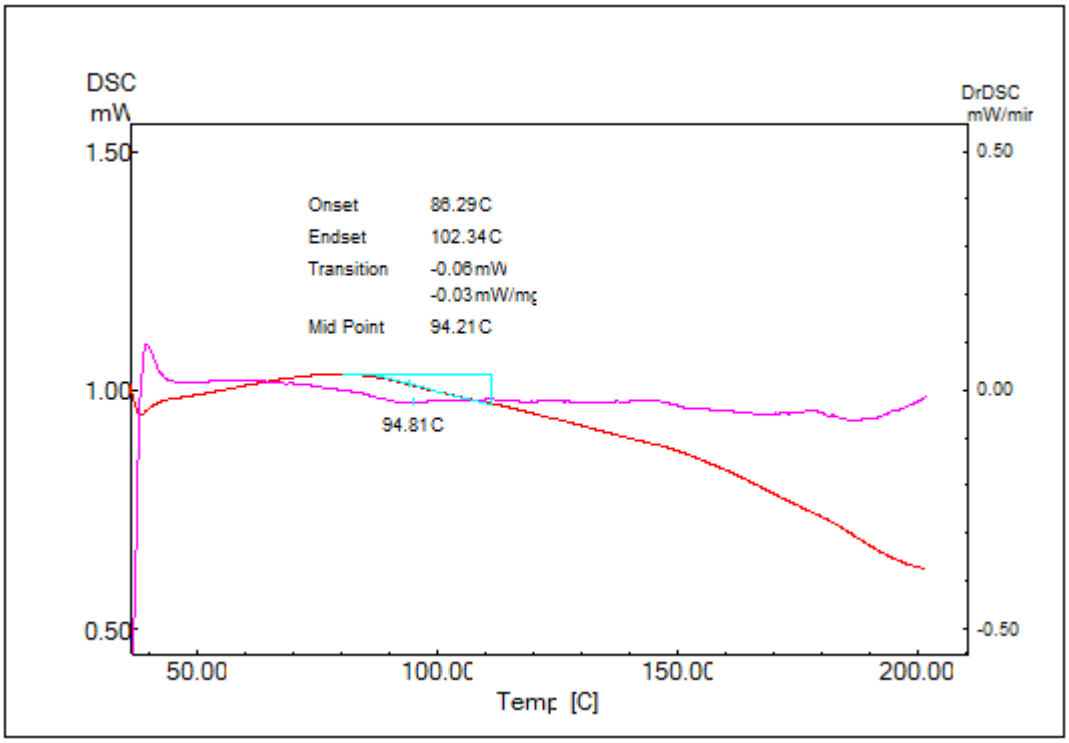

Figure D.2 DSC Thermogram of EP/0.5B_4C.

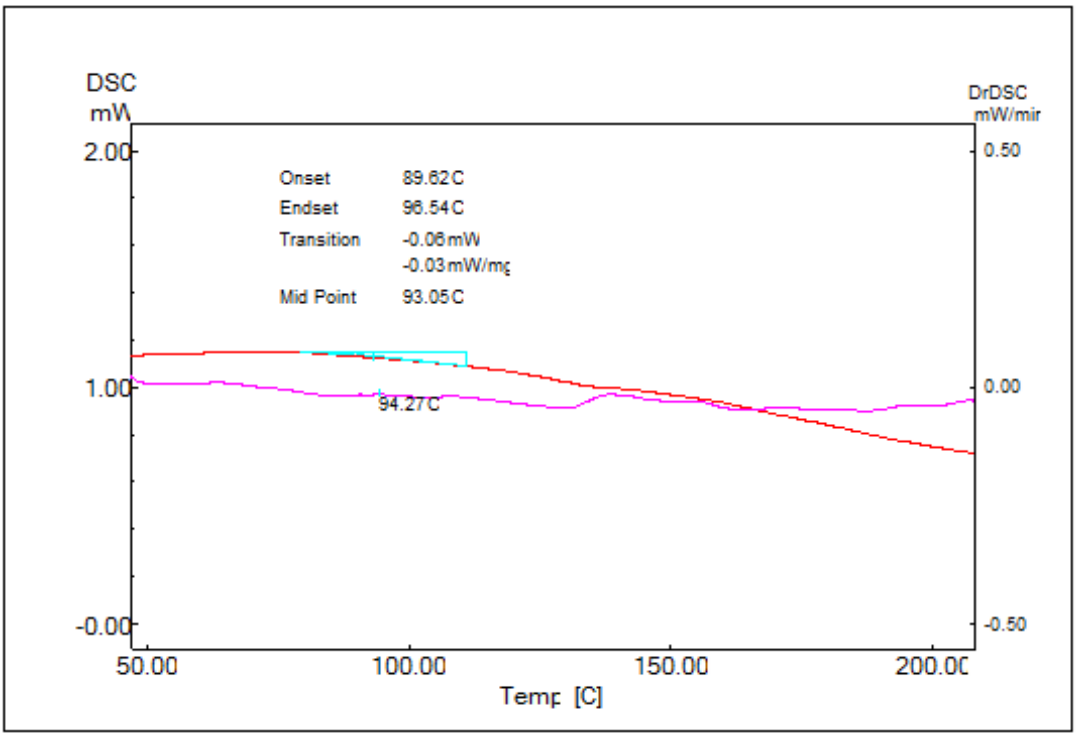

Figure D.3 DSC Thermogram of EP/1B_4C.

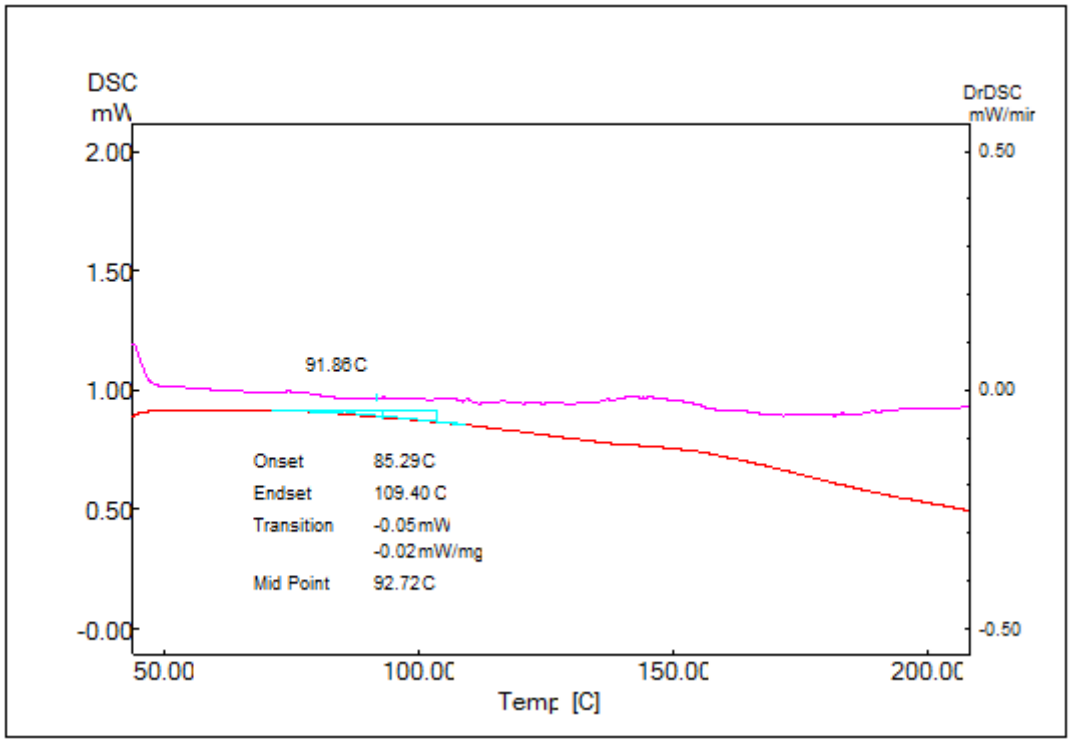

Figure D.4 DSC Thermogram of EP/3B_4C.

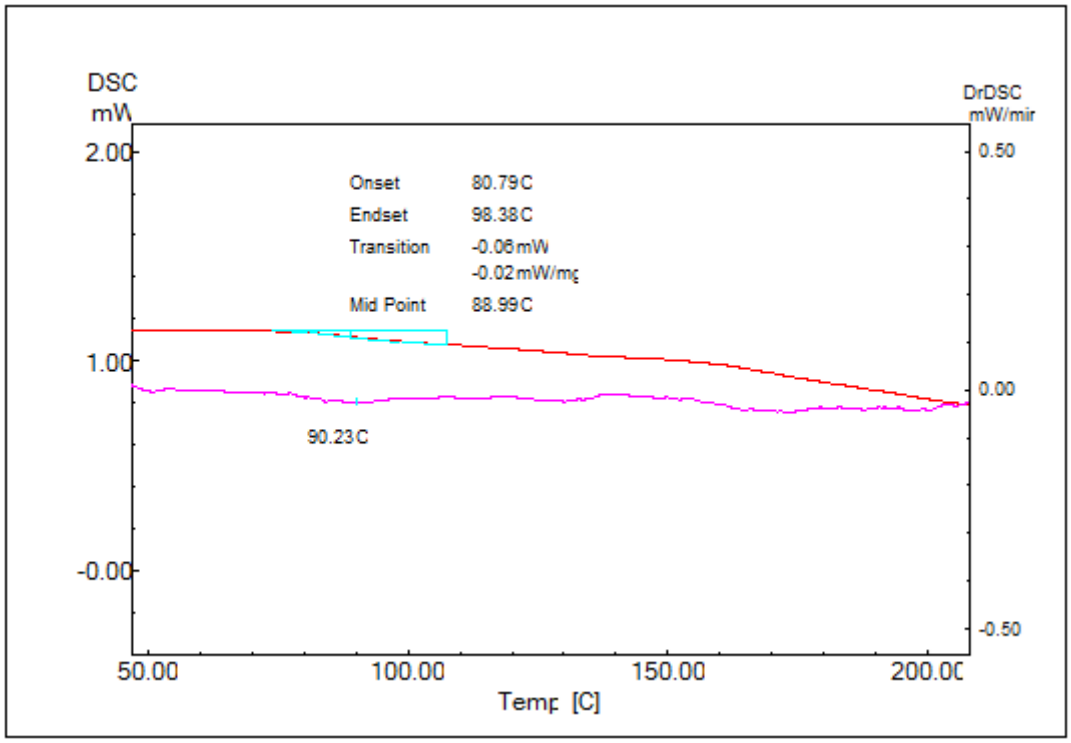

Figure D.5 DSC Thermogram of EP/5B_4C.

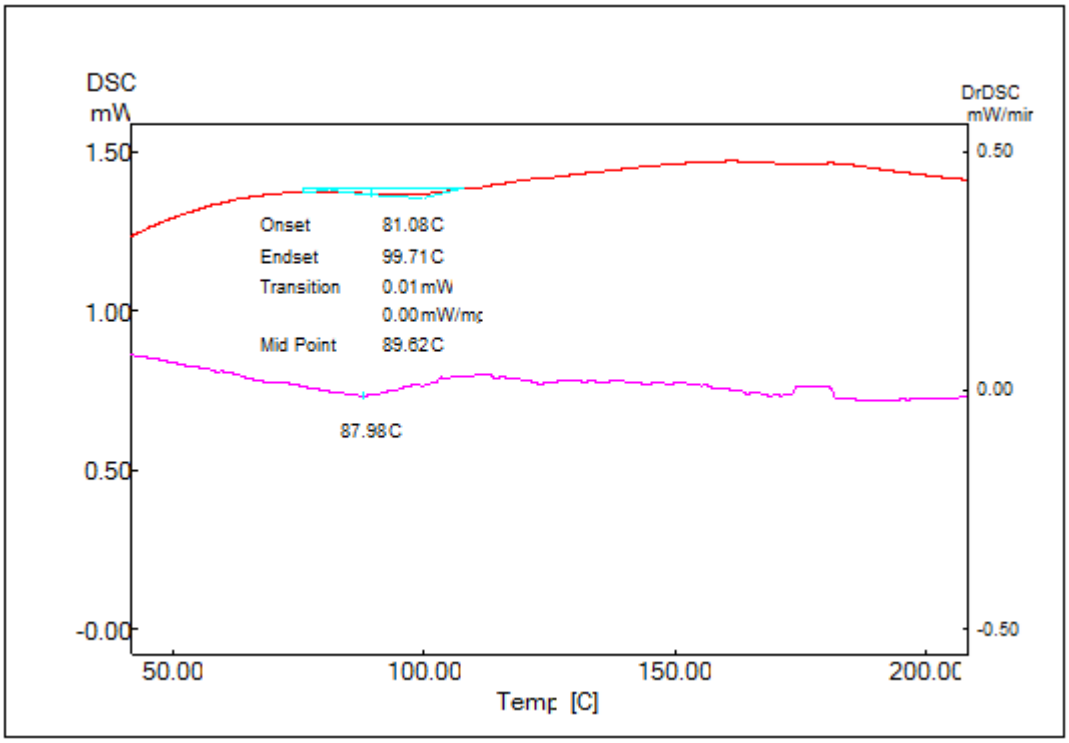

Figure D.6 DSC Thermogram of EP/8B_4C.

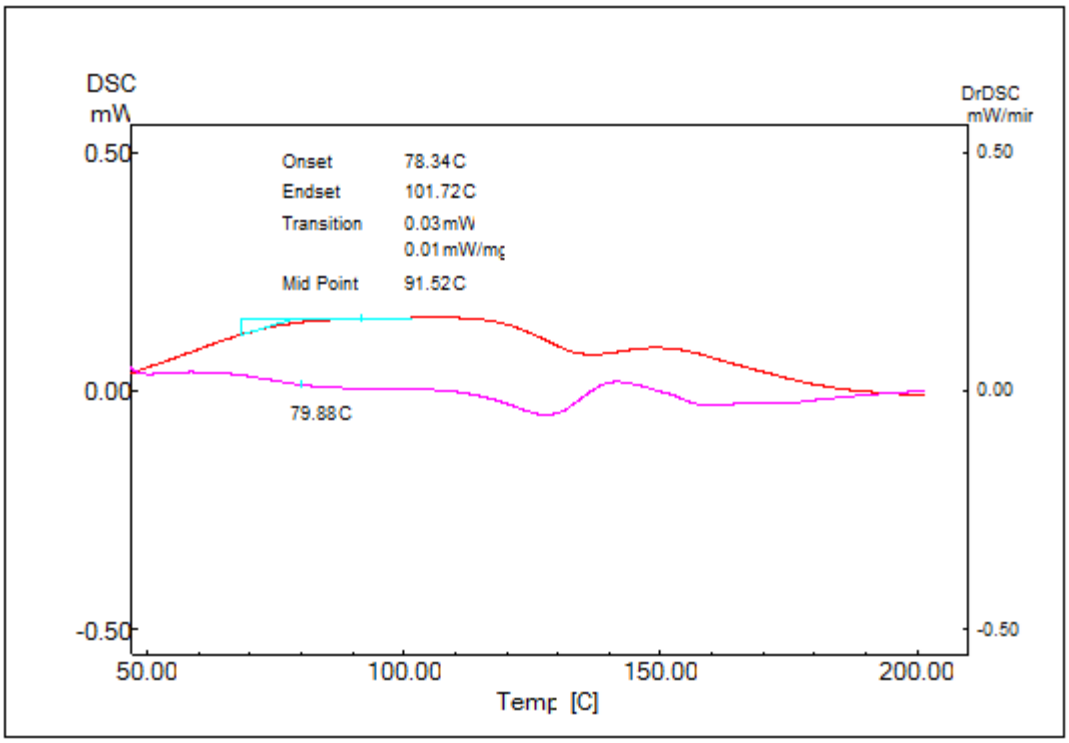

Figure D.7 DSC Thermogram of EP/1ZnB.

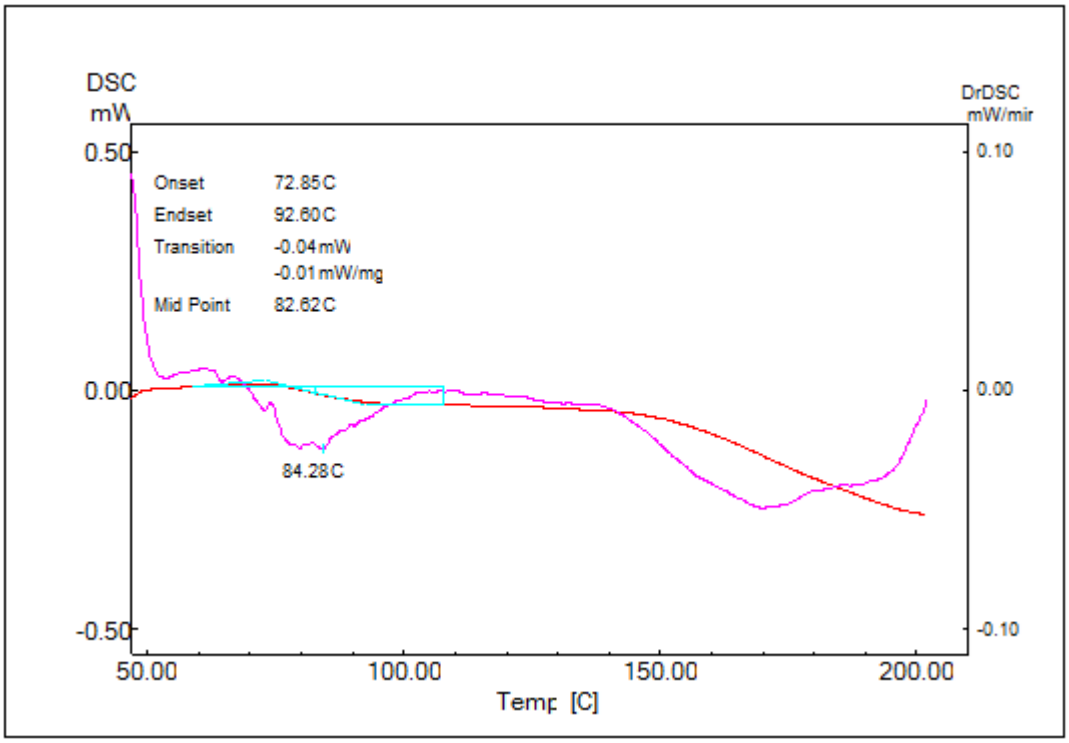

Figure D.8 DSC Thermogram of EP/1BA.

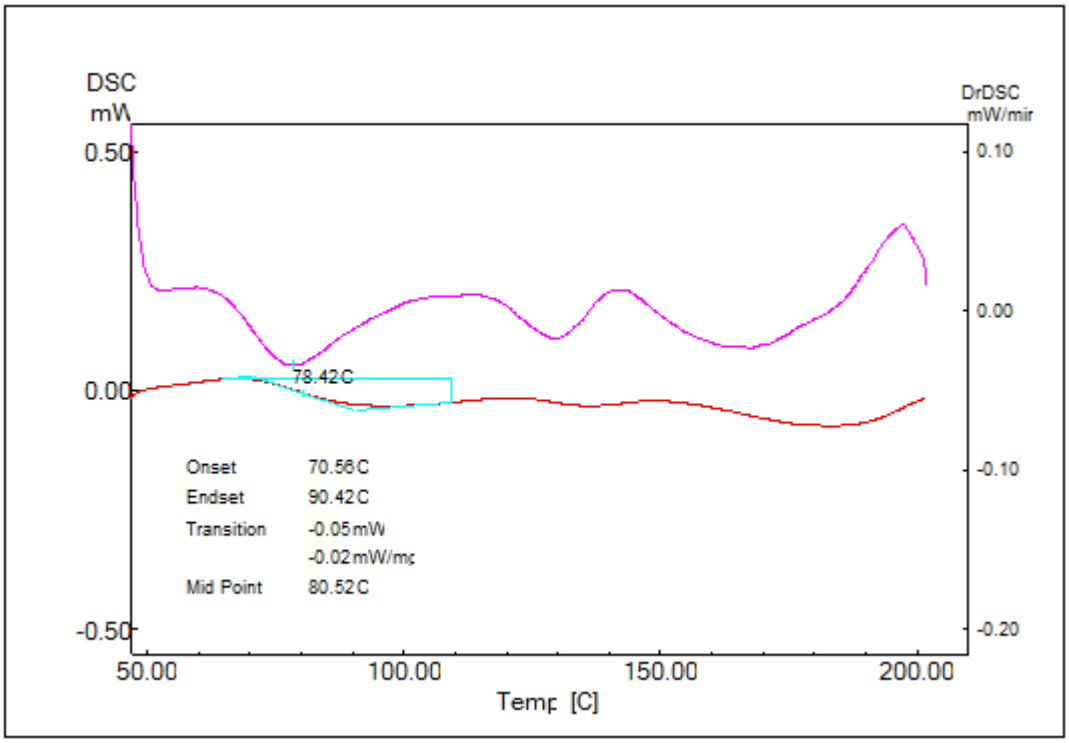

Figure D.9 DSC Thermogram of EP/1CaB.

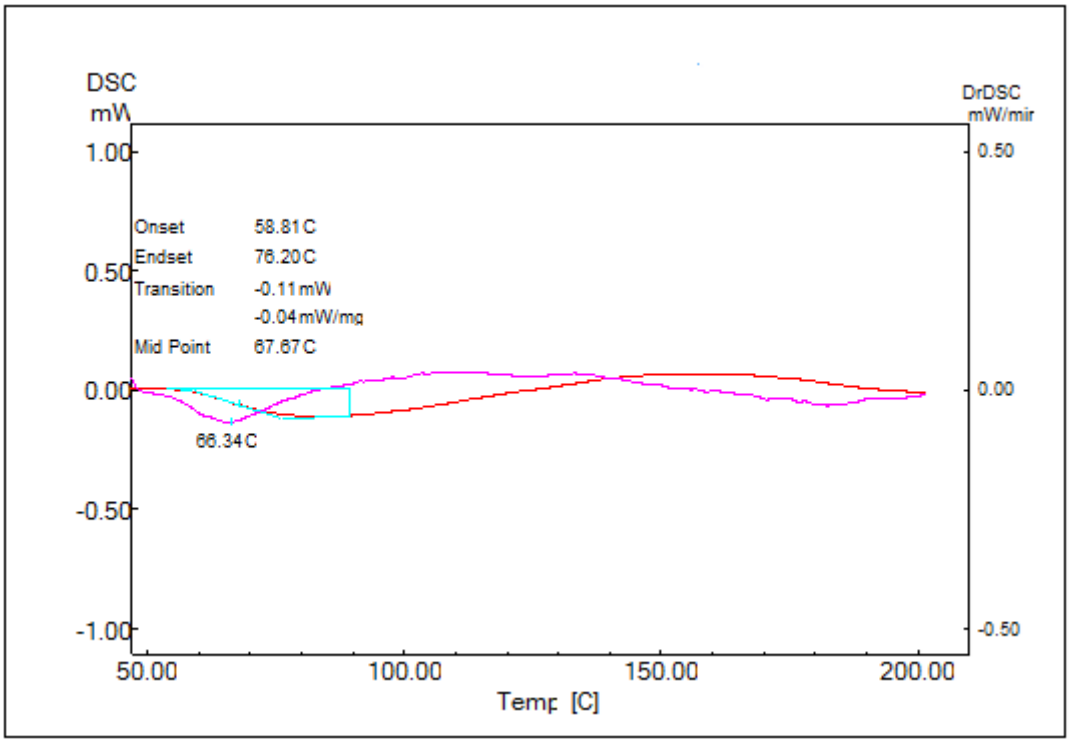

Figure D.10 DSC Thermogram of EP/3B_4C/1ZnB.

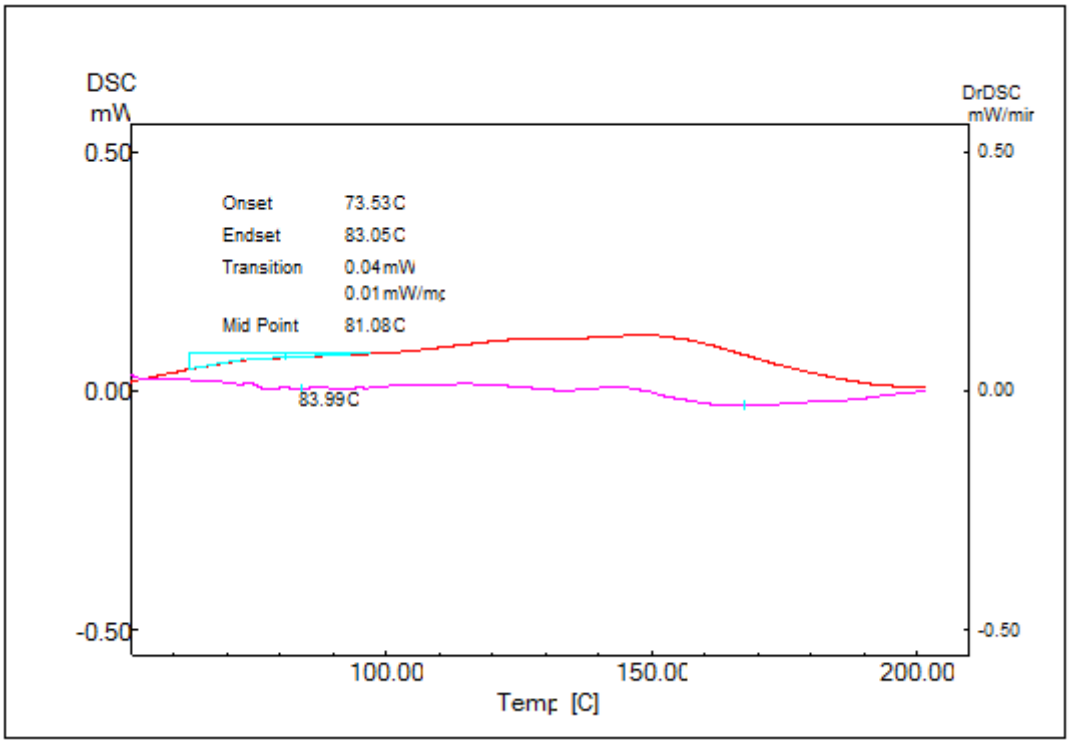

Figure D.11 DSC Thermogram of EP/3B_4C/1BA.

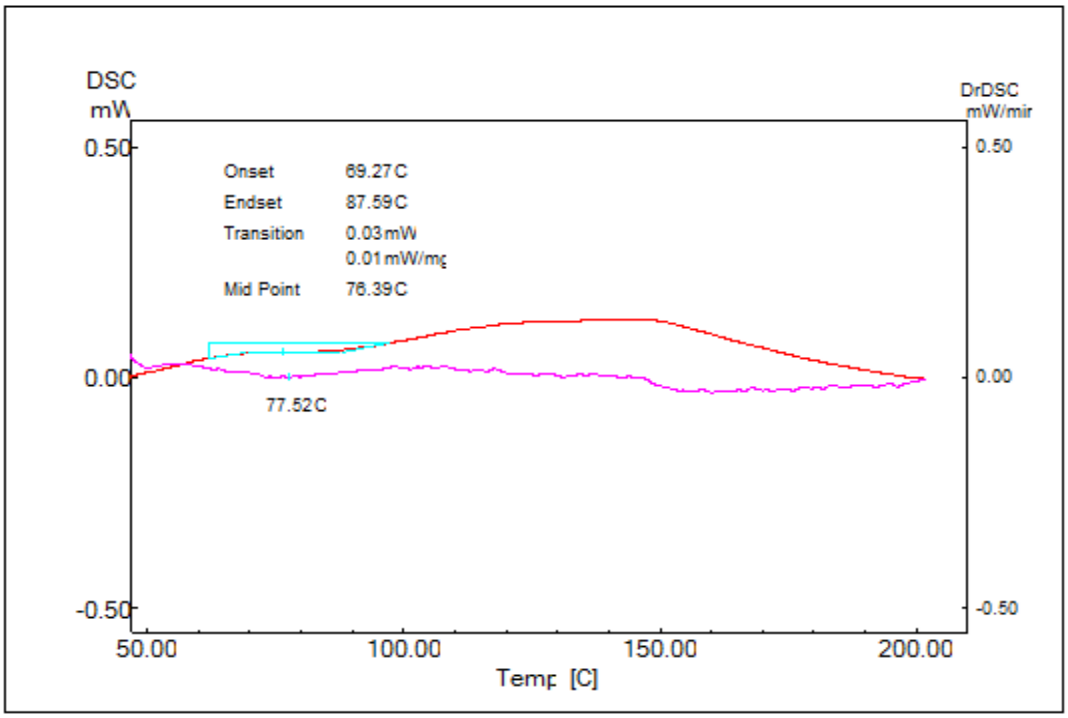

Figure D.12 DSC Thermogram of EP/3B_4C/1CaB.

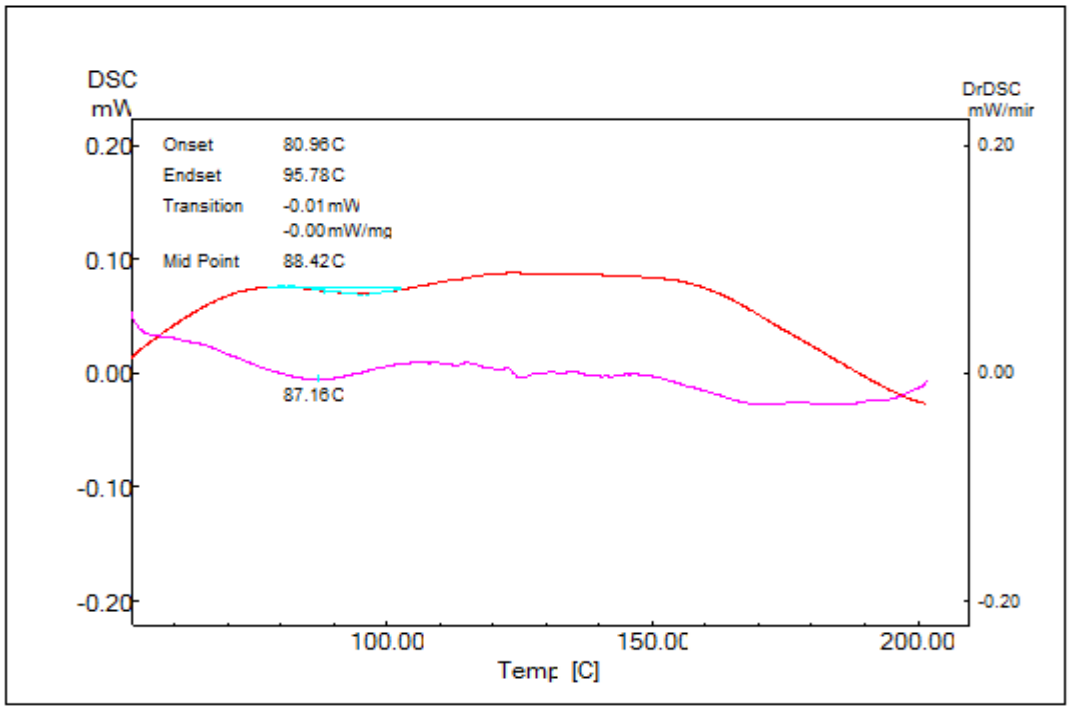

Figure D.13 DSC Thermogram of EP/10MP.

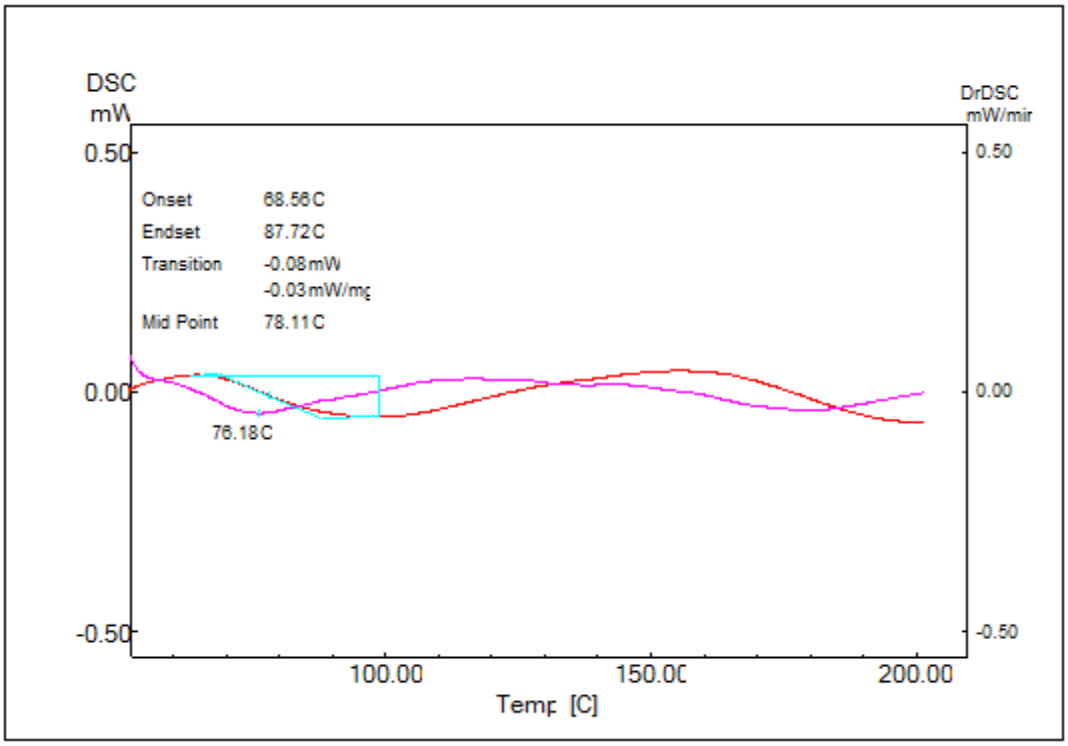

Figure D.14 DSC Thermogram of EP/10MP/3B_4C.

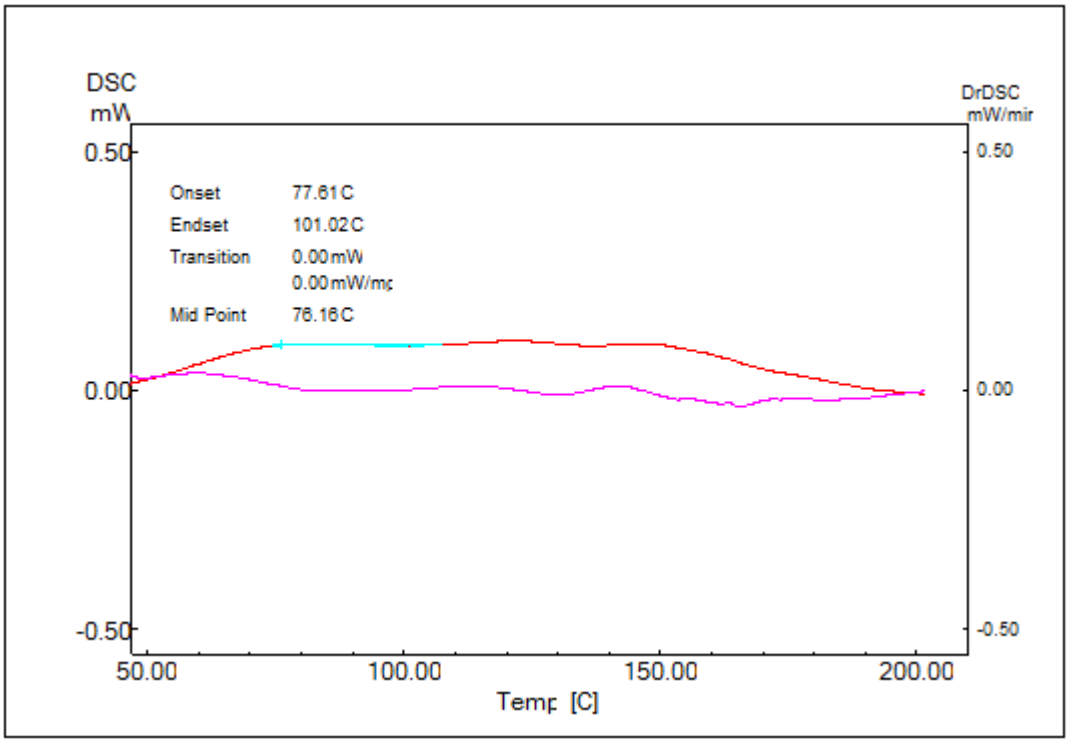

Figure D.15 DSC Thermogram of EP/10MP/3B_4C/1ZnB.

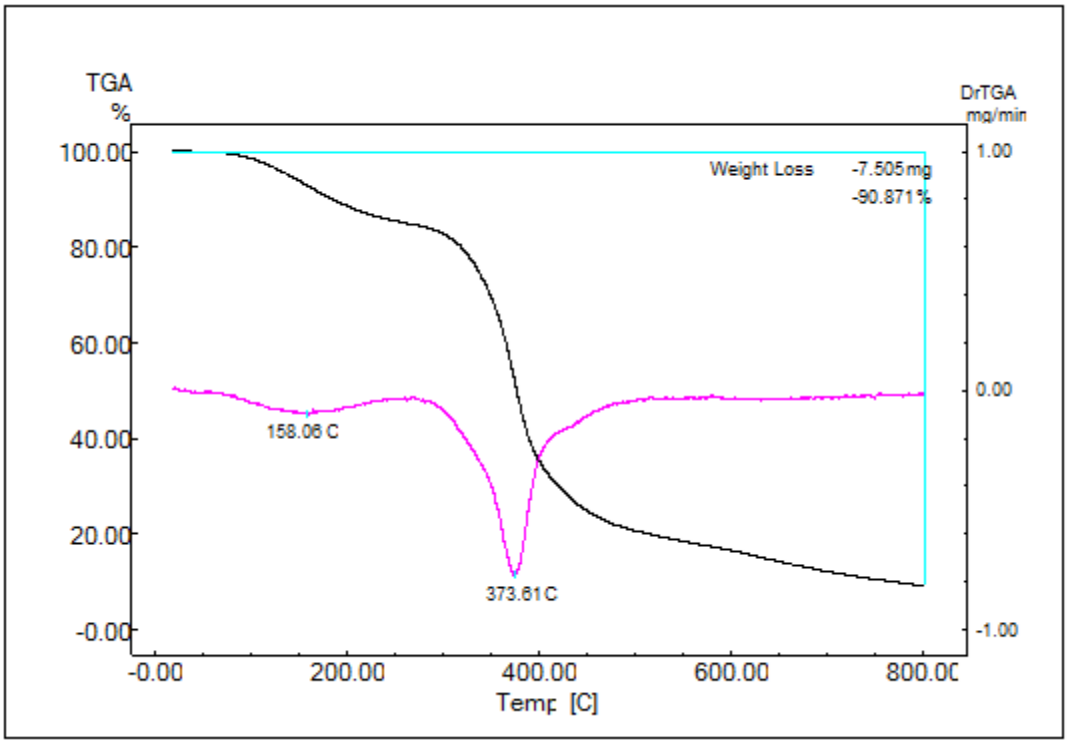

Figure D.16 Dr-TGA Thermogram of Neat EP.

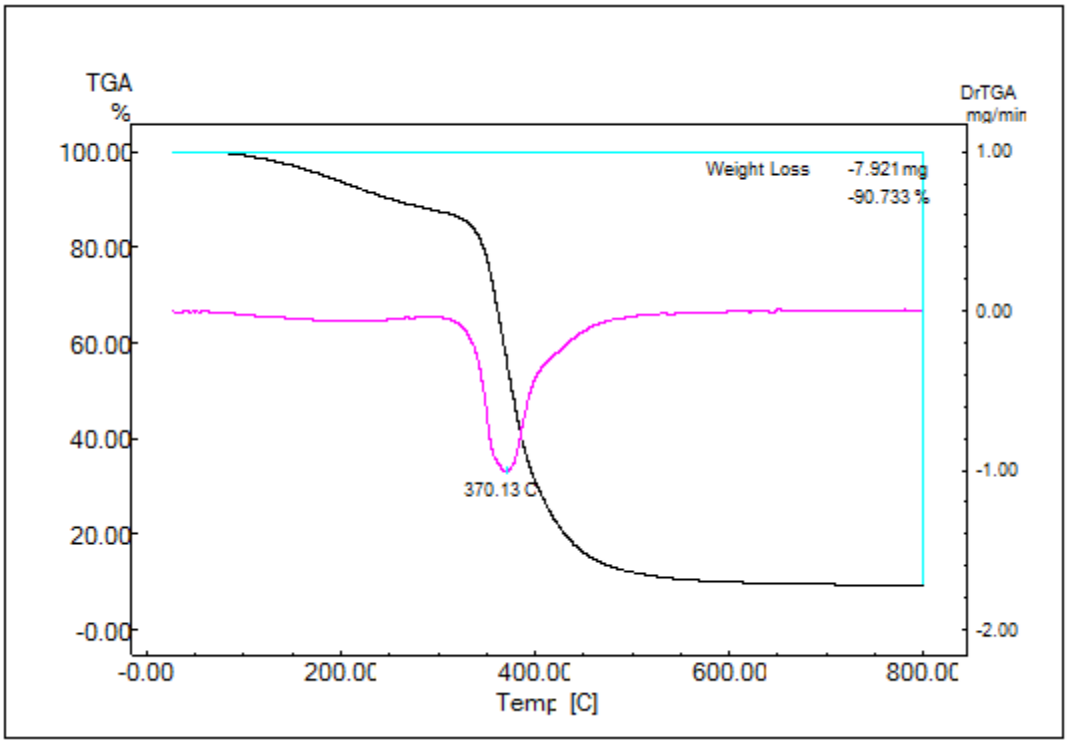

Figure D.17 Dr-TGA Thermogram of EP/0.5B_4C.

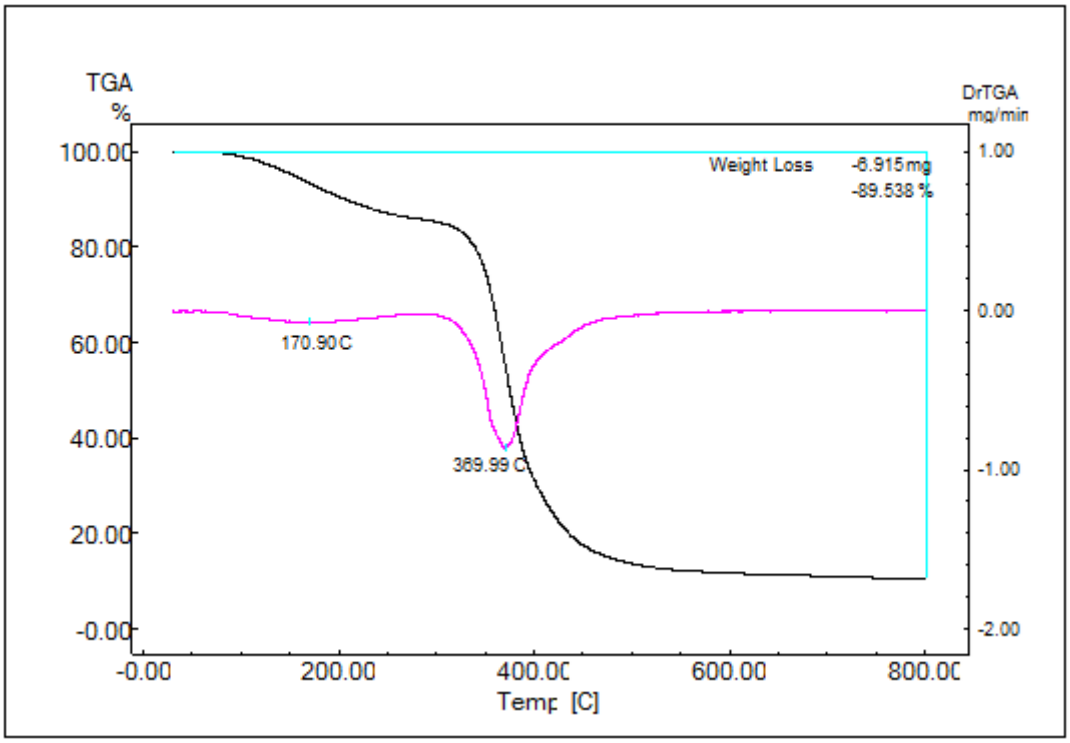

Figure D.18 Dr-TGA Thermogram of EP/1B_4C.

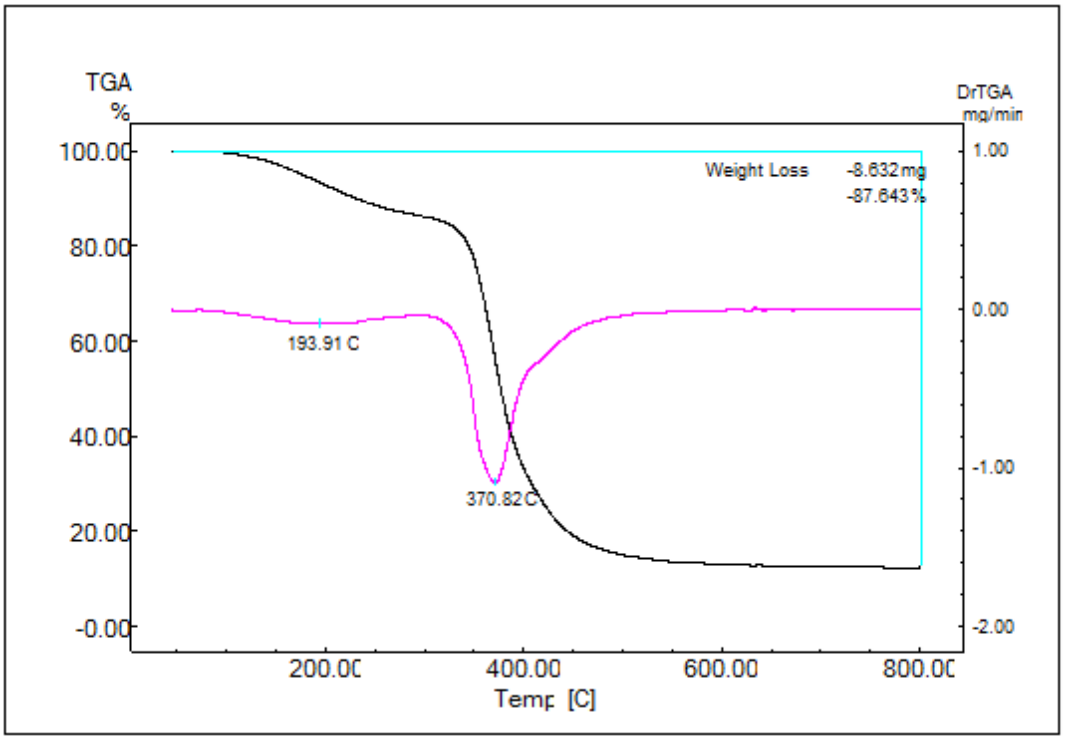

Figure D.19 Dr-TGA Thermogram of EP/3B_4C.

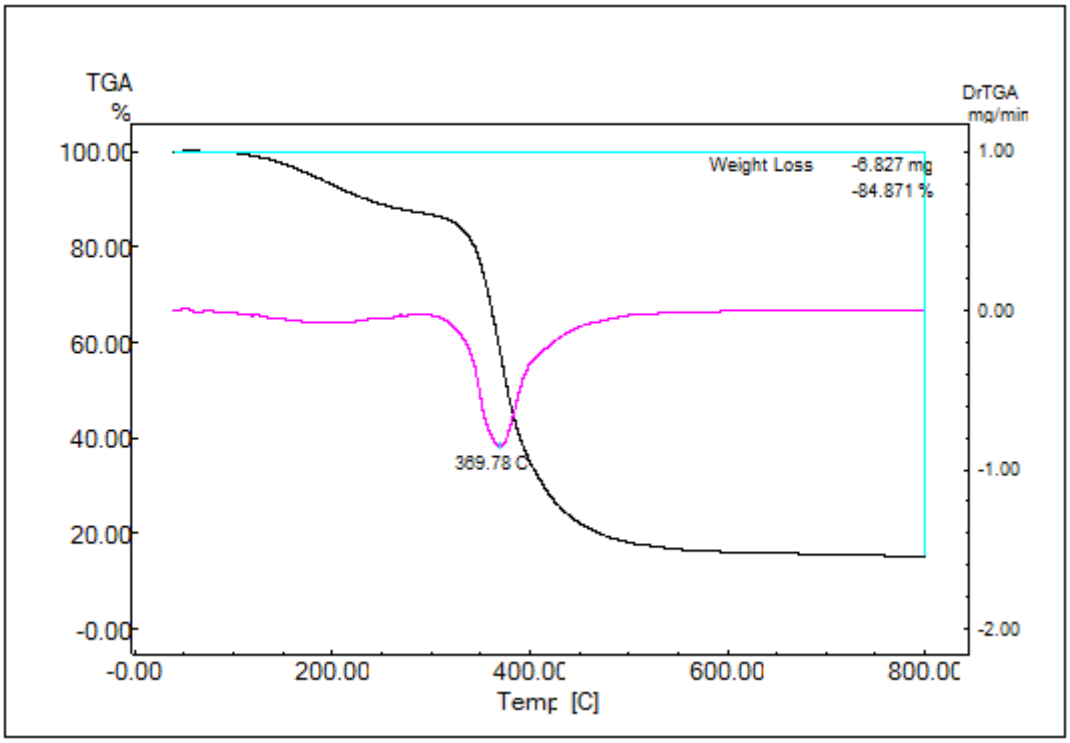

Figure D.20 Dr-TGA Thermogram of EP/5B_4C.

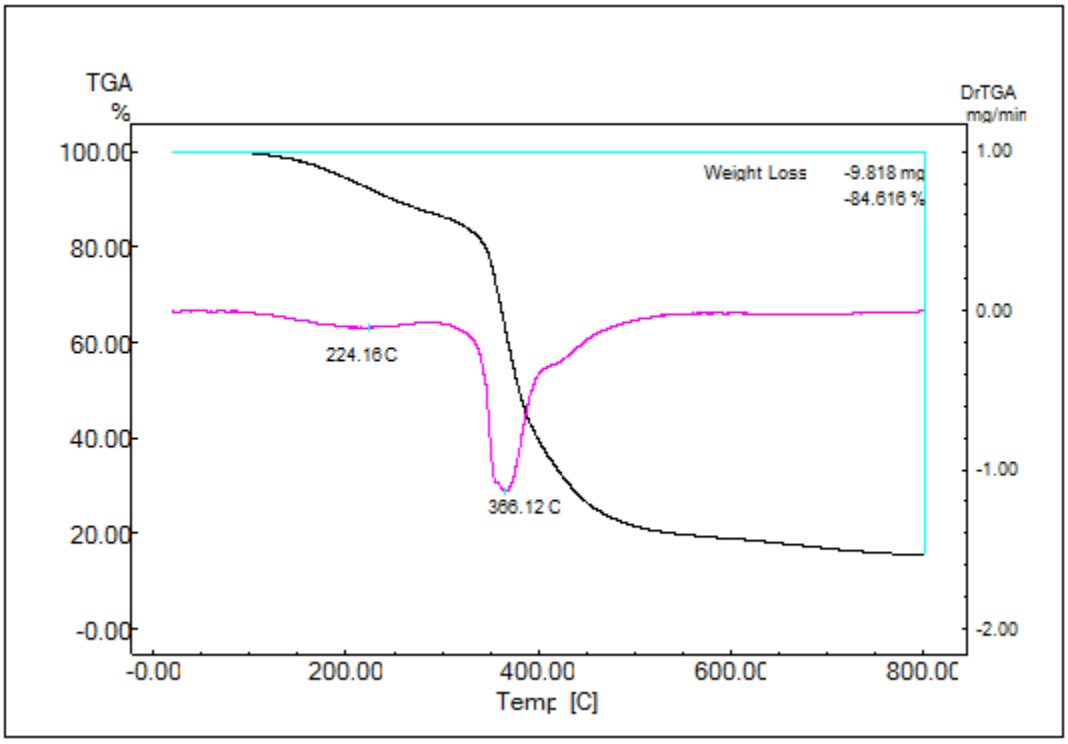

Figure D.21 Dr-TGA Thermogram of EP/8B_4C.

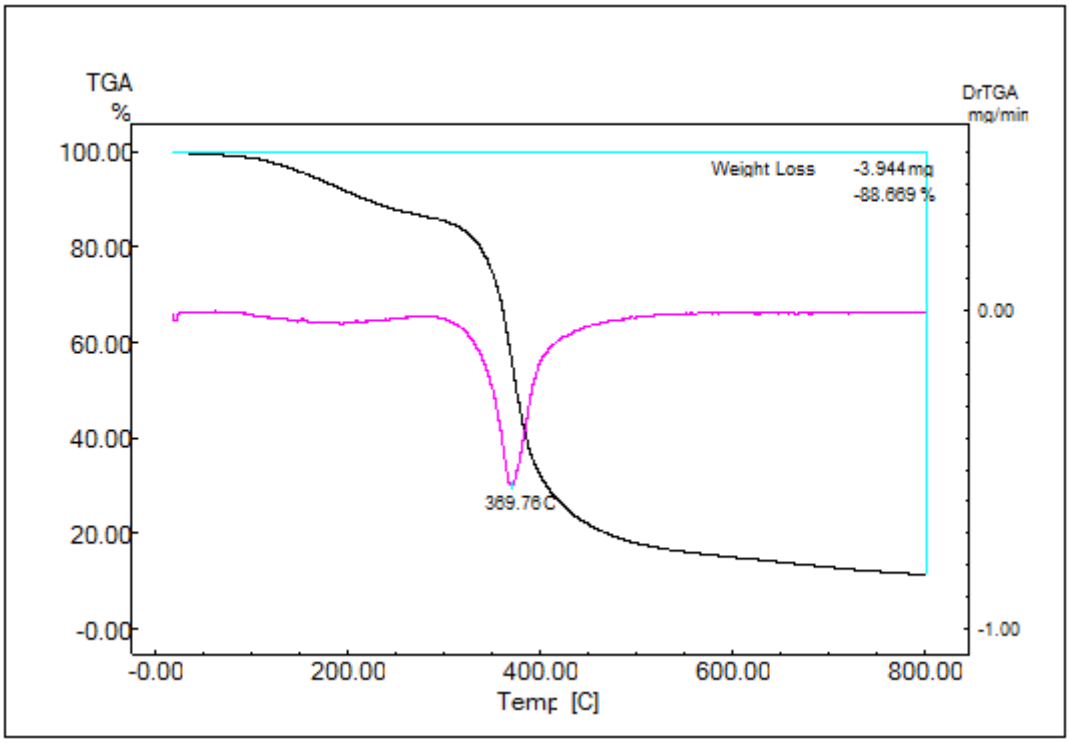

Figure D.22 Dr-TGA Thermogram of EP/1ZnB.

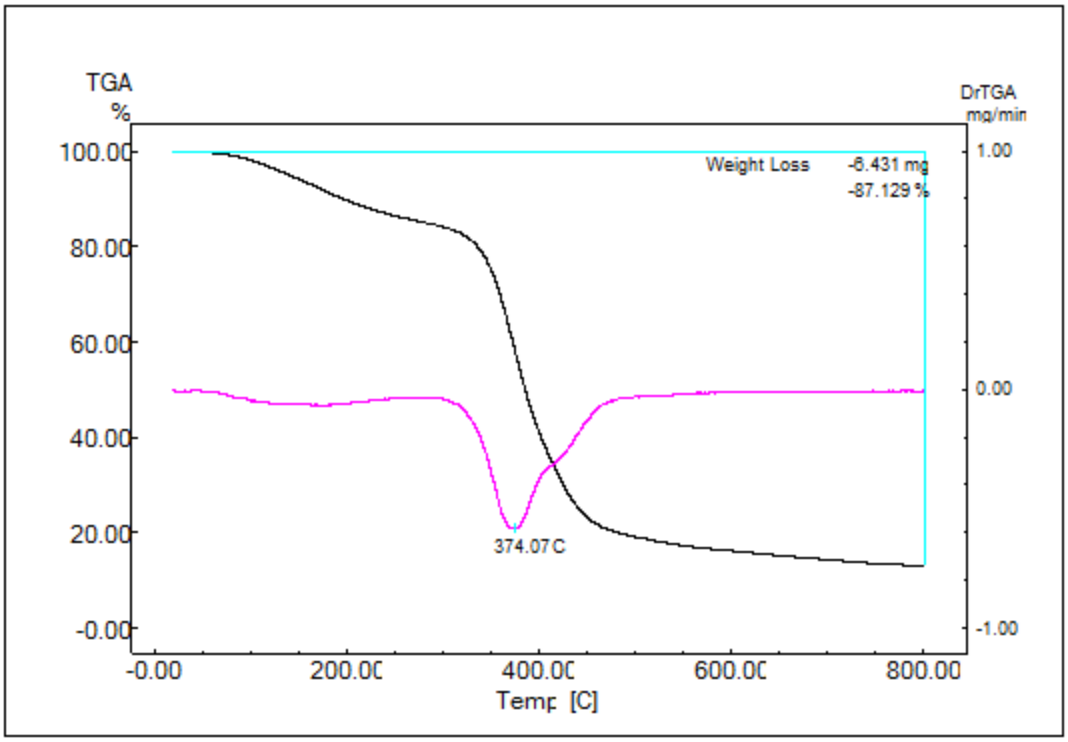

Figure D.23 Dr-TGA Thermogram of EP/1BA.

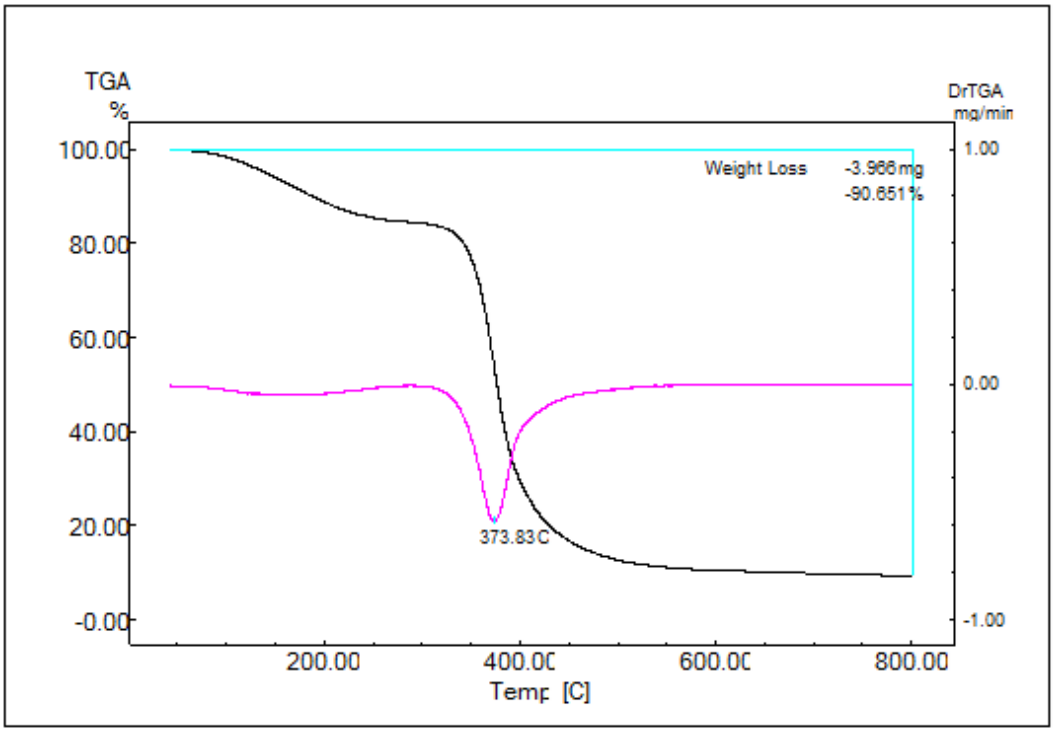

Figure D.24 Dr-TGA Thermogram of EP/1CaB.

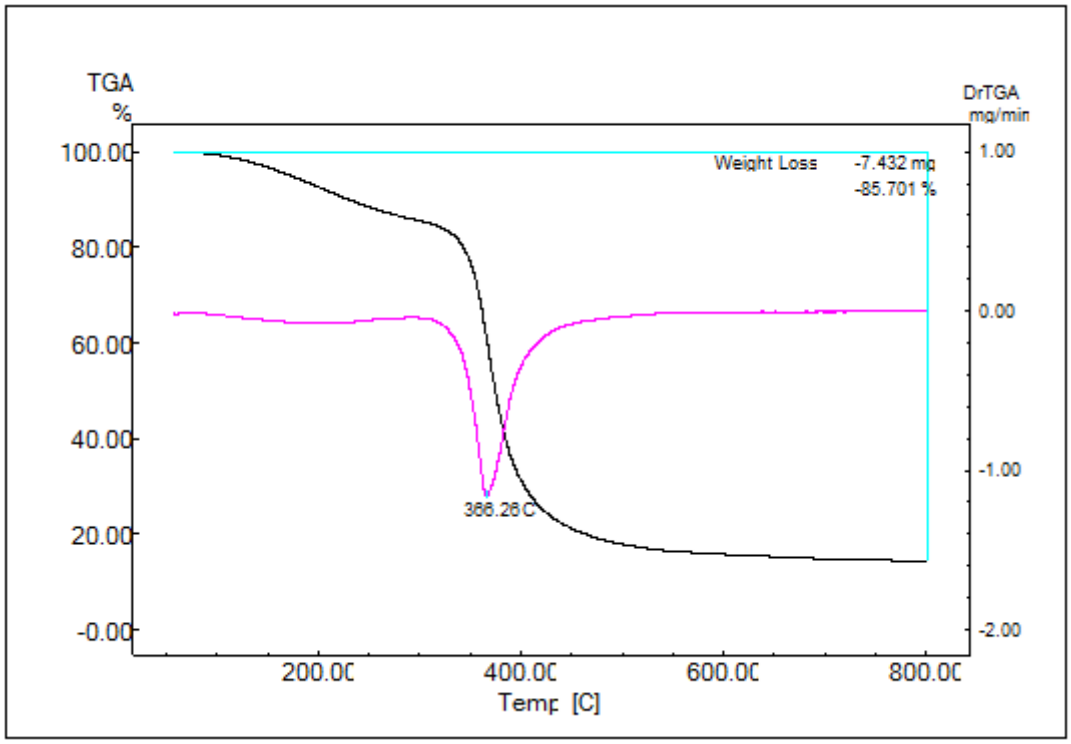

Figure D.25 Dr-TGA Thermogram of EP/3B_4C/1ZnB.

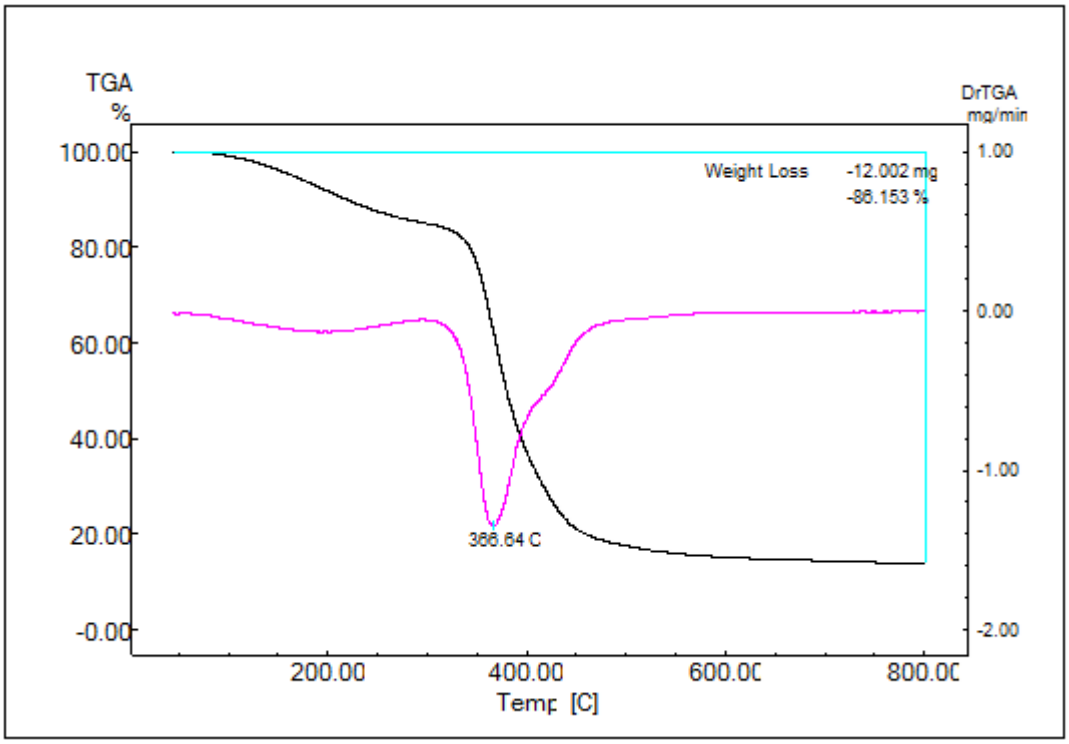

Figure D.26 Dr-TGA Thermogram of EP/3B_4C/1BA.

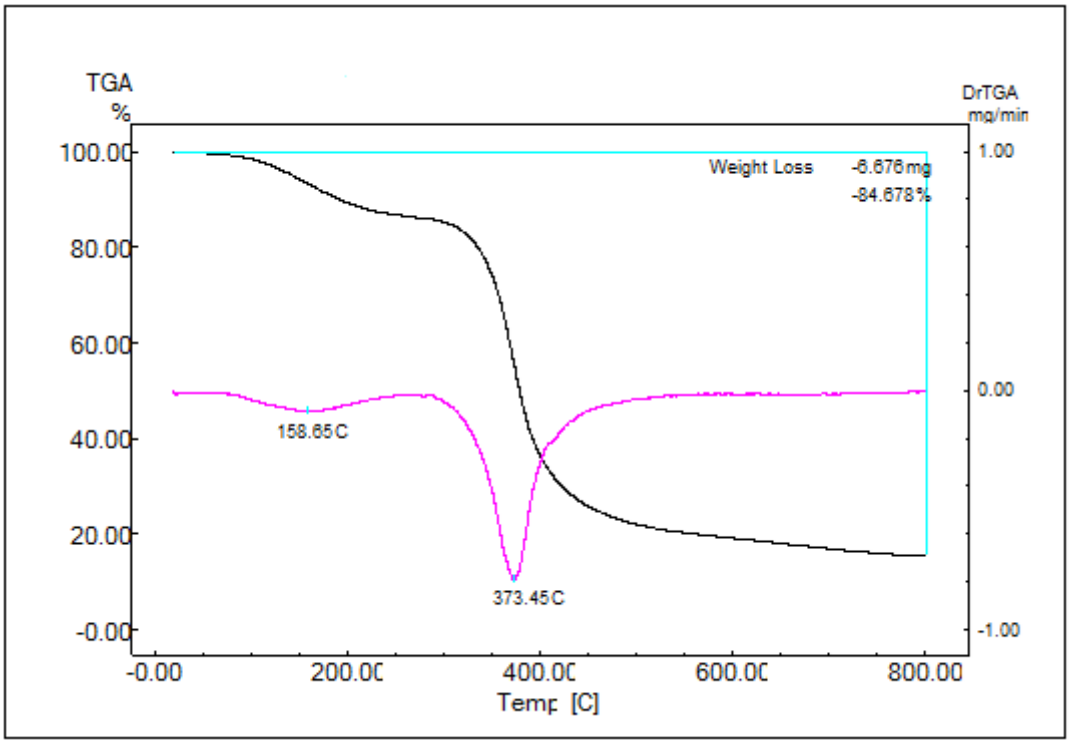

Figure D.27 Dr-TGA Thermogram of EP/3B_4C/1CaB.

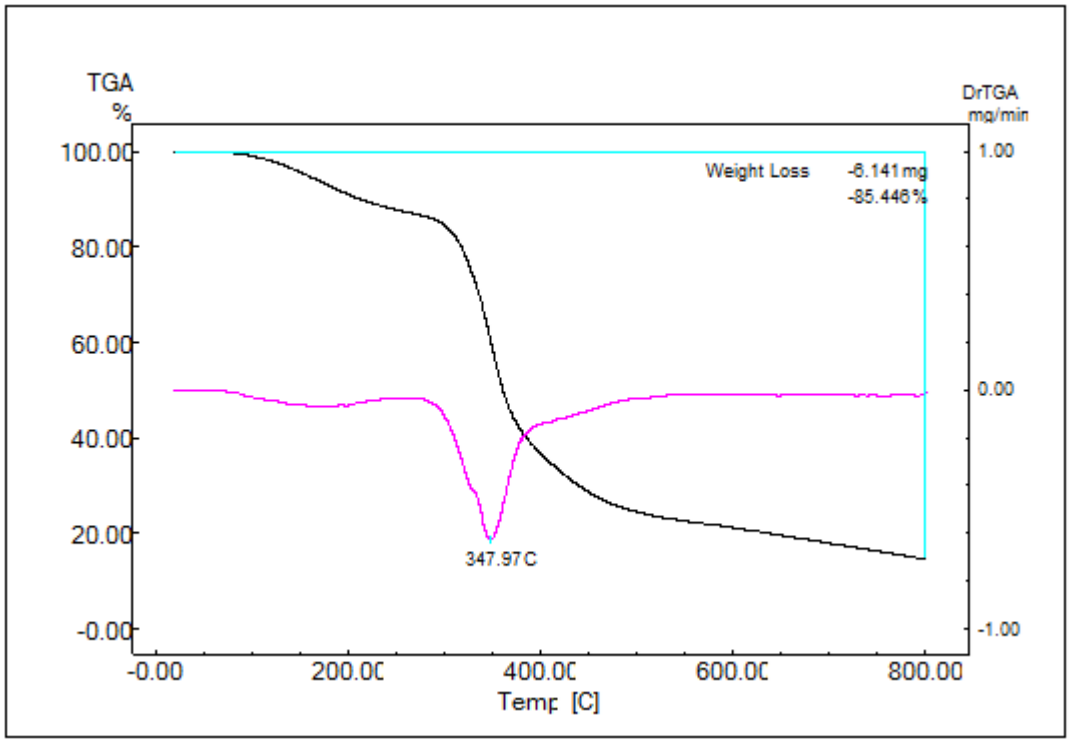

Figure D.28 Dr-TGA Thermogram of EP/10MP.

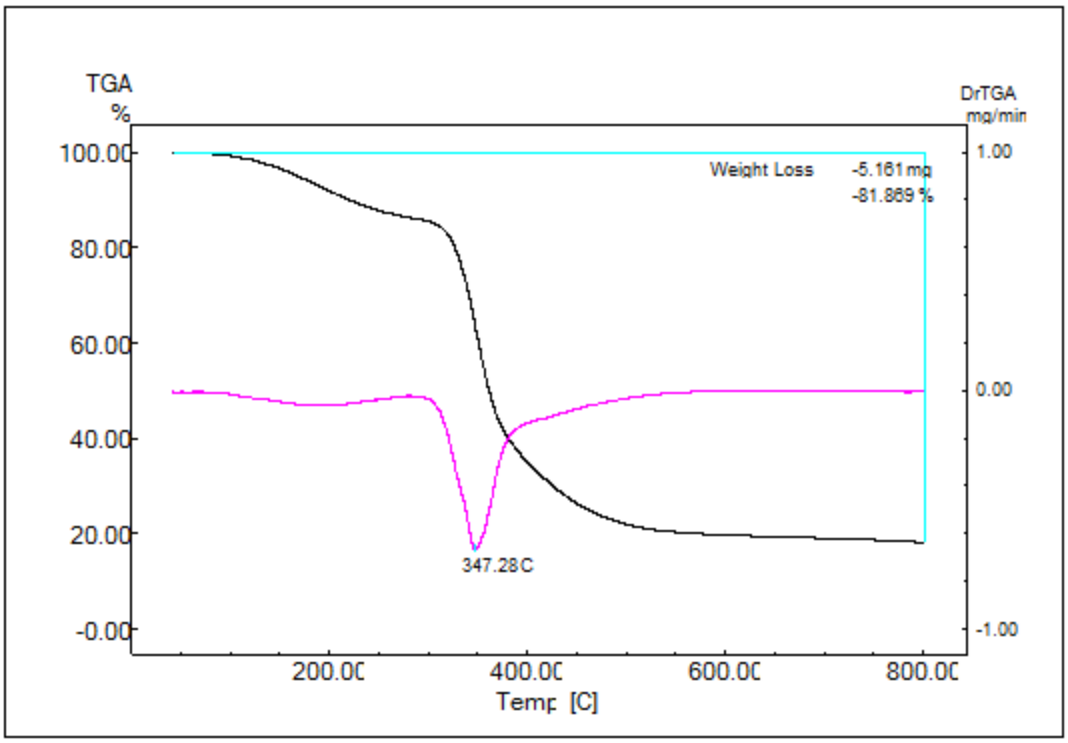

Figure D.29 Dr-TGA Thermogram of EP/10MP/3B_4C.

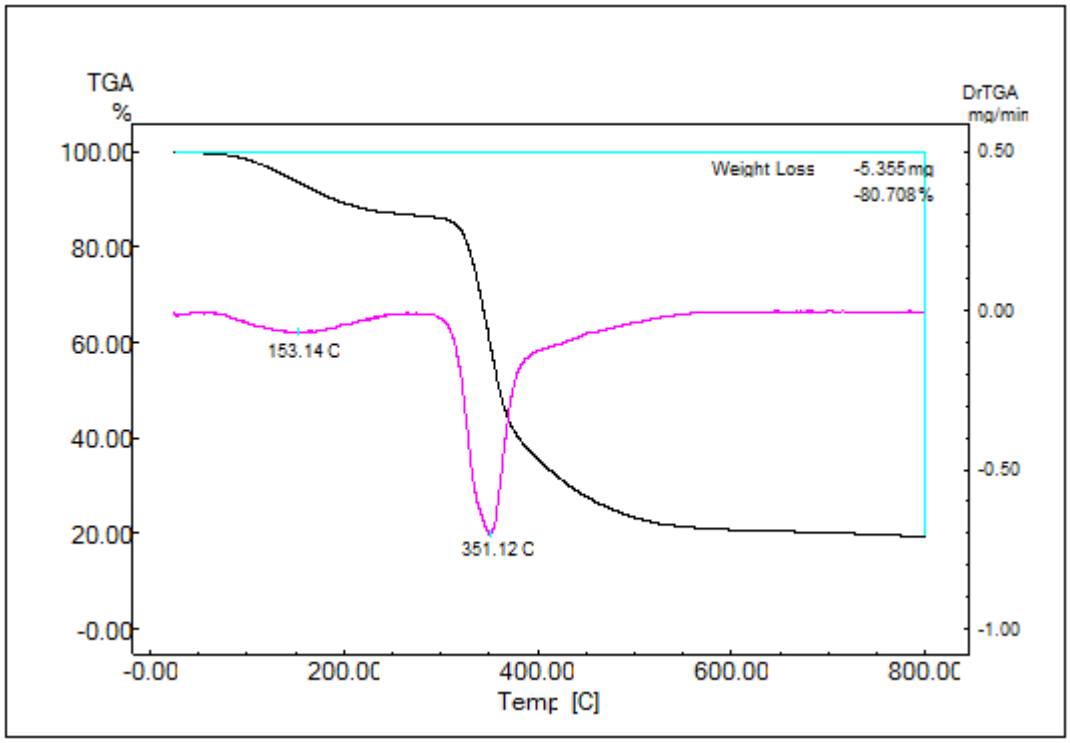

Figure D.30 Dr-TGA Thermogram of EP/10MP/3B_4C/1ZnB.

APPENDIX E

SINTERING OF BORON CARBIDE

In this study boron carbide was sintered using distilled water as binding agent. 5 grams of B_4C is mixed with 1 drop of water and mixed in a muller. Then this cohesive boron carbide was pressurized with a cold press with a pressure of 100 bar. After 25 minutes of pressing, the boron carbide was removed from the cold press and put into an oven at 1350°C for 4 hours. Then the electrical measurements were carried out with two point probe electrical resistivity measuring method with this sintered boron carbide.

Figure E.1 Pressed boron carbide.